Fall 11-1-2020

Uncertainties and Robustness in Fisheries Stock Assessment and Management: Data Processing, Modeling and Socioeconomic Aspects

Luoliang Xu
luoliang.xu@maine.edu

UNCERTAINTIES AND ROBUSTNESS IN FISHERIES STOCK ASSESSMENT AND MANAGEMENT: DATA PROCESSING, MODELING AND SOCIOECONOMIC ASPECTS

BY

LUOLIANG XU

A DISSERTATION

Submitted in Partial Fulfillment of the

Requirements for the Degree of

Doctor of Philosophy

(in Ecology and Environmental Sciences)

The Graduate School

The University of Maine

December 2020

Advisory Committee:

Yong Chen, Professor, School of Marine Sciences, Advisor

David E. Hiebeler, Professor, Department of Mathematics and Statistics

James N. Ianelli, Senior Research Scientist, NOAA

Joshua S. Stoll, Assistant Professor, School of Marine Sciences

Walt Golet, Assistant Professor, School of Marine Sciences

UNCERTAINTIES AND ROBUSTNESS IN FISHERIES STOCK ASSESSMENT AND MANAGEMENT: DATA PROCESSING, MODELING AND SOCIOECONOMIC ASPECTS

By Luoliang Xu

Dissertation Adviser: Dr. Yong Chen

An Abstract of the Dissertation Presented
in Partial Fulfillment of the Requirements for the
Degree of Doctor of Philosophy
(in Ecology and Environmental Sciences)
December 2020

The main uncertainties that affect the quality of fisheries stock assessment and pose great challenges to fisheries management can stem from a wide range of sources including observation errors associated with model input data, dynamic model process errors, model structure misspecifications, and/or volatile fishery-related socioeconomic environment. Many assessment and management failures are attributed to inappropriate consideration of different uncertainties.

Using simulations or case studies, this project aims to evaluate the performance of existing approaches (including estimators, data processing methods, management strategies) when confronting uncertainties from different sources and develop new approaches that can better quantify the level of, or are more robust to the key uncertainties.

This study shows that using robust distributions in the likelihood function can locate outliers caused by atypical observation error in biomass index data. The advantage of the state-space production model over the observation-error-estimator diminishes with increased model

specification errors. Using multiple time series instead of one time series of biomass index as model inputs can substantially improve the performance of state-space production models and especially improves the accuracy of the error estimates. A new indicator (i.e., $B_{highest\_S}$: the biomass at which surplus production is at its highest) is proposed for identifying stock status when only biomass and catch data are available. Understanding the reason for the fluctuation of American lobster price suggests that providing resources gradually through the extent of price recovery rather than large and immediate injections of resources may be more efficient for fishing sectors experiencing crises.

This study provides several approaches that can better quantify or are more robust to the uncertainties commonly seen in fisheries stock assessment. While the results of the simulations and case studies are produced approximating conditions for the particular stocks (jumbo flying squid, pacific saury, American lobster), the findings regarding the uncertainty issues are relevant to many stocks that have the similar characteristics. This study evaluates error estimation in state-space production models in considerably more depth than previous studies. The recommendations made in this study can help address uncertainties in stock assessment and management.

ACKNOWLEDGEMENTS

I was born in a small town of an inland province in China. I have been beyond fortunate in my life to have the opportunity to study abroad. I would like to thank my advisor, Yong Chen, for taking me as a doctoral student and for providing me with opportunities to learn and grow. His steadfast support throughout my program have been invaluable over the years. I thank my committee members, David E. Hiebeler, James N. Ianelli, Joshua S. Stoll, Walt Golet, for their guidance and support. Chen lab members helped me from start to end. Specifically, this work would not have run as smoothly without Kisei Tanaka, Bai Li, Cameron Hodgdon, and Mackenzie Mazur. I thank Xinjun Chen in Shanghai Ocean University for encouraging me to take on challenges at the very beginning of my research when I was an undergraduate. I would like to thank University of Maine and Shanghai Ocean University for providing me with generous financial support throughout my study. Finally, I want to thank my wife Mingming Zou and my families, who have always supported me.

CONTENTS

LIST OF TABLES

LIST OF FIGURES

CHAPTER 1

INTRODUCTION

It is widely accepted that the fundamental objective of fisheries management is to ensure sustainable production from fish stocks, thereby promoting the long-term economic and social well-being of the fishermen and industries that use the production (Hilborn and Walters, 1992). To achieve this goal, a collection of management measures on fishing activities should be designed and enforced (Haddon, 2011). Fishery stock assessment is a process to develop scientific advice for fishery management. A complete stock assessment framework often consists of the processes of data collection; stock assessment modeling; fisheries parameters and biological reference points estimation; stock status identification; and development and evaluation of management strategies (Hilborn and Walters, 1992).

Uncertainty pervades in different components of fisheries stock assessment and management (Fulton et al., 2011; Magnusson et al., 2013). Many management failures are in part attributed to inappropriate consideration of different uncertainties (Hilborn and Walters, 1992). It is therefore crucial to explicitly deal with the key uncertainties that affect the quality of fisheries stock assessment and pose great challenges to fisheries management.

Several studies have been carried out to categorize different types of sources of uncertainties (Francis and Shotton, 1997; Haddon, 2011; Punt et al., 2014). In this study, four key uncertainties including observation error, process error, model error, and socioeconomic uncertainty are discussed. Observation error refers to the difference between the observed value and the true value. It arises in the process of data collection, usually through measurement and sampling error. Model error (or so-called model mismatch or model misspecification) and process error are both associated with the model that describes the population dynamics of

fisheries through mathematical functions in stock assessment. A model error occurs when the function form of the dynamic model mismatches the true population dynamic process; for example, misusing asymptotic function to model the fishery selectivity while the real relationship is dome-shaped (Hordyk et al., 2019). The model error can be reduced through a more accurate and deeper understanding of the fishery. The process error refers to the random variations associated with the dynamic model. It reflects the internal stochasticity of a fishery system and can not be reduced by improving knowledge. The process error is usually described as an added random effect on top of a deterministic model (de Valpine, 2002; Punt, 2003; de Valpine and Hilborn, 2005). The socioeconomic uncertainties in this study refer to the abnormal socioeconomic events that affect the prosperity of the fishery industry and the well-being of the fishermen.

For many traditional stock assessment models, the observation error is the only source of uncertainty that modelers explicitly deal with. The observation error is usually assumed to be random and the objective functions are formulated by the corresponding distributions (e.g., log-normal distribution for biomass index data; multinomial distribution for size composition data). However, the distributional assumption regarding observation error is often violated by the fact that outliers caused by atypical observation error frequently occur in fishery data (Chen, 2003). Robust distributions have been applied in both frequentist and Bayesian fish stock assessment models to overcome the sensitivity to outliers (Chen et al., 2003; Methot and Wetzel, 2013). Parameter estimates derived from robust distributions are more accurate than those from normal distributions when outliers exist in the biomass index data (Chen et al., 2003). Previous studies, however, have not attempted to locate outliers. Locating outliers enables us to further analyze the

particular reasons for the emergence of outliers. In chapter 2, a simulation is conducted to test the performance of a robust distribution for identifying outliers in biomass index data.

The assumption that the observation error is the only source of uncertainty in modeling is challenged by advocators of state-space models. State-space models can simultaneously account for both observation and process errors (de Valpine and Hilborn, 2005). Although previous simulation studies have shown the state-space model outperformed the observation-error-estimator in various cases (de Valpine, 2002; Punt, 2003; Ono et al., 2012), it is still unclear how the performance of the two estimators is affected when there are model misspecifications. Chapter 3 explores the role of model errors in determining the performance of the two estimators using simulation. The Pella-Tomlinson model with different values for the shape parameter is used as the operating model and the Schaefer model is used as the assessment model. The objective of this chapter is to evaluate the performance of two estimators under different levels of model, process and observation errors.

Despite the fact that the state-space models are advertised as providing the means to differentiate process error from observation error, the estimates of the two errors tend to be biased (Auger-Méthé et al., 2016). How to improve the accuracy of error estimates remains a major question for state-space models. In chapter 4, a simulation study is conducted to demonstrate that the routine survey data processing approach of aggregating all observations into a single annual biomass index undermines state-space models' ability to distinguish between process error and observation error. Using multiple time series of biomass index as model inputs substantially improves the performance of state-space models and especially improves the accuracy of the error estimates. Without additional sampling efforts, appropriately adjusting the

protocol of processing survey data can gain considerable benefits when state-space models are used for fishery stock assessment.

Data-limited methods (DLM) coupled with empirical harvest strategies, considered as an alternative to the stock assessment modeling approach, have been drawing extensive attention in recent decades (Sun et al., 2018; Carruthers and Hordyk, 2018). However, more research is needed to better understand the robustness of certain DLMs and empirical harvest strategies to key uncertainties. In chapter 5, two simulations are conducted to compare a suite of surplus-production-based DLMs and corresponding harvest strategies. The first simulation is to evaluate the performance of the production modeling approaches and indicator-based DLMs on identifying stock status when only biomass and catch data are available. The simulation results show that the newly proposed indicator (i.e., $B_{highest\_S}$: the biomass at which surplus production is at its highest) is more robust to observation errors or model misspecification than the modeling approach for stock status identification. In the second simulation, the management procedure that incorporates $B_{highest\_S}$ in the harvest control rule is evaluated based on age-structured population dynamics models parameterized by the outputs of ten fisheries stock assessments.

A biologically sustainable fishery is not warranted to be immune to socioeconomic uncertainties that may impair the wellbeing of fishermen. The exceptional slow price recovery of the American lobster in the wake of socioeconomic shocks is a living example. Chapter 6 uses an inflation-adjusted simple moving average analysis of the monthly ex-vessel price of American lobster in tandem with a content analysis of more than 6,000 newspaper articles about lobster to systematically analyze the recovery process following socioeconomic shocks of different magnitude over a 25-year time frame from 1995 to early 2020. Results show that recovery duration ranges from 23 months to more than 12 years and the process can be stalled by

compounding local and regional disturbances. Understanding recovery dynamics in food production systems following global crises and that full recovery can take more than a decade is critical to framing effective response strategies in the aftermath of crises. Analyzing the socioeconomic shocks in history provides insights on how to help the fishery industry confront future uncertainties.

In a nutshell, my dissertation aims to evaluate the performance of existing approaches (including estimators, data processing methods, management strategies) when confronting uncertainties from different sources and develop new approaches that can better quantify the level of, or are more robust to the key uncertainties in stock assessment and management. The recommendations made in this study can help address certain uncertainties in stock assessment and management.

CHAPTER 2

IMPROVING THE ROBUSTNESS OF FISHERIES STOCK ASSESSMENT MODELS TO OUTLIERS IN INPUT DATA

2.1 Introduction

The development of an optimal management strategy for a fishery requires a good understanding of population dynamics (e.g., growth, mortality, maturity, reproduction) and the status (e.g., overfishing, overfished) of the fish stock (Hilborn and Walters, 1992; Chen et al., 2003). This is usually obtained through quantitative modelling (Quinn and Deriso,1999); therefore, reliable estimation of the model parameters and biological reference points (BRPs), which are subject to input data quality, is essential to fisheries stock assessment and management (Chen and Fournier, 1999; Chen et al., 2000).

The data quality can be measured by observation error, which is the difference between the observed value and the true value. Observation error may arise from different sources and in general can be divided into three components according to different statistical properties: random errors, systematic errors and atypical errors (Barnett and Lewis, 1994; Chen, 2003). Random error causes unbiased data to fluctuate around the true value. In fishery stock assessment models, the observation error is usually assumed random and the objective functions are formulated by the corresponding distributions (e.g., log-normal distribution for biomass index data; multinomial distribution for size composition data). Systematic error causes data to consistently deviate in one direction from the true value. Systematic error can be potentially detected by analyzing the non-random patterns in model residuals. For example, the continual overestimation of biomass over a given period may be reflected in the routine model diagnostics, in which positive residuals cluster in corresponding years. Atypical errors refer to the errors only affecting a small portion of the data set, in which the statistical properties of the error are significantly

different from errors occurring in other data points (Chen and Fournier, 1999). Some unusual events in the data collection process, such as a substantial reduction in the sample size for a certain year, may lead to atypical error.

The data contaminated by atypical error may contain outliers. The outliers caused by atypical error are best eliminated because the erroneous data do not represent the realistic process under study, and outliers often have a great and adverse impact on the accuracy of model outputs (Barnett and Lewis, 1994). However, outliers emerged in data sets are not necessarily the result of observational errors and caution should be exercised when dealing with them. Some abnormal environment events (so-called "black swan") lead to the emergence of outliers that often contribute to a comprehensive understanding of population dynamics of the species (Hinrichsen, 2011; Anderson et al., 2017). Other outliers are due to the mismatch between the model and the realistic fishery dynamics, where the so called "outliers" are actually accurate but the model predictions are significantly biased. The outliers from different sources require different treatments. Thus, understanding the nature of an outlier by carefully checking the background information regarding how the data are collected, model configurations and abnormal environmental variations is important. Nevertheless, locating the outliers in a data set is the preliminary step.

Many formal statistical methods have been developed to detect outliers, of which the use of robust distribution is the most common (Hampel et al., 1986; Rousseeuw and Leroy, 1987; Motulsky and Brown, 2006). The virtue of using robust distribution is that the model fits remain unbiased when a certain amount of data is contaminated by atypical error. Therefore, the outliers far away from the robust fits can be detected by their large residuals, whereas the residuals from non-robust distribution estimators (e.g. normal distribution) may not expose outliers due to the

biased model fits. Robust distributions have been applied in both frequentist and Bayesian fish stock assessment models to overcome the sensitivity to outliers (Chen et al., 2003; Methot and Wetzel, 2013). Previous studies, however, have not evaluated whether removing detected outliers in fishery data using robust distribution would improve the model performance.

Herein, a simulation study was conducted in which a surplus production model was used to mimic the fishery population dynamics and the outliers caused by atypical error were imposed in the biomass index data. The observation error was assumed to follow a robust distribution and the data points that deviate significantly far away from the corresponding model predictions were defined as outliers. We then removed the defined outliers and fit the model to the remaining data points, assuming the observation error follows the normal distribution. We raised two questions specifically for a typical fishery stock assessment model: (1) Can the outliers be correctly detected using robust distribution; and (2) Does deleting the detected error-induced outliers improve the accuracy of parameter estimation.

2.2 Materials and Methods

2.2.1 A robust distribution and pre-specified threshold for outlier identification

A number of robust distribution functions, which are otherwise similar to normal distributions except for the heavier tails, have been developed to deal with the outlier problem in model fitting (Chen et al., 2003; Methot and Wetzel, 2013). In this study, the normal distribution function was modified by adding a parameter (θ) to serve the purpose of being robust to outliers (Fig. 2.1). This modified normal distribution function can be described as follows:

$$f(x) = \frac{1}{\sqrt{2\pi}\sigma}(e^{-\frac{x^2}{2\sigma^2}} + \theta) \quad (2.1)$$

where x represents the residuals; σ is the standard deviation of the residuals; and θ is a parameter used to adjust the tail of the distribution. Both σ and θ are estimable parameters. However, θ is often a pre-specified small fixed value (0.01 here; Fournier, 1996; Andrew, 1999).

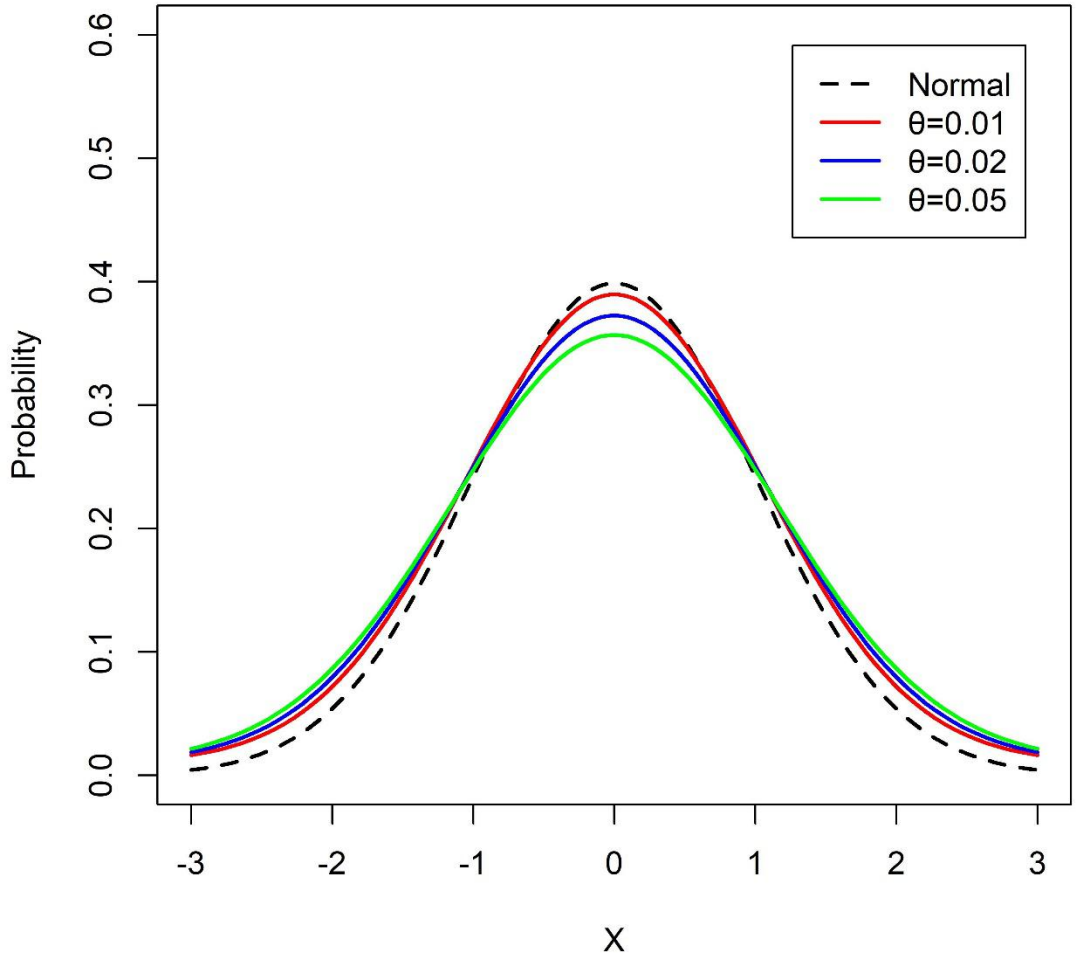

Figure 2.1. Normal distribution and robust distributions.

A threshold is needed for determining whether a data point is far enough from the model prediction to be defined as an outlier. To this end, a normal distribution with a mean zero and a standard deviation the same as the standard deviation estimate of the observation error in the

robust distribution was used to measure the probability of the emergence of each residual. The data points of which the corresponding residuals fall out of the range of 1% to 99% of the probability density function of the normal distribution are defined as outliers in this simulation study.

2.2.2 Simulation study

For simplicity in model structures, we chose the Schaefer production model to describe the population dynamics. The model is written as:

$$B_{y+1} = B_y + rB_y(1 - \frac{B_y}{k}) - C_y \qquad (2.2)$$

$$\log\left(I_y\right) = \log\left(qB_y\right) + \varepsilon_y \qquad (2.3)$$

where B_y is the biomass in year y; C_y is the catch in year y; q is the catchability coefficient; I_y is the index of biomass in year y; r is the intrinsic growth rate; k is the environmental carrying capacity; and ε_y is the observation error which is assumed to follow a robust distribution or normal distribution.

The BRPs, maximum sustainable yield (*MSY*) and exploitation rate which leads to *MSY* (*Emsy*) can be calculated as:

$$MSY = \frac{rk}{4} \qquad (2.4)$$

$$E_{msy} = \frac{r}{2} \qquad (2.5)$$

The maximum likelihood estimation method was used to estimate the model parameters. The objective functions for normal distribution and robust distribution were respectively written as follows:

$$\mathrm{L}(\varepsilon,r,k,q|I_y) = \prod_y \left(\frac{1}{\sigma_n I_y\sqrt{2\pi}} e^{-\frac{(lnI_y - \ln(qB_y))^2}{2\sigma_n^2}}\right) \quad (2.6)$$

$$\mathrm{L}(\varepsilon,r,k,q|I_y) = \prod_y \left(\frac{1}{\sigma_n I_y\sqrt{2\pi}} e^{-\frac{(lnI_y - \ln(qB_y))^2}{2\sigma_n^2}} + 0.01\right) \quad (2.7)$$

The values of the parameters were set based on the results of a stock assessment for jumbo flying squid in the Southeast Pacific Ocean (Xu et al., 2019). We parameterized the operating model such that k=11.62 million tons, r=0.64 year^{-1} and q=0.006 (day*vessel)$^{-1}$. The initial biomass was set to equal to k.

Two catch histories, which represent informative and non-informative input data, were simulated for 45 years. The two types of catch histories were used to assess whether the effectiveness of the outlier detection method relied on volume of information contained in the input data. The informative catch history was simulated to manipulate the biomass to decrease below *Bmsy* followed by a recovery to status over *Bmsy* to generate good contrast in biomass index and fishing effort. The other catch history led to a decline in biomass from k to *Bmsy* ("one-way trip"), which created relatively uninformative input data for the surplus production model (Fig. 2.2).

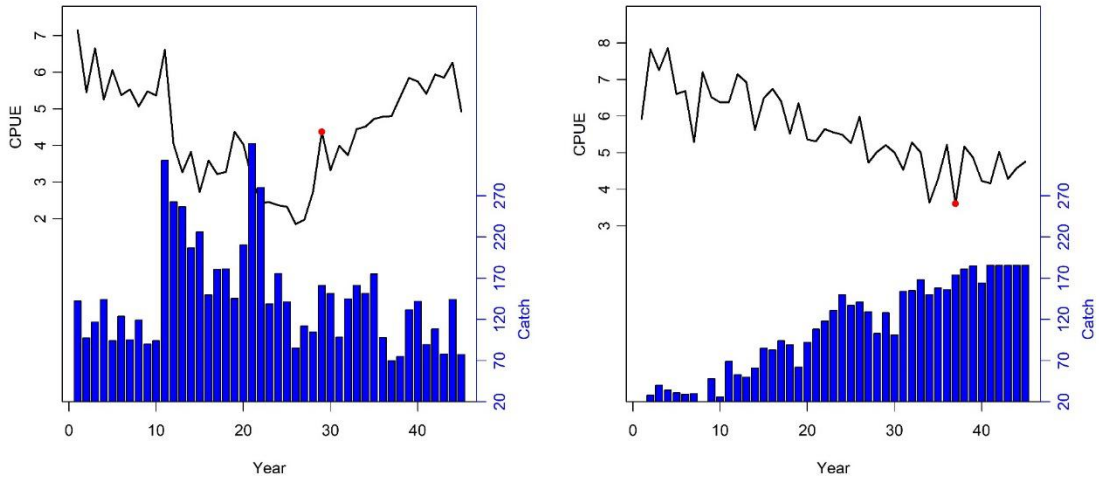

Figure 2.2. Simulated CPUE data when the standard deviation of random error is 0.1. The left and right figures represent informative and uninformative data, respectively. The red points are the outliers.

Four levels of random observation errors (σ = 0.1, 0.15, 0.20 and 0.25) were simulated to represent different data collecting processes. Usually, the random observation errors of fishery-dependent data tend to be greater than that from a well-designed survey program. The process and model errors associated with the dynamics model were assumed to be absent.

The outliers were randomly placed in the time series of the biomass index data. The difference between the outliers and the true values were 0.1% or 99.9% quantile of a normal distribution with zero mean and a variance equal to the corresponding variance of the random observation error (σ_ε). Although the difference between the outliers and the true values seems to be large, which is actually a key characteristic of outliers, determining outliers by observing the plot of biomass index against time is still impossible (Fig. 2.2). We assumed that the number of outliers was from one to four in different scenarios with the maximum proportion of outliers less than 10% of the total time series of data. For each of the scenarios (different number of outliers and different random observation errors), the experiment was repeated 1000 times.

2.2.3 Evaluation of the performance of the method

The method validation involves two criteria. Primarily, the robust distribution should have the ability to discover the true outliers and avoid mistakenly identifying “good” data points as outliers. In addition, the parameter estimates of the stock assessment model should be more accurate by deleting the detected outliers.

2.2.3.1 False discovery rate and correct discovery rate

Two metrics were used to evaluate the ability of the robust distribution in outlier detection. The false discovery rate (FDR) was defined as the ratio of the number of mistakenly identified outliers over the number of identified outliers. The correct discovery rate (CDR) was defined as the ratio of the number of correctly identified outliers over the total number of true outliers. A low FDR indicates that the proposed robust distribution can avoid identifying "good" data points as outliers whereas a high CDR indicates that the method can discover the true outliers.

2.2.3.2 The parameter estimates of the fishery stock assessment model

For each simulation trial, the parameters and BRPs, including *r*, *k*, *q*, *MSY*, and *E_msy* were estimated by using the data with and without the detected outliers. The estimates of the parameters and BRPs were then compared with the corresponding true values. Two metrics, median relative error (MRE) and median absolute relative error (MARE), were calculated to indicate the accuracy of the parameter estimates. The two performance metrics are described as follows:

$$\text{MRE} = \text{median}\left(\frac{\theta_{est}-\theta_{true}}{\theta_{true}}\right) \qquad (2.8)$$

$$\text{MARE} = \text{median}\left|\frac{\theta_{est}-\theta_{true}}{\theta_{true}}\right| \qquad (2.9)$$

where θ_{est} and θ_{true} denote the parameter estimates and true values, respectively. Both MRE and MARE quantify the bias of the parameter estimates. MRE provides information on bias direction whereas MARE is always positive and monotonically increases as the bias level elevates. A general linear model (GLM) was used to fit the logarithms of MARE. The number of outliers, the levels of random observation error, the model parameters and BRPs, and the types of input data (i.e., informative or not) were treated as independent variables in the GLM and the

coefficients associated with them represented the magnitude of impact on the bias of estimates by different variables.

2.3. Results

2.3.1 False discovery rate and correct discovery rate

With informative input data, the proposed robust distribution performs well in both identifying the true outliers and avoiding erroneously defining "good" data points as outliers (Fig. 2.3). The method successfully discovered all the outliers in 42.5% of the simulation trials. In more than 70% of the simulation trials, the method discovered at least half of the total outliers. Also, the FDR was zero in 71.5% of the simulation trials. Only in 3.7% of the simulation trials, all the detected outliers were actually "good" data points. Similar results were found in the scenarios with uninformative input data (Fig. S2.1 in appendix). The corresponding FDR and CDR with respect to different numbers of outliers were included in the appendix (Fig. S2.2 ~S2.5).

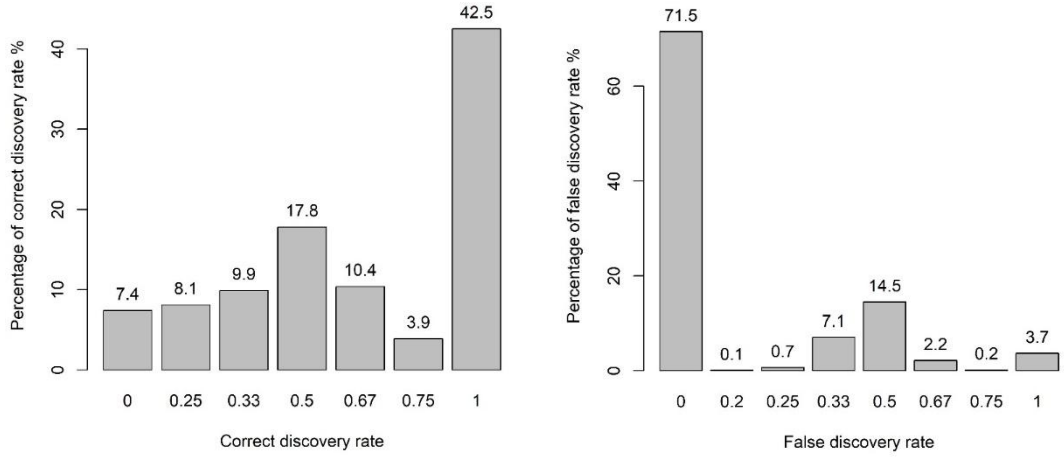

Figure 2.3. The percentage of different levels of correct discovery rate (CDR) (left) and false discovery rate (FDR) (right) of the proposed method when the input data are informative.

2.3.2 Parameter estimation of the fishery stock assessment model

In the GLM for MARE, the coefficient of the proposed method (i.e., deleting the detected outliers) was negative, suggesting that the parameters and BRPs estimated by data without detected outliers were less biased than those estimated by the whole dataset (Table 2.1). Unsurprisingly, the coefficient of the uninformative input data in the GLM was positive, meaning that the uninformative data will lead to more biased parameter estimation. The median of MRE estimates from the proposed method was closer to zero than that estimated by the whole dataset. The parameter estimation by the proposed method was robust to the number of outliers originally existing in the dataset. In contrast, the accuracy of estimating parameters using the entire dataset was sensitive to the number of outliers (Fig. 2.4).

Table 2.1. Summarized statistics of the linear model.

Dependent variable log(MARE)	Estimate	Std. Error	P Value
Intercept	-3.315	0.041	0.000
Continuous variables			
Observation error (σε)	4.559	0.154	0.000
Number of outliers	0.060	0.008	0.000
factor(parameters & BRPs)			
K	-0.136	0.030	0.000

MSY	-1.923	0.030	0.000
q	-0.066	0.030	0.027
r	0.000	0.030	1.000
factor(model type)			
Proposed method	-0.119	0.017	0.000
factor(data type)			
Uninformative data	2.101	0.017	0.000

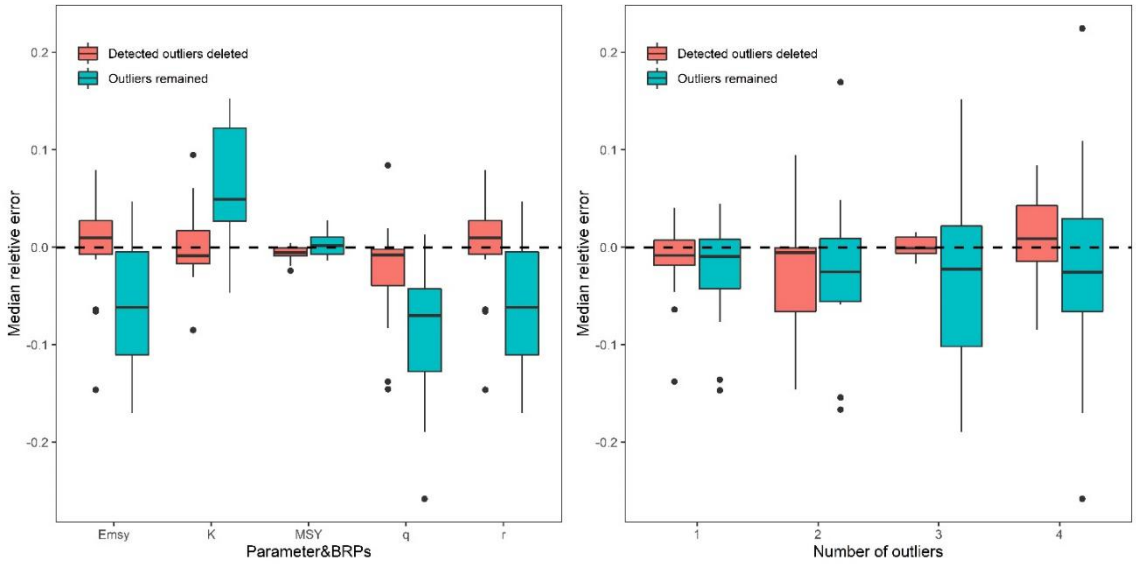

Figure 2.4. MREs (median relative errors) of parameters and biological reference points (BRPs) estimated with and without detected outliers for the informative input data. The results are grouped by parameters and BRPs (left), and the number of outliers (right).

2.4. Discussion

We demonstrated that the outliers caused by atypical observation error in the biomass index data can be identified by evaluating residuals in a robust-distribution-based estimator for surplus production models. By removing the detected outliers in biomass index data, though in some cases there are still undetected outliers in the data or some good data points are removed, the

performance in parameter estimation is generally improved. The biomass index data have been widely used as an input in different stock assessment models. We suggest that this method can potentially be used to provide a higher-quality input for more sophisticated stock assessment models (e.g., ASAP, SAM, SS3) other than surplus production models.

Many distributions with larger tails than the normal distribution can be used to formulate robust likelihood functions. The robust distribution used in this study is flexible and conceptually easy to understand. The parameter θ is used to adjust the size of the tail of the distribution, and pre-specified value 0.01 is appropriate for this simulation study according to some preliminary tests. The parameter θ may also be estimated along with all the other parameters in the model. In theory, the number of outliers and their degree of deviation from the true value can inform the parameter θ. In most of the practical cases, however, fishery data is hardly so informative to provide an appropriate estimate for θ. Another essential step is to define an appropriate threshold to determine the range of non-outliers; overly narrow ranges will cause some data points mistakenly to be defined as outliers and overly wide range tends to lose the sensitivity to the true outliers. In practice, the threshold could be tuned based on the total number of data points and the quality of the data collection process.

Whether a data point will be detected as an outlier by its large residual also depends on the choice of the model. An outlier identified in biomass index data for a production model may be well accommodated in an age-structured model when the fluctuation of annual recruitment is incorporated. In such case, the outliers are caused by the violation of assumptions of the simplified model (or so called “model error”) instead of observation error. It is important to understand whether the “error” is associated with the data points or the model structure before

we treat outliers. At all events, the emergence of outliers is a sign that the model results may be biased.

Using a robust distribution assumption could potentially identify the outliers for other types of input data of fishery stock assessment models. For example, Fournier et al (1990) proposed a robust distribution for length composition data. The robust distribution was found to be less sensitive to the outliers than the more commonly used multinomial distribution in parameter estimation. It is possible, therefore, that by using a proper robust distribution, the outliers in the length composition data could be identified. There is abundant room for further progress in developing and testing robust distributions suitable for identifying outliers in different types of input data for fisheries stock assessment models.

CHAPTER 3

A COMPARATIVE STUDY OF OBSERVATION-ERROR ESTIMATORS AND STATE-SPACE PRODUCTION MODELS IN FISHERIES ASSESSMENT AND MANAGEMENT

3.1. Introduction

Surplus production models can provide management advice in data limited situations (Hilborn and Walters, 1992; Punt, 2003). Using a time-series of catch and an index of relative abundance, a surplus production model can estimate biological reference points (BRPs) and infer unknown current and historical stock biomass (Schaefer, 1954; Schaefer, 1957; Hilborn and Walters, 1992).

The approach to fitting production models to observed data varies, for example, assuming errors in the abundance index or the dynamic model or both. Only one of the two error sources was considered historically due to computation limits (Chen and Andrew, 1998). Simulation studies have shown that a model with observation error (i.e., an observation-error estimator) performed better than a model with only process error (i.e., a process-error estimator; Polacheck et al., 1993; Chen and Andrew, 1998; Ono et al., 2012). Here, we test an observation-error estimator against a state-space model approach.

State-space production models can simultaneously account for both observation and process errors. Explicit incorporation of both errors in state-space production models complicates the process of estimating parameters compared with observation-error estimators. Methods for estimating parameters in state-space production models are numerous, e.g.: the errors-in-variables (EV) method (de Valpine and Hilborn, 2005), the extended Kalman filter (Reed, 1986; Kimura et al., 1996), the numerical integration state-space (NISS) approach (de Valpine and Hastings, 2002), the Monte Carlo Kernel Likelihoods (MCKL) method (de Valpine, 2004) and

the Bayesian approach (Ono et al., 2012). Some of these methods treat the unknown biomass states as random variables while others treat them as as fixed parameters. The methods (e.g., EV) that treat the biomass states as fixed parameters were originally thought to be an improvement over simply assuming the absence of either process or observation errors (Ludwig and Walters, 1981). However, they were criticized due to their systematic estimation bias (de Valpine and Hilborn, 2005). In this study, we treated biomass states as random variables and adhered to maximum likelihood for parameter estimation.

Previous simulation studies have shown the state-space model, which can match the assumed error structure in operating models that consider observation and process error, outperformed the observation-error estimator (de Valpine, 2002; Punt, 2003; de Valpine and Hilborn, 2005; Ono et al., 2012). We therefore explored the role of model errors in determining the performance of the two estimators using simulation. The Pella-Tomlinson model with different values for the shape parameter was used as the operating model and the Schaefer model was used as the assessment model. The goal of this study was to compare the performances of two estimators under different types and levels of errors.

The following hypotheses were developed; (1) the state-space model will outperform the observation-error estimator when confronted with process, observation and model errors, (2) the state-space model may outperform the observation-error estimator when the model error is small, but the advantage of the state-space model may diminish as the level of model error increases, and (3) the observation-error estimator may outperform the state-space model when the level of model error increases to a certain point.

3.2. Materials and Methods

3.2.1 Schaefer model and Pella-Tomlinson model

Following Schaefer (1954), the surplus production model can be formulated as:

$$B_{y+1} = \left(B_y + rB_y(1 - \frac{B_y}{k}) - C_y\right) e^{\varepsilon_y} \quad (3.1)$$

$$I_y = qB_y e^{\eta_y} \quad (3.2)$$

where B_y is the biomass in year y; C_y is the catch in year y; q is the catchability coefficient; I_y is the index of biomass in year y; ε_y and η_y are respectively process and observation errors, assumed to follow the normal distribution, i.e., $\varepsilon_y \sim N(-\frac{\sigma_\varepsilon}{2}, \sigma_\varepsilon^2)$; $\eta_y \sim N(-\frac{\sigma_\eta}{2}, \sigma_\eta^2)$; σ_ε^2 and σ_η^2 are respectively the variances of the process and observation errors; $-\frac{\sigma_\varepsilon}{2}$ and $-\frac{\sigma_\eta}{2}$ are bias-correction terms for the lognormal distributions; r is the intrinsic growth rate; and k is the environmental carrying capacity.

The Pella-Tomlinson population dynamic model can be written as follows:

$$B_{y+1} = \left(B_y + \frac{r}{s}B_y(1 - (\frac{B_y}{k})^s) - C_y\right) e^{\varepsilon_y} \quad (3.3)$$

where the shape parameter s relaxes the assumption of symmetric surplus production curve. Other parameters are the same as in equation 3.1.

3.2.2 Simulation scenarios

Thirteen levels of model error (*Bmsy*/*k* from 0.2 to 0.8 in steps of 0.05, with the shape parameter for each *Bmsy*/*k* then calculated), four levels of observation error (σ_ε = 0.1, 0.15, 0.20 and 0.25), and four levels of process error (σ_η = 0.05, 0.1, 0.15 and 0.20) were used to develop 208 scenarios. The levels of model error were based on the ratio of *Bmsy*/*k* for 149 marine

species (Thorson et al., 2012). The lowest process and observation errors represented the scenario where the models performed well when the assumed population function matched the true data-generating process. The upper error limit was set because higher levels of errors did not allow an accurate estimate of model scale (i.e., q and k) for surplus production models, even when the models were correctly specified (Thorson et al., 2014).

The simulation study was designed to evaluate the impact of various errors on model performance by allowing the biases of estimates to only stem from errors and not from uninformative input data. Catch history was therefore simulated for 45 years. The simulated catches allowed the biomass to decrease below *Bmsy* followed by a recovery to a status over *Bmsy* in a deterministic version of the model to generate good contrast in CPUE and effort (Fig. S3.1). The simulated fishery consists of data points at high stock size with low fishing effort (years 1~10; to inform $k*q$), low stock size with low fishing effort (years 25~30; to inform r) and high fishing effort (years 10~20; to inform q; Hilborn and Walters, 1992).

The values for the parameters were set based on the results of a stock assessment for jumbo flying squid in the Southeast Pacific Ocean (SPRFMO, 2017). The operating models were parameterized such that k=11.62 million tons, r=0.64 $year^{-1}$ and q=0.006 $(day*vessel)^{-1}$. The initial biomass for each simulation trial was sampled from a lognormal distribution with a median k and a variance that was the same as the corresponding process error. The data generation procedure was repeated 500 times for each scenario.

3.2.3 Parameters estimation

The observation-error estimator and the state-space Schaefer model were used as assessment models to estimate the parameters and calculate the BRPs (*MSY*, *E_msy* and

Yield_Emsy – the estimate of terminal biomass multiplied by *E_msy*). For the observation-error estimator, the likelihood function was as follows:

$$\mathrm{L}\left(\sigma_{\eta},r,k,q,B_0\middle|I_y\right)=\prod_y\left(\frac{1}{\sigma_{\eta}I_y\sqrt{2\pi}}e^{-\frac{(lnI_y-\ln(qB_y))^2}{2\sigma_{\eta}^2}}\right) \quad (3.4)$$

For the state-space model, the likelihood function was as follows:

$$\mathrm{L}\left(\sigma_{\eta},\sigma_{\varepsilon},r,k,q,B_y\middle|I_y\right)=\int\prod_y\left(\frac{1}{\sigma_{\eta}I_y\sqrt{2\pi}}e^{-\frac{(lnI_y-\ln(qB_y))^2}{2\sigma_{\eta}^2}}\right)\mathrm{d}\varepsilon \quad (3.5)$$

The parameters were estimated by maximizing the likelihood function. This process was implemented using the R package "TMB" (Kristensen et al., 2016).

A Bayesian approach was avoided in this study because any seemingly "uninformative" priors might affect the parameter estimates (Thorson and Cope, 2017), which would inevitably influence the results of model performance comparison.

3.2.4 The convergence efficiency and parameter correlations of the two models

In TMB, the gradient descent algorithm is used to obtain the global minimum of an objective function formulated by parameters and/or random effects (Kristensen et al., 2016). The following three criteria were used to examine the model convergence: (1) the Hessian matrix is positive definite; (2) the maximum gradient is small (e.g., <0.0001); and (3) alternative parameter starting points result in the same final parameter estimates. Two combinations of values randomly selected from reasonable ranges were used as starting points for the parameters for each simulation trial (Table S3.1 in appendix). If the model did not attain the identical estimates for the parameters, that particular trial would be marked as a failure to obtain the global minimum and would not be used for further analysis. The correlations of the estimated parameters from the two estimators were evaluated by Pearson correlation coefficient.

3.2.5 Accuracy of the parameters and BRPs estimates from the two models

For each simulation, the parameters and BRPs (*r*, *k*, *q*, *MSY*, *E_msy* and *Yield_Emsy*) were estimated by the two models. The estimates of the parameters and BRPs were then compared with the corresponding true values. The model performance was evaluated using three metrics: the median relative error (MRE), median absolute relative error (MARE), and the percentage of parameters and BRPs that are estimated more accurately by the state-space model than by the observation-error estimator (P_S). The MRE, MARE and P_S were calculated as follows:

$$\text{MRE} = \text{median}\left(\frac{\theta_{est}-\theta_{true}}{\theta_{true}}\right) \quad (3.6)$$

$$\text{MARE} = \text{median}\left|\frac{\theta_{est}-\theta_{true}}{\theta_{true}}\right| \quad (3.7)$$

$$\text{P\_S} = \frac{\sum_i^n S_i}{N};\ S_i = 1 \text{ if ARE(s,ɵ)} < \text{ARE(o,ɵ)};\ S_i = 0 \text{ if ARE(s,ɵ)} \geq \text{ARE(o,ɵ)} \quad (3.8)$$

where θ_{est} and θ_{true} denote the estimates and true values of the parameters and BRPs, respectively. ARE(s,ɵ) and ARE(o,ɵ) denote the absolute relative errors of the estimates of a parameter or BRP, ɵ, by the state-space model and the observation-error estimator, respectively. *N* is the total number of parameters and BRPs over 500 simulations. MRE is the median of relative errors between estimates and true values across 500 simulations. A general linear model (GLM) was used to fit the logarithms of MARE. The three errors were treated as continuous variables and the coefficients associated with them represented the magnitude of impact on the bias of estimates (Punt and Szuwalski, 2012). P_S represents the advantage of the state-space production model over the observation-error estimator. The simulation study is summarized graphically in Fig. 3.1.

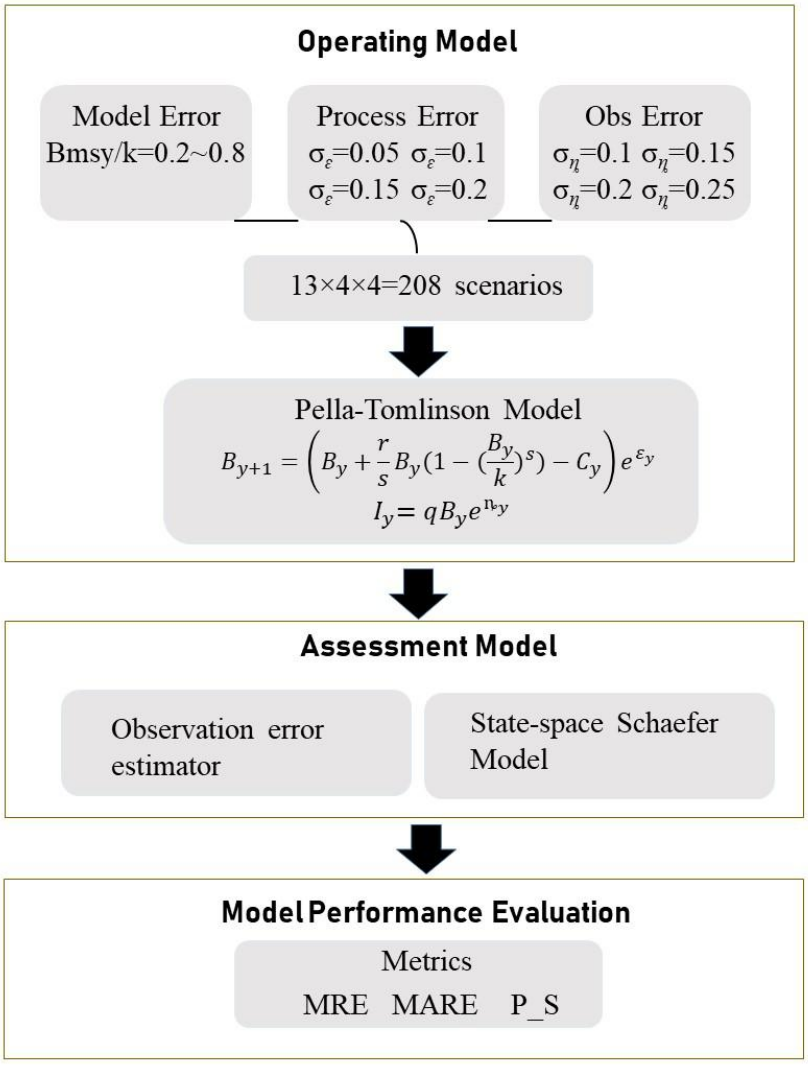

Figure 3.1. Flow chart of the simulation-estimation approach.

3.3. Results

3.3.1 Convergence efficiency and parameter correlations

Both models effectively found the global minimum of the objective function. More than 97% of the simulations led to the same parameter estimates with different starting points. The observation error estimator was slightly better than the state-space model in terms of locating the

global minimum of the objective function. For both the models, the percentages of simulation for which the global minimum was found had no impact on the level of model error (Fig. S3.2). The time that it took to fit the state-space production model was roughly thirty times that of the observation-error estimator.

The estimated standard deviations of process and observation errors from the state-space models shown high negative correlations (Fig. 3.2). From both estimators, the estimated r and q were negatively correlated with estimated k. However, the level of the negative correlation decreased with the true process and observation error (Fig. 3.2 and 3.3). These patterns were similar in different model error scenarios (Fig. S3.3~S3.14).

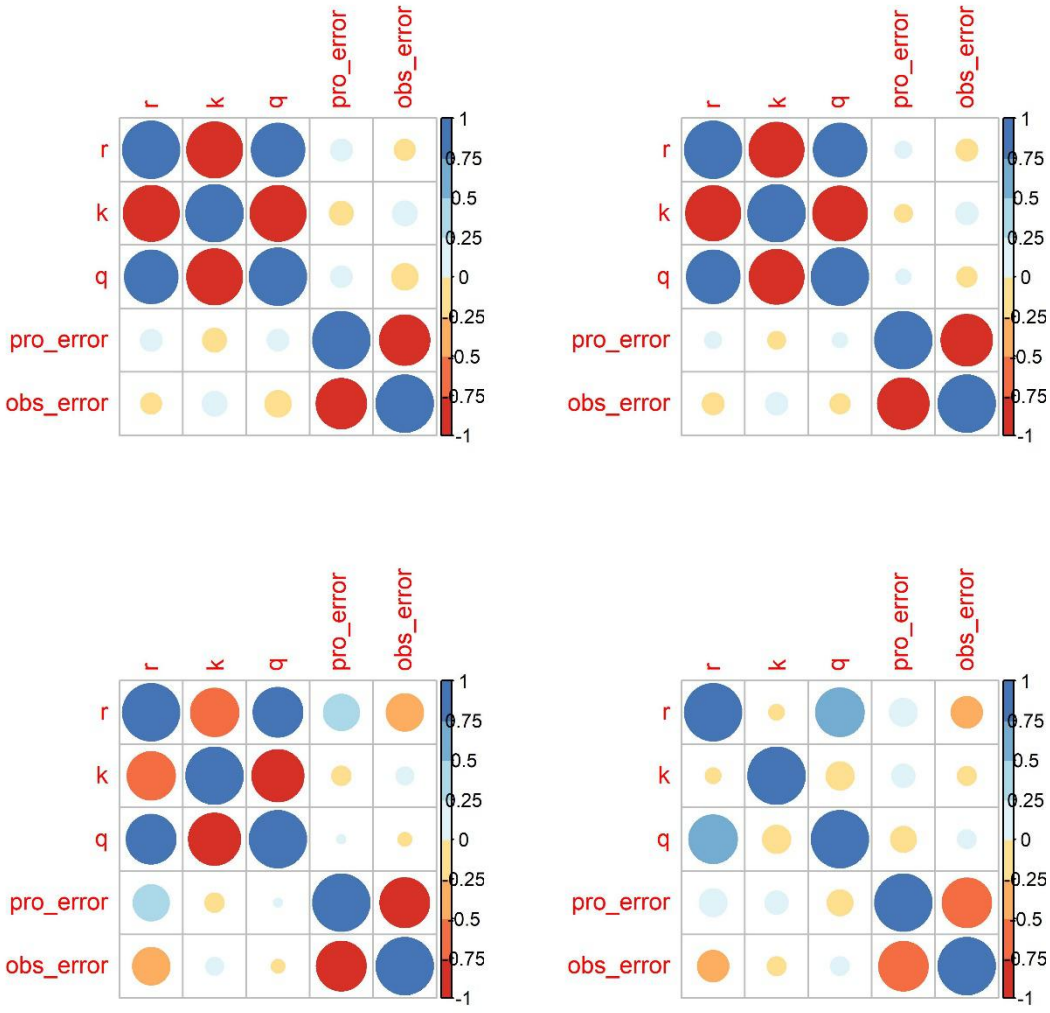

Figure 3.2. The Pearson correlation coefficients of estimated parameters from state-space models when there is no model error and the standard deviations of true process and observation errors are 0.05 (top-left), 0.1 (top-right), 0.15 (bottom-left), and 0.2 (bottom-right).

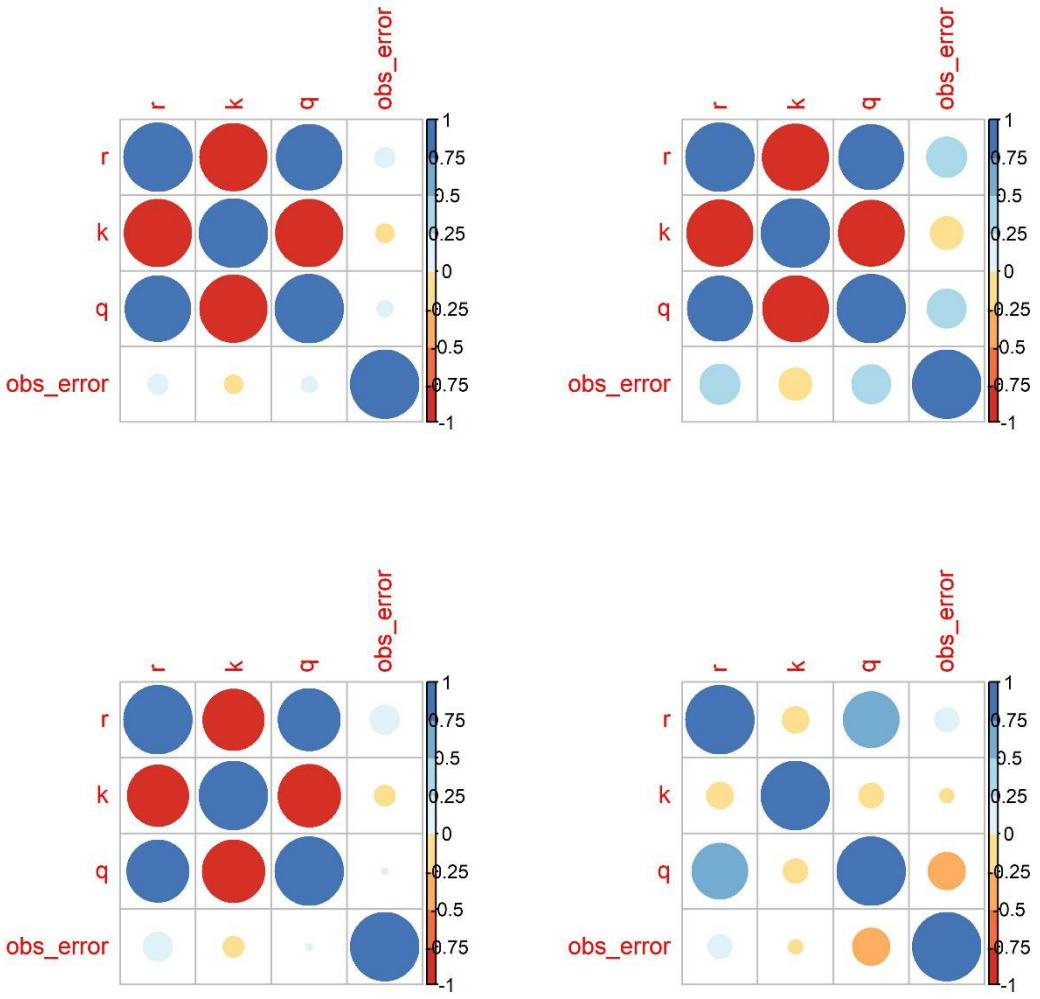

Figure 3.3. The Pearson correlation coefficients of estimated parameters from observation-error estimators when there is no model error the standard deviations of true process and observation errors are 0.05 (top-left), 0.1 (top-right), 0.15 (bottom-left), and 0.2 (bottom-right).

3.3.2 Hypothesis 1

The coefficient of the state-space production model in the GLM was negative, suggesting that overall, the estimates of the parameters and BRPs by the state-space production model were less biased than those of the observation-error estimator (Table. 3.1). The median of the MREs

from the state-space production model were closer to zero than those for the observation-error estimator (Fig. 3.4).

Table 3.1. Summarized statistics for the GLM analysis.

MARE	Estimate	Std. Error	P Value
Intercept	-2.645	0.038	0.000
Continuous variables			
Process error (ση)	5.993	0.149	0.000
Observation error (σε)	0.721	0.149	0.000
Model error (abs(s-1))	0.361	0.019	0.000
factor(Parameters&BRPs)			
k	-0.066	0.020	0.001
MSY	-1.250	0.020	0.000
q	-0.047	0.020	0.020
r	0.321	0.020	0.000
Yield_Emsy	-0.452	0.020	0.000
factor(Model type)			
State-space model	-0.105	0.051	0.041
interaction terms			
*State-space model*abs(s-1)*	-0.020	0.027	0.451
*State-space model*Observation error*	0.932	0.210	0.000
*State-space model*Process error*	-1.208	0.210	0.000

*the percentage of variance explained by the model is 81.5%; the levels of model error are represented by the absolute value of (s-1)

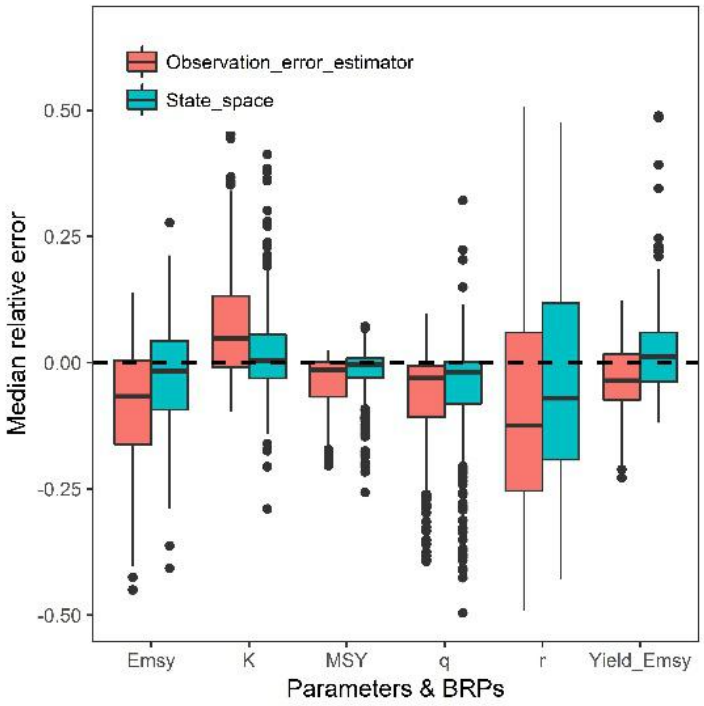
Observation_error_estimator
State_space
0.50
0.25
0.00
-0.25
-0.50
Median relative error
Emsy
K
MSY
q
r
Yield_Emsy
Parameters & BRPs

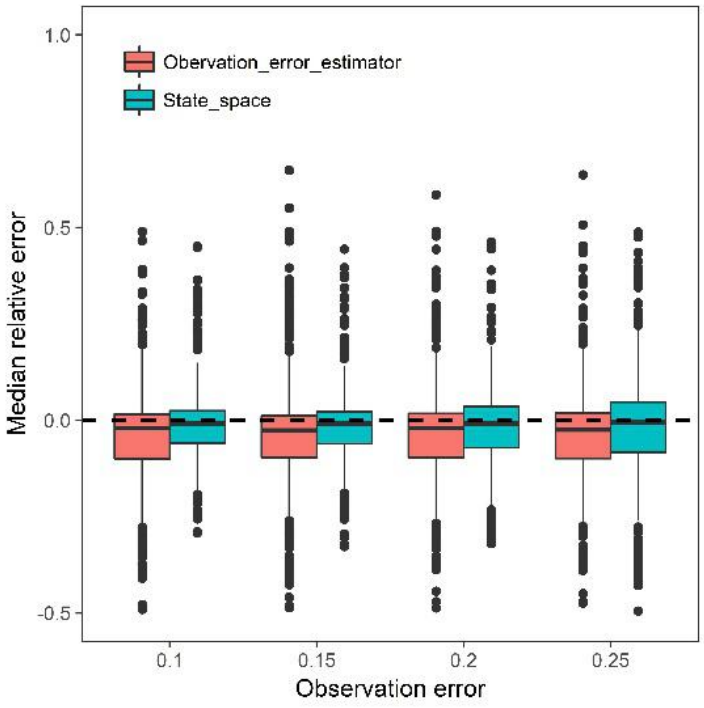
Obervation_error_estimator
State_space
1.0
0.5
0.0
-0.5
Median relative error
0.1
0.15
0.2
0.25
Observation error

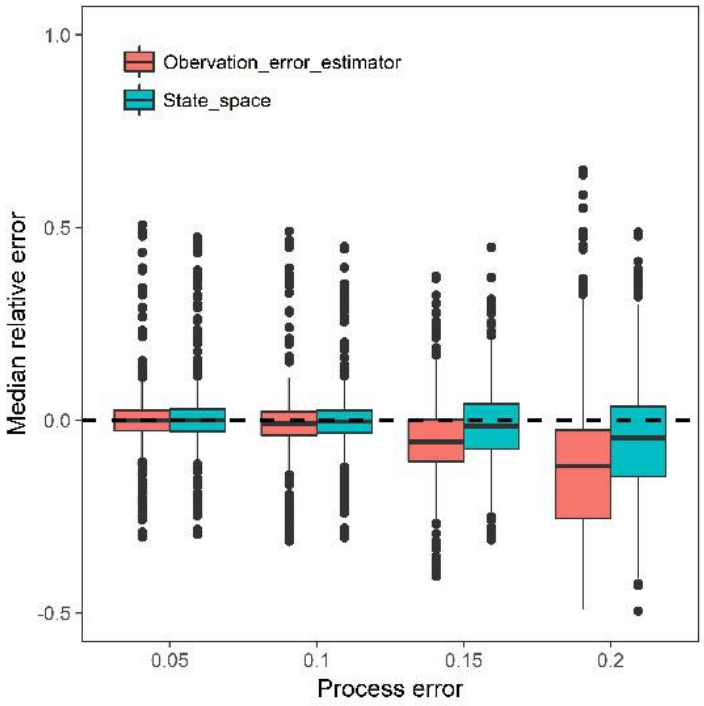

Figure 3.4. Median relative errors for the estimates of the parameters and BRPs from the two assessment models grouped by (top) parameters and BRPs (middle) observation error standard deviations, and (bottom) process error standard deviations.

In most of cases except when the model error was large, more than 50% of the estimates of the parameters and BRPs derived from the state-space production model were more accurate (Fig. 3.5). These findings support Hypothesis 1 in that the state-space production model is generally superior to the observation-error estimator when all three types of errors exist.

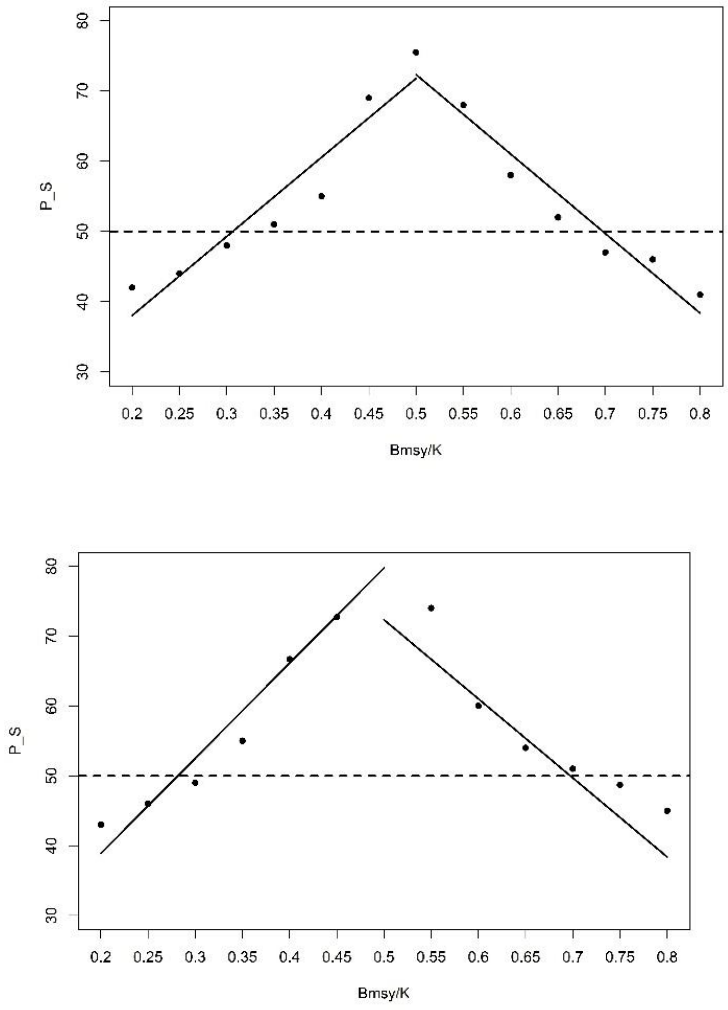

Figure 3.5. The percentage of parameters and BRPs in which the state-space model provides more accurate estimates than the observation-error estimator, when (top) all the parameters and BRPs are considered; (bottom) only the BRPs are considered

3.3.3 Hypothesis 2

As the shape parameter *s* deviated from one to both directions, P_S tended to decrease (Fig. 3.5). Given the importance of BRPs to management, we evaluated the advantage of the state-space model over the observation-error estimator by only considering the estimates of the BRPs.

These results also support Hypothesis 2, where the advantage of the state-space model diminishes as the model error increases (Fig. 3.5).

3.3.4 Hypothesis 3

The P_S tended to be smaller than 50% when the model error became large (*Bmsy/k* smaller than 0.3 or greater than 0.7), indicating that the observation-error estimator outperformed the state-space model when the model error exceeded a certain level (Fig. 3.5).

3.3.5 Biases of parameter and BRPs estimates

Estimates of intrinsic growth rate were more biased than that of the carrying capacity and catchability coefficient. Estimates of *MSY* were less biased compared with other BRPs (Table 3.1; Fig. 3.4).

3.3.6 Estimates of process and observation errors

Many small (< 0.0001) estimates of the process and observation error standard deviations were observed when the state-space model was fitted to the model (Fig. 3.6). The state-space production model tended to overestimate process error standard deviation and underestimate observation error standard deviation when the process error standard deviation was smaller than observation error standard deviation, and vice versa. The observation error standard deviations were overestimated by the observation-error estimator except when the ratio of process error to observation error was small (i.e., 0.2; 0.4; Fig. 3.6).

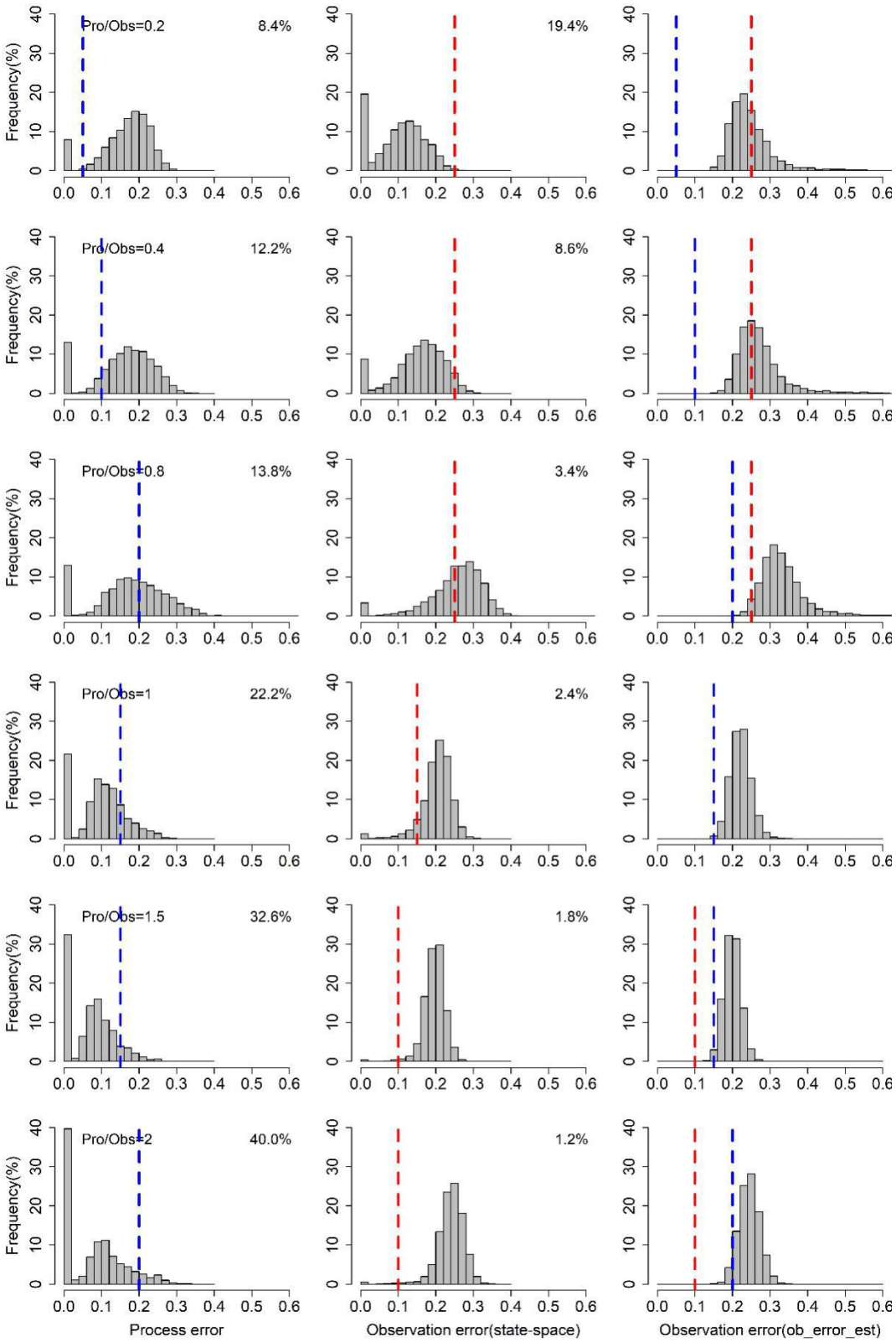
Pro/Obs=0.2
8.4%
19.4%
Pro/Obs=0.4
12.2%
8.6%
Pro/Obs=0.8
13.8%
3.4%
Pro/Obs=1
22.2%
2.4%
Pro/Obs=1.5
32.6%
1.8%
Pro/Obs=2
40.0%
1.2%
Frequency(%)
Process error
Observation error(state-space)
Observation error(ob_error_est)

Figure 3.6. The estimates of process error and observation error standard deviations in the state-space model (left two columns); the estimates of observation error standard deviation in the observation-error estimator (rightmost column).

3.4. Discussion

3.4.1 The comparison of stock assessment models

Both assessment models effectively achieved the global minimum of the objective function. The state-space production model required much more computation time and generally yielded more accurate and precise parameter estimates than the observation-error estimator when all three errors existed. However, as the model error increased, the advantage of the state-space production model tended to decrease. The observation-error estimator tended to perform better than the state-space production model when the model errors became large. Few previous studies comparing the two models considered the impact of model errors on the model performance. The results of this study suggest that the state-space production model may be not preferable when the assumed functional form of the model for population dynamics is badly mis-specified.

3.4.2 Model errors in the production models

The shape parameter in Pella-Tomlinson model could be estimated in principle, though in practice, it is notoriously difficult to estimate with any precision using an individual data set even when the process and observation errors are small. Thorson et al. (2012) estimated the ratio of *Bmsy*/*k* for 147 exploited marine species from different taxonomic orders using the Pella-Tomlinson model. The ratio varies greatly among species in different taxonomic orders. The model error can be introduced when we use the Schaefer model as a default surplus production function regardless of the species' taxonomic order, hence leading to biased estimation of

parameters and BRPs. Pre-specifying a reasonable range for the shape parameter by considering the species' taxonomic order may mitigate the impact of model errors on parameter estimation. However, the effectiveness of this approach relies on how accurately and precisely the prior on *Bmsy/k* can be defined given species' taxonomic order.

It should also be noted that the model errors considered in this simulation are specific (i.e., misspecification of production curve). The results may not be representative of the impacts of other model errors. Fishery population dynamics consist of complex and usually unstable processes of growth, mortality and reproduction, and do not necessarily follow the Pella-Tomlinson function. Alternative population growth functions, for example, depensatory population growth which incorporates an Allee effect at low population sizes, may be more realistic for some species. The impacts of model errors are more difficult to determine in that case.

3.4.3 The process error in the state-space model

Estimates of process errors in the state-space production model were badly biased. Process errors, if available, are often used in projecting future biomass dynamics (e.g., Cadigan, 2016). The projected future biomass can be compared with reference points to quantify the risk of a stock being overfished. However, the quantification of the risk of the stock being overfished may not be accurate if the process error standard deviations are badly biased.

This study found that the ratio of process error standard deviation to observation error standard deviation could affect their estimates. This finding was also reported by Auger-méthé et al (2016) for a state-space Gompertz model. Pre-defining the relative magnitude of the two standard deviations has been used. However, this approach is somewhat arbitrary (Millar and

Meyer, 2000; de Valpine and Hilborn, 2005). The question of how to accurately estimate process and observation error standard deviations in a state-space production model remains.

3.4.4 Model performance evaluation and implications for management

The impact of different error levels on model performance was evaluated using a GLM. This approach allows managers to understand the relative values of reducing different errors. Reducing the observation error of an abundance index often requires increasing sample effort, which may be economically and/or logically difficult. Many studies for optimizing survey designs aim to find a balance between the costs of the survey and the quality of the observed data. The evaluation of the link between the quality of the observed data and the reliability of the model outputs can serve as additional information to those task with designing surveys.

The GLM analysis also evaluated the bias of BRPs estimates, which can be useful to managers when they select BRPs for setting quota or harvest control rules. The estimates of *MSY* were the least biased in this study. This might result from the reciprocal relationship between estimates of *k* and *r*. Any overestimates of *r* were likely to be compensated for by underestimates of *k*, making *MSY* more reliable than the other BRPs. In theory, if *MSY* is greater than *Yield_Emsy*, the current stock biomass is below *Bmsy* and vice versa. In practice, this is not necessarily true because of possible estimation bias. One precautionary approach is to choose the smaller value of *MSY* and *Yield_Emsy* for quota setting.

3.4.5 Recommendation

This simulation study shows that the state-space production model generally outperformed the observation-error estimator when there was process, observation and model error. However, differences in performance between these two methods decreased with increased model errors.

The observation-error estimator could even outperform the state-space model when the model errors became large. Therefore, the state-space production model is recommended when there is no prior knowledge of the error levels. Ensuring low model errors is critical for state-space models to perform well.

CHAPTER 4

MULTIPLE TIME SERIES OF INPUT DATA IMPROVE THE PERFORMANCE OF STATE-SPACE FISHERY STOCK ASSESSMENT MODELS

4.1. Introduction

State-space fishery stock assessment models (e.g., JABBA, SAM) are increasingly being used in fishery stock assessment and management (Nielsen and Berg, 2014; Berg and Nielsen, 2016; Pedersen and Berg, 2017; Winker et al., 2018). A typical fishery stock assessment model includes two components: 1) equations that model the fishery population dynamics; 2) observation models that link unknown states in dynamic models to observed data. State-space models are favored because their model structure is designed to differentiate between sources of errors respectively associated with the two model components, that is, the process error mainly due to environmental variation and the observation error related to sampling method (Fig. 4.1). Previous studies have shown that outputs from state-space fishery stock assessment models are more reliable than outputs from models only accounting for one error source (i.e., process error estimator or observation error estimator; de Valpine and Hastings, 2002; Punt, 2003; Ono et al., 2012; Xu et al., 2019).

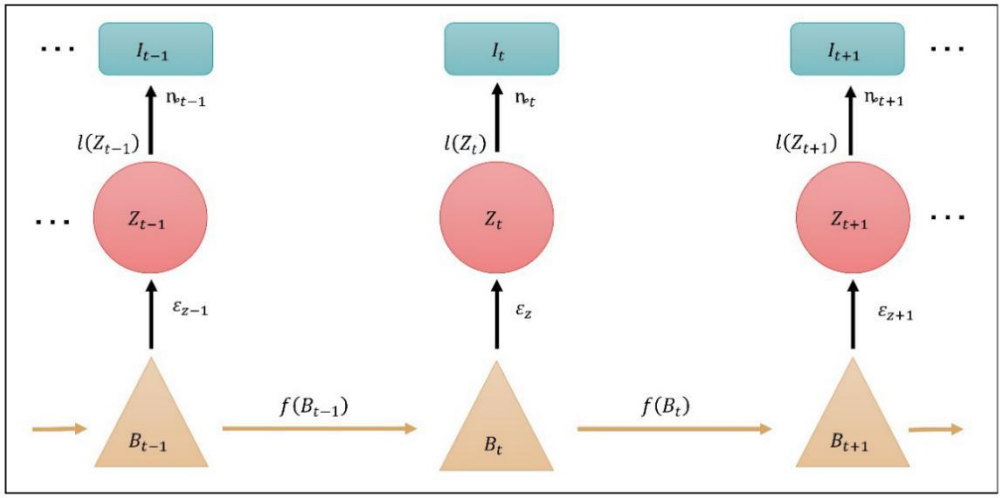

Figure 4.1. The diagram of a typical state-space model's structure.

Statistical methods used in state-space fishery stock assessment models for estimating parameters are numerous in both frequentist and Bayesian inference, e.g.: the Laplace approximation (Fournier et al., 2012), the errors-in-variables method (de Valpine and Hilborn, 2005), the extended Kalman filter (Reed, 1986), the Monte Carlo Kernel Likelihoods method (de Valpine, 2004) and the Metropolis-Hastings sampler (Millar and Meyer, 2000). Accompanying the emergence of statistical methods came the development of R packages and corresponding computer software (e.g., BUGS, JAGS, ADMB, TMB) that facilitate the model fitting (Meyer and Millar, 1999; Fournier et al., 2012; Denwood, 2016; Kristensen et al., 2016). In this study, we focus on the Laplace approximation method and TMB due to their increasing popularity in fishery stock assessment modelling (Stewart et al., 2013; Taylor and Methot, 2013; Thorson et al., 2015; Cao et al., 2020).

While the state-space model has demonstrated its practicability and flexibility in fishery stock assessment modelling, its model fitting problems are still challenging. Even parameters in structurally simplified state-space models can not be estimated effectively given available data. Unfortunately, estimates of process and observation errors for state-space models are notoriously often significantly biased (Auger-Méthé et al., 2016). The two errors' estimates are greatly affected by the ratio of their true values, which indicates that the two errors generally confound each other and are subject to estimability problem (Xu et al., 2019). This quality is particularly discouraging given that state-space models are advertised as providing the means to separate the two errors. The estimability problem, which refers to the maximum value of the objective function occurring at more than one parameter values (i.e., the profile likelihood is flat around

global maximum), causes the state-space model to fail to converge or estimate extremely large confidence intervals for parameters (Auger-Méthé et al., 2020).

Various methods have been explored to address this problem of estimability, with a focus on effectively separating the two errors. The most commonly used methods include fixing some of the parameters, or using informative priors if the model is developed within a Bayesian framework (Dennis et al., 2006; Auger-Méthé et al., 2020). In particular, one may estimate the observation error externally or fix the ratio of the two errors to facilitate the model fitting (Ono et al., 2012). While these methods can often solve the estimability problem, it is usually hard to verify that the pre-specified value or the priors are not biased. One method that has somehow escaped the notice of fishery scientists involves repeating observations for each state of the dynamic models. Dennis et al. (2010) found that using replicated observations of bird counts improved the parameter estimation of the Gompertz state-space model. This method is promising for fishery stock assessment modeling because fish biomass surveys usually consist of large numbers of independent subsamples that may serve as replications of observations. The routine practice is to aggregate all the samples and produce a single estimate of population biomass for each year. We argue that this routine data processing approach may result in the loss of useful information for the state-space model.

In the present paper, we demonstrate that using multiple time series of biomass index extracted from raw survey data may solve the estimability problem and improve the performance of state-space models. To this end, we conducted a simulation mimicking the fishery system that includes fish population dynamics, spatial distribution, biomass survey, data processing, and stock assessment. We compared the stock assessment results to show the potential gains of relevant information for state-space models when more than one time series of biomass index is

used as an input. The simulation is based on the jumbo flying squid fishery in the Southeast Pacific.

4.2. Materials and methods

4.2.1 The jumbo flying squid fishery in the Southeast Pacific

The jumbo flying squid (*Dosidicus gigas*) is widely distributed in the eastern Pacific Ocean (Nigmatullin et al., 2001). In the Southeast Pacific, the species supports the world's largest squid fishery, with a catch of over one million metric tons in 2014 (Fig. 4.2). Seven fishing entities have been targeting jumbo flying squid in the Southeast Pacific Ocean. The fishing grounds of jumbo flying squid are located in the area within 0°~30°S, 70°~95°W. The stock has been assessed using the state-space surplus production model, with the results showing that the stock is not overfished and overfishing is not occurring.

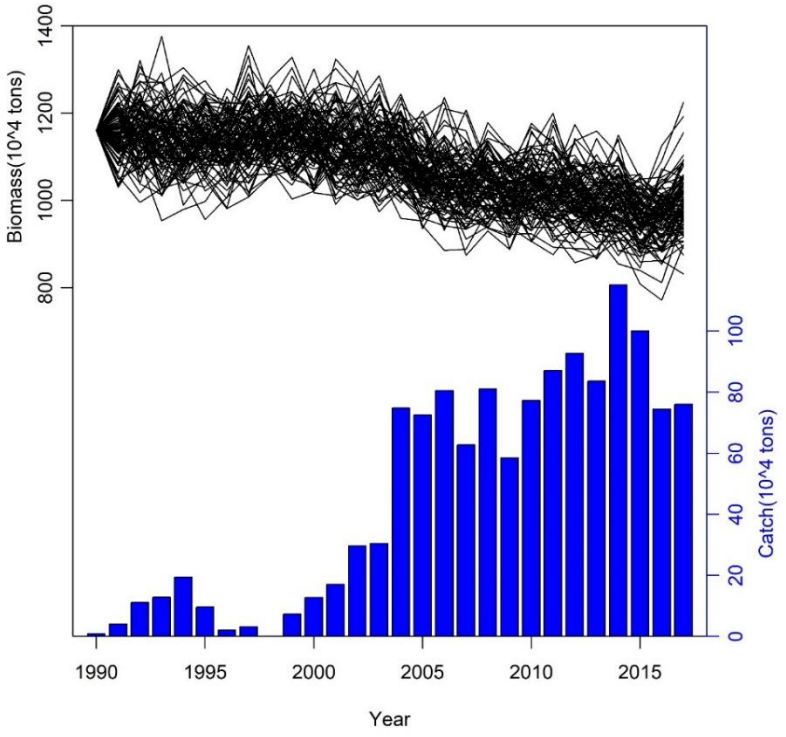

Figure 4.2. The biomass and catch of jumbo flying squid in the simulation. The figure shows 100 biomass trajectories when the standard deviation of the process error was 0.05.

4.2.2 The simulation

4.2.2.1 The population dynamics

We used the state-space Schaefer production model to describe population dynamics. The model is written as:

$$B_{y+1} = \left(B_y + rB_y(1 - \frac{B_y}{k}) - C_y\right) e^{\varepsilon_y} \qquad (4.1)$$

where B_y is the biomass in year y; C_y is the catch in year y; q is the catchability coefficient; ε is process error assumed to follow the normal distribution, i.e.,$\varepsilon \sim N(-\frac{\sigma_\varepsilon}{2}, \sigma_\varepsilon^2)$; σ_ε^2 is the variance of the process error; $-\frac{\sigma_\varepsilon}{2}$ is a bias-correction term for the lognormal distributions; r is the intrinsic growth rate; k is the environmental carrying capacity. The biological reference points, maximum sustainable yield (*MSY*) can be calculated as:

$$MSY = \frac{rk}{4} \qquad (4.2)$$

The values of the parameters were set based on the results of a stock assessment for jumbo flying squid in the Southeast Pacific Ocean (Xu et al., 2019). We parameterized the operating model such that k=11.62 million tons, and r=0.64 year^{-1}. The time series of catch data used in the model was from 1990 to 2017. Since the pre-1990 catch was minuscule, the initial biomass was set as equal to k. Three levels of process error (σ_ε=0.05, 0.1, 0.15) were used in the simulation (Fig. 4.2).

4.2.2.2 The spatial distribution and the biomass survey

The spatial distribution of jumbo flying squid varies over the years and is affected by many environmental factors, among which sea surface temperature is the most influential (Yu et al., 2016) . In this simulation, the jumbo flying squid was assumed to distribute in accordance with the spatial habitat suitability index (HSI). The spatial HSI for each year from 1990 to 2017 was calculated based on the difference between the local temperature and the optimal temperature for the species (Fig. 4.3):

$$HSI_{y,i} = 1 - \frac{|T_{y,i} - T_{optimal}|}{Maximum|T_{y,i} - T_{optimal}|} \qquad (4.3)$$

$$B_{y,i} = \frac{B_y * HSI_{y,i}}{\sum HSI_{y,i}} \qquad (4.4)$$

where the $HSI_{y,i}$ is the habitat suitability index in year y and location i; $T_{y,i}$ is the local sea surface temperature of location i in year y; $T_{optimal}$ is the optimal temperature favored by jumbo flying squid; B_y is the total biomass in year y calculated by the population dynamic model (1); $B_{y,i}$ is the biomass of squid occurring in location i and year y. The sea surface temperature data are downloaded from OceanWatch (NOAA; https://oceanwatch.pifsc.noaa.gov/).

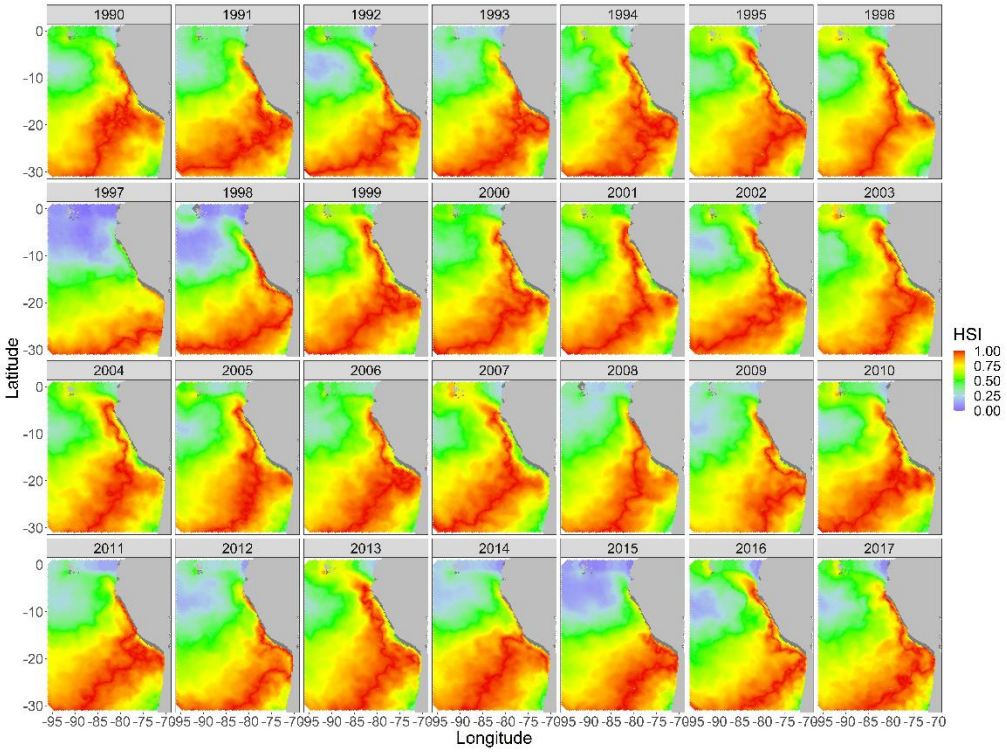

Figure 4.3. Spatial distribution of habitat suitability index of jumbo flying squid from 1990 to 2017.

23955 potential sample sites evenly distributed over the ocean area bounded by 0°~30°S, 70°~95°W were considered as the sampling framework of this simulation. A certain number of sample stations were randomly selected from the potential sample sites each year (Fig. 4.4). The catch of squid in each sample station and the annual biomass index were calculated as:

$$I_{y,i} = qB_{y,i}e^{n_y} \qquad (4.5)$$

$$I_y = \frac{\sum I_{y,i}}{n} \qquad (4.6)$$

where $I_{y,i}$ is the catch of the squid by the survey occurs in year y and location i; I_y is the annual biomass index in year y; q is the catchability coefficient; n is the number of sample stations; η_y is

measurement error and $n_y \sim N(-\frac{\sigma_n}{2}, \sigma_n^2)$; σ_n^2 is the variance of the measurement error; and $-\frac{\sigma_n}{2}$ is bias-correction terms for the lognormal distributions. We set q=0.006 and σ_n=0.1. Please note that the measurement error here differs from the observation error. The observation error is formed by two parts: the measurement error and the sampling error caused by finite sample sizes.

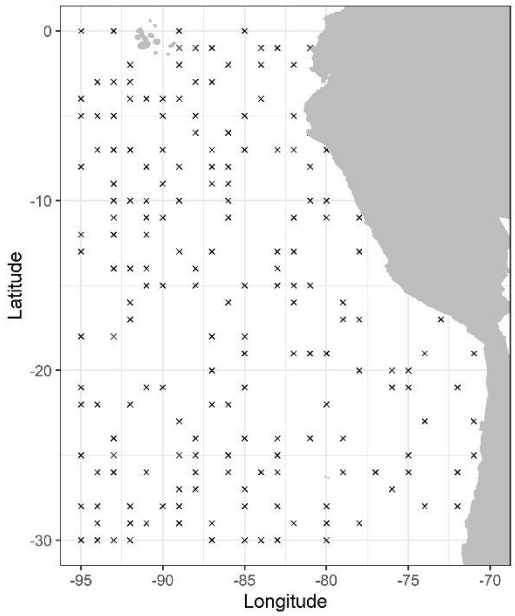

Figure 4.4. An example of the layout of survey stations based on random sample design

The routine data processing approach is to aggregate the catch data from the 200 sample stations to calculate one biomass index each year using equation 4.5. Here, using the same raw survey data, we extracted multiple time series of the biomass index. The sample stations were allocated equally and randomly for calculating each biomass index. We calculated 1~4 time series of biomass index in four different scenarios with the sample size respectively being 200, 100, 67, and 50. The observation error for each biomass index increased with the number of time series of biomass index (Fig. 4.5). For each scenario, the simulation procedure was repeated 400 times.

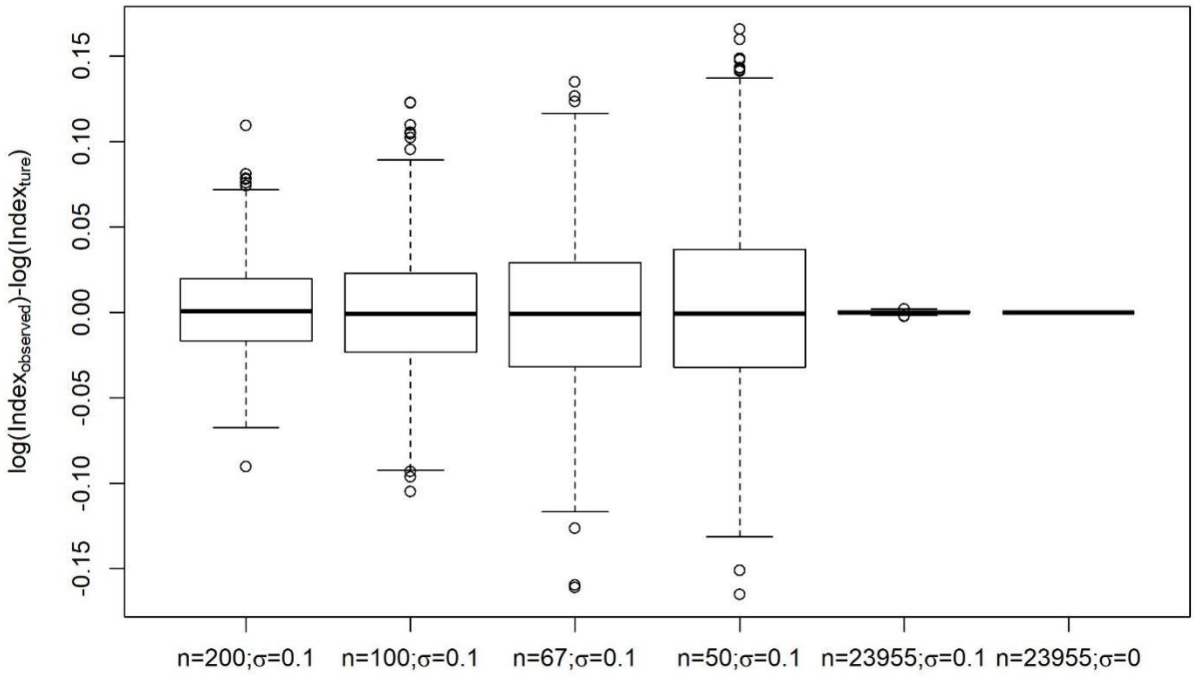

Figure 4.5. The difference between the observed annual biomass index and the true annual biomass index (logarithm) when different sample size and measurement error was set for the biomass survey in the simulation.

4.2.2.3 Model fitting and results comparing

The maximum likelihood estimation method was used to fit the state-space model to the biomass index data. Template Model Builder (TMB) and R were used to maximize the objective function. Model convergence was checked by two criteria: 1) the Hessian Matrix was positive definite; and 2) the gradient was near zero (<0.0001). The simulation trials that failed to converge were recorded and replaced.

For each simulation trial, the key parameters r, k and biological reference point *MSY* were estimated and compared to the corresponding true values. Relative error (RE) calculated as follows was used to indicate the accuracy and precision of the estimates:

$$\mathrm{RE} = \frac{\theta_{est} - \theta_{true}}{\theta_{true}} \qquad (4.7)$$

where θ_{est} and θ_{true} denote the estimates and true values, respectively. The profile likelihoods of key parameters r and k from the state-space model were compared. A flowchart of this simulation is shown in Fig. 4.6.

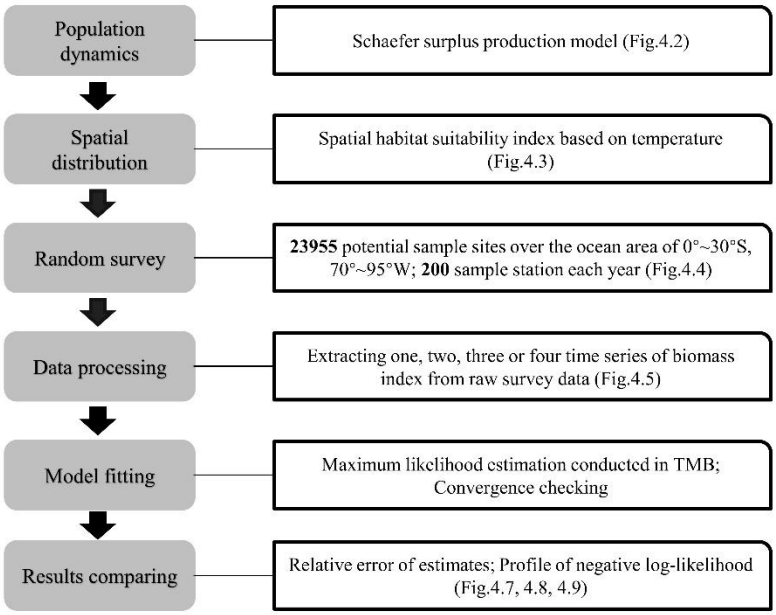

Figure 4.6. Flowchart of the simulation study.

4.3. Results

4.3.1 Model convergence

31.25% of the initial simulation trials with a single biomass index time series data did not converge, showing a severe estimability problem. However, all of them converged when

additional time series of biomass index were inputted into the model. The results suggest that providing multiple observations for each state of the dynamic model was sufficient enough to solve the estimability problem. The trials that failed to converge were replaced and not included for later analysis.

4.3.2 The profile of the likelihood of the key parameters' estimates

When multiple time series of biomass index were used as inputs, the profiles of negative log-likelihoods were unimodal and approximately parabolic. The profile was relatively flat around the global minimum when only a single time series of biomass index was inputted (Fig. 4.7). The parabolic shape of the profile likelihood enabled the parameters to swiftly converge to the theoretically unbiased point estimates and yield reliable interval estimates. The shapes of the profile likelihood explain why lots of initial simulation trials with a single time series of biomass data failed to converge. Adding one more time series of biomass index makes a substantial contribution to model fitting. When it came to the convergence speed, fitting the state-space model with a single time series of biomass index data took roughly sixty times longer than fitting the model with multiple time series data.

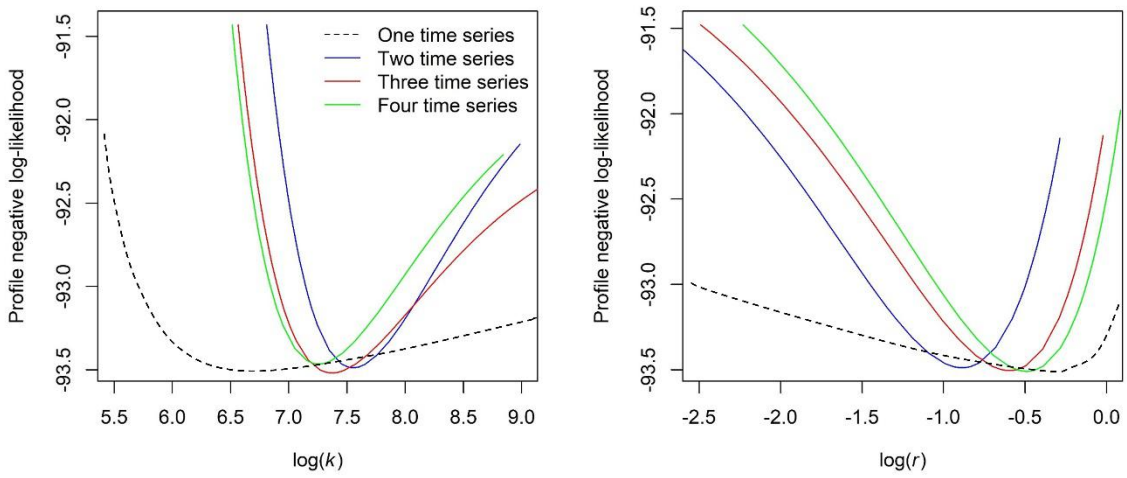

Figure 4.7. One profile negative log-likelihood for the key parameters k and r (logarithm) from simulation trials with the same biomass trajectory and raw survey data.

4.3.3 The accuracy of estimates of key parameters and the biological reference point

In general, *r*, *k,* and *MSY* estimated from state-space models using multiple time series of biomass index data were much less biased than those from the models using a single time series. The relative error of *r*, *k,* and *MSY* had a narrower range when multiple time series of biomass index data were used as model inputs instead of singular time series. The median relative error of estimated parameters *k* and biological reference point *MSY* were close to zero using multiple time series of biomass index as model inputs (Fig. 4.8). There was no visible difference in the accuracy of estimates when the number of time series increased from two to four.

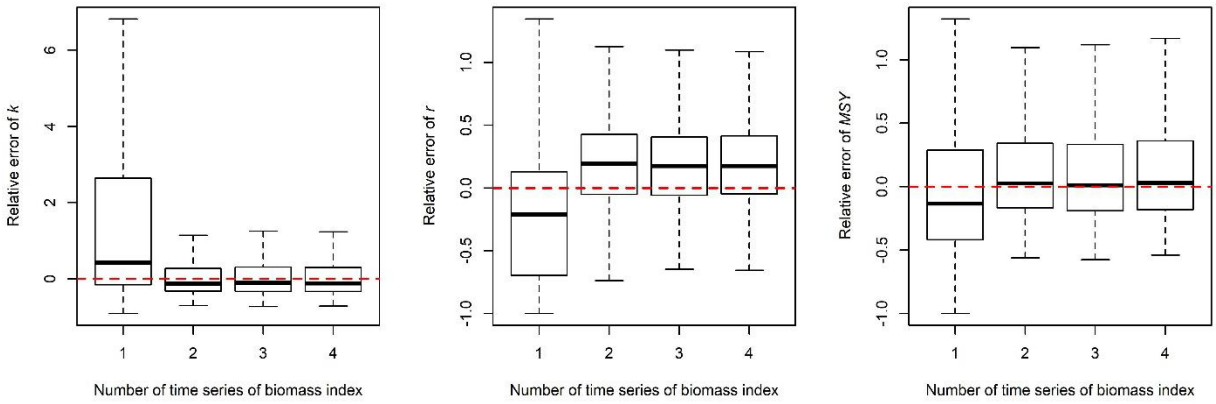

Figure 4.8. The relative errors of estimates of k, r, and MSY when the model input data consist of one, two, three, or four time series of biomass index.

A large proportion of extremely negative biased estimates (<0.0001) of the process error standard deviation emerged when a single time series of biomass index data was used as an input for the state-space models. No such extremely small estimates were observed when using multiple time series. The standard deviations of process error estimated from the state-space model using multiple time series were overall more accurate and precise compared with those using a single time series. Similarly, the results did not show visible differences in the accuracy between the estimates when the number of time series of biomass index increased from two to four (Fig. 4.9).

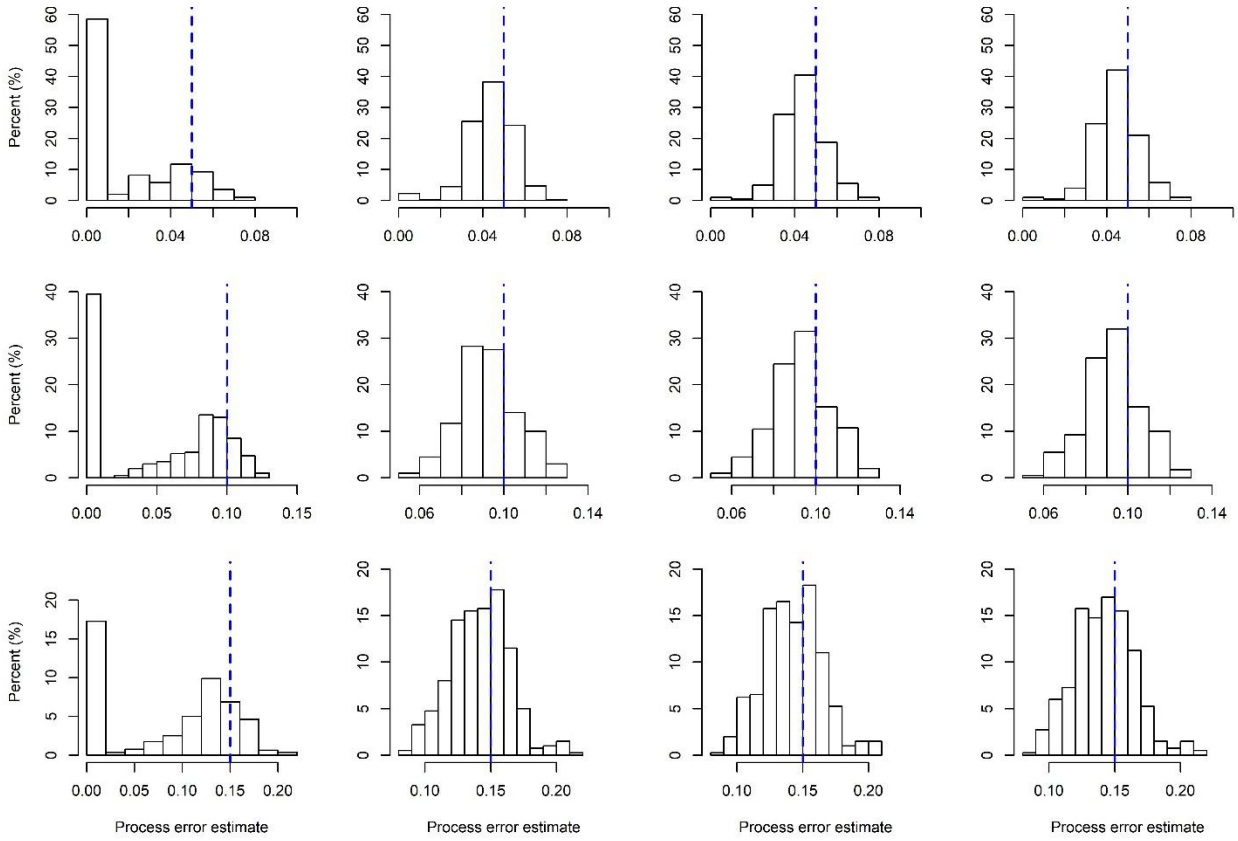

Figure 4.9. The estimates of the standard deviation of process error when the inputted biomass index data of the state-space model consisted of one (leftmost), two (second column from the left), three (third column from the left), or four (rightmost) time-series. The dotted blue lines represent the value of 0.05, 0.1, and 0.15 for the true corresponding standard deviation from the top to the bottom, respectively.

4.4. Discussions

The simulation results show that multiple time series of biomass index offer substantial information-related benefits for the state-space surplus production model. The data can be obtained by dividing the survey stations into multiple groups with no additional costs from the sampling efforts. Therefore, state-space model performance could be greatly improved by simply

converting the routine data processing protocol from calculating a single time series to calculating multiple time series of biomass index.

The contrasts in model convergence and the shapes of profile likelihood indicate that using multiple time series of biomass index solves the estimability problem for state-space models. The estimates of the process error standard deviation are strikingly accurate when using multiple time series of biomass index, whereas the estimates are severely biased when using a single time series of data. This suggests that a single observation for each state of the dynamic models lacks sufficient information to distinguish between process error and observation error, while repeated observations for each state can provide relevant information to estimate errors accurately. Some studies have discussed the benefits of replicating the observations for state-space models (Brian et al., 2010; Knape et al., 2011). It would be interesting to continue similar studies in the field of fishery sciences as state-space models become more commonly used in fishery stock assessment, and a typical biomass survey is able to provide replications of observations.

The simulation results also indicate that the number of repeating observations, whether it is two or four, only slightly affects the model performance. However, this tendency may not hold if some other factors are considered in the simulation. Firstly, compared with the real sample size in a marine survey, 200 out of 23955 potential sampling sites is a very large proportion. The population of potential sampling sites could go near-infinite if we take into consideration a finer spatial and temporal resolution. Secondly, the jumbo flying squid is a pelagic species with high swimming speed and frequent vertical and horizontal migration. Although catchability was assumed to be constant in different sampling stations, in practice it is likely to vary, which could result in a nonlinear relationship between the catch and biomass. Thirdly, different biomass index extracted from the survey data showed similar temporal trends in the simulation trials,

indicating that there was no contradictory information in the input data and that it was ideal for model fitting. However, model inputs with opposing pieces of information are possible if sampling error is huge and multiple time series are used. In short, the setting of this simulation makes the data quality (their representativeness of the biomass trend) be much better than what is likely to be a less ideal reality. Therefore, although the observation error increases as more time series of biomass index are extracted from the survey data, each one of the time series still provides representative and consistent information for the state-space model. In real application, we argue that deciding the optimal number of time series for the state-space model needs investigation on a case-by-case basis.

We demonstrated that even the most structurally simple state-space fishery stock assessment model can have estimability problem and biased parameter estimates when input data are not informative enough. Similar issues could likely occur in more structurally complex state-space fishery stock assessment models. With very sophisticated state-space models being increasingly used in the fishery stock assessment, relatively little attention has been paid toward the intricate problem related to model fitting. Ignorance of such problems may cause inappropriate interpretations of misleading model results and, by extension, lead to fisheries mismanagement. The model fitting problems as expounded upon in this paper can hardly be detected by conventional model diagnostics. Using a simulation-estimation approach, the intrinsic flaw of model configuration may potentially be discovered. We suggest that state-space fishery stock assessment models be evaluated by the simulation-estimation approach, and that their ability to separate process and observation errors be emphatically investigated.

CHAPTER 5

COMPARING A SUITE OF SURPLUS-PRODUCTION-BASED DATA-LIMITED METHODS AND MANAGEMENT PROCEDURES

5.1 Introduction

The majority of commercially exploited fish stocks lack sufficient data for sophisticated age/size-structured assessment models. This incapacity poses a significant challenge for the sustainable management of these stocks (Froese et al., 2012). Nevertheless, most exploited stocks, including those with limited data, are required to be managed by law in many countries and regions (e.g., DAFF, 2007; MFNZ, 2008). For example, the 2006 amendment to the U.S. Magnuson-Stevens Act mandated the implementation of annual catch limits (ACL) for all federally managed fisheries (MSA, 2007). The lack of sufficient data in many fisheries worldwide coupled with strict laws and regulations requiring management of said fisheries spurred the development of what is known as data-limited methods (DLMs). DLMs combined with management procedures (MPs) could provide appropriate management advice (i.e., total allowable catch) using limited information about the stock and fishery without relying on sophisticated models (Geromont and Butterworth, 2015). DLMs and corresponding MPs are constantly evolving and dozens of new approaches have been developed in recent decades (Hordyk et al., 2016; Froese et al., 2017; Rudd and Thorson, 2018).

Management strategy evaluation (MSE), an alternative to the traditional stock assessment model approach to fisheries management, has been drawing extensive attention both in scientific and management communities (Punt et al., 2016; Miller et al., 2019). MSE is a simulation-based framework with the purpose of evaluating the performance of candidate MPs in meeting management objectives. The rise in interest of MSE has also brought corresponding developments with various simulation tools (e.g., DLMtool and FLR; Kell et al., 2007; Sun et al.,

2018; Carruthers and Hordyk, 2018). Many previous studies have compared DLMs and MPs using these frameworks (Wiedenmann et al., 2013; Carruthers et al., 2014; Newman et al., 2015; Carruthers et al., 2016), but there remain concerns that the results derived from broad comparisons may not extend to all stock-specific cases (Dowling et al., 2019; Sagarese et al., 2019). A lack of comprehensive review of DLMs may lead to mismanagement when the methods are taken out of their original design context or their assumptions (especially implicit ones) are ignored (Deroba et al., 2015).

In this study, a suite of DLMs and corresponding MPs relying on estimates of surplus production are evaluated and compared using simulations. The only data requirements of the methods are time-series data of catch and absolute biomass. The methods are based on a simple population dynamics equation:

$$B_{y+1} = B_y + S_y - C_y \qquad (5.1)$$

where S_y, B_y, and C_y represent surplus production, biomass, and catch, respectively, in year y.

Surplus production models formulate surplus production using fixed function forms. Commonly used surplus production models include the Schaefer model, Fox model, and Pella-Tomlinson model, which can all be expressed as follows:

$$B_{y+1} = \left(B_y + \frac{r}{s} B_y \left(1 - \left(\frac{B_y}{k}\right)^s\right) - C_y\right) \qquad (5.2)$$

where r is the intrinsic growth rate, k is the environmental carrying capacity, and s is the parameter that determines the shape of the surplus production curve. For the Schaefer model, s equals one and the surplus production curve is symmetric. For the Fox model, $s \approx 0$ and the

surplus production curve is asymmetric. For the Pella-Tomlinson model, s is a freely estimable parameter (larger than -1).

Surplus production can also be estimated in a non-model approach using a modified version of equation 1 relying on catch and biomass data:

$$S_y = B_{y+1} - B_y + C_y \qquad (5.3)$$

Both the model approaches and non-model approaches can be used to determine fishery stock status. For model approaches, the biological reference point B_{MSY} can be estimated and compared with the current biomass to identify the fishery stock status. For non-model approaches, the derivative of surplus production with respect to biomass (dS/dB) can be approximated by the coefficient ($slope_{S/B}$) of the linear regression between the calculated surplus production and the observed biomass in recent years (Fig.5.1). A positive $slope_{S/B}$ indicates that the current biomass is less than B_{MSY}, and vice versa. One management procedure called *Gcontrol* has been developed based on $slope_{S/B}$. Maximum yield is achieved by having $slope_{S/B} \approx 0$ through regulating catch and maintaining biomass close to B_{MSY}. In this study, an alternative indicator ($B_{highest\_S}$) was proposed for the non-model approach, which serves to identify the stock status by comparing current biomass with the biomass at which surplus production was at its highest. $B_{highest\_S}$ can be considered a proxy of B_{MSY} if the stock biomass has ever been around B_{MSY} and the corresponding biomass and catch data are recorded with certain level of accuracy.

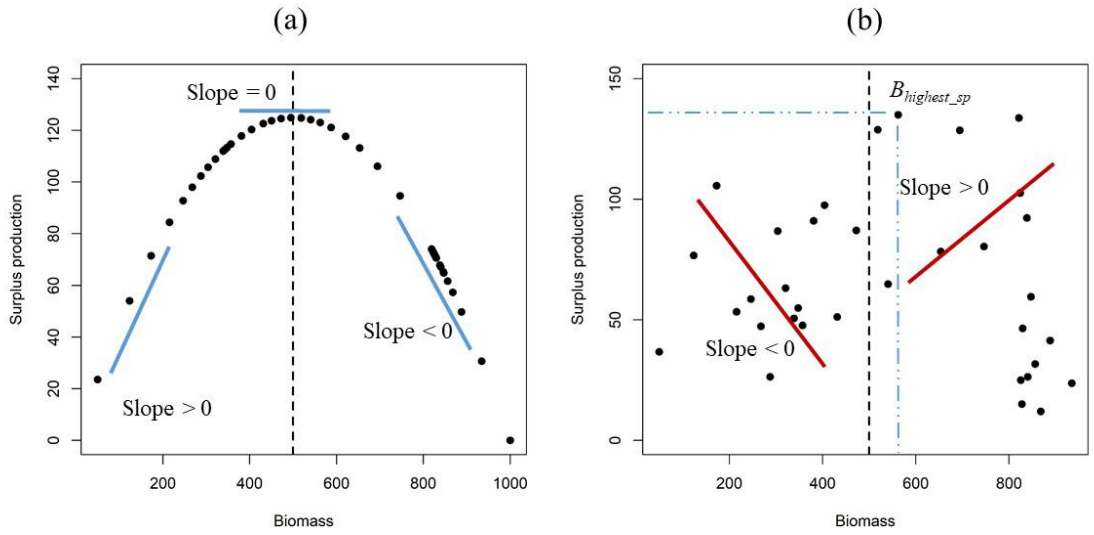

Figure 5.1. The relationship between biomass and surplus production when observation error is (a) absent and (b) present.

One advantage of the non-model approach is that it does not rely on the assumption that surplus production must strictly follow a fixed function. Therefore, the approach is immune to the possible misspecifications of model structure and may be able to adapt to temporal shifts in stock productivity. Surplus production models with one-way trip fishing history, which lacks contrast in fishing efforts and biomass, are known to provide unreliable parameter and reference points estimates. The performance of the non-model approach with different fishing histories needs to be further examined. In addition, the observation error associated with biomass, which is inevitable, has the potential to degrade the performance of both model and non-model approaches.

The main purpose of this paper is to explore various methods for identifying the stock status and provides an appropriate recommendation on catch limits when only catch and biomass data

are available. To this end, we conduct two simulations. The operating models of the first simulation are constructed based on surplus production models with different assumptions. This simulation is to evaluate and compare the performance of model-based and non-model approaches on identifying stock status. Based on the results, we propose five new surplus-production-based MPs. For the second simulation, we use the well-developed simulation tool "DLMtool" to compare the new proposed MPs with the original surplus-production-based MP *Gcontrol*. The operating models of the second simulation are constructed based on age-structured population dynamics models parameterized by the outputs of ten real fisheries stock assessments.

5.2 Materials and Methods

5.2.1 Simulation 1: Evaluating the performance of approaches in identifying stock status

5.2.1.1 Approaches to identify stock status

Two non-model approaches and two model approaches to identify stock status are detailed as follows:

Approach 1 (**A1**): Use catch and biomass to calculate the surplus production based on Equation (5.3). Estimate the coefficient of the linear regression between the calculated surplus production and the observed biomass ($slope_{S/B}$) for the most recent ten years' data. A positive $slope_{S/B}$ indicates that the current biomass is below B_{MSY}, and vice versa. This approach is the basis for *Gcontrol* to identify the stock status and recommend total allowable catch (TAC).

Approach 2 (**A2**): Use catch and biomass data to calculate the surplus production based on Equation (5.3). Identify $B_{highest\_S}$ as the observed biomass at which surplus production was at its highest. Compare the current observed biomass with $B_{highest\_S}$ to determine the stock status. The biomass being less than $B_{highest\_S}$ indicates that the current stock biomass is below B_{MSY}, and vice versa.

Approach 3 (**A3**): Fit the Schaefer model with catch and biomass data to estimate B_{MSY} and compare the current observed biomass with the estimated B_{MSY}. The maximum likelihood estimation method was used to estimate the model parameters and biological reference points. The Schaefer form of the population dynamics model, the observation model, the objective function, and the biological reference points are written as follows:

$$B_{y+1} = B_y + rB_y(1 - \frac{B_y}{k}) - C_y \quad (5.4)$$

$$I_y = B_y e^{\varepsilon_y} \quad (5.5)$$

$$\mathrm{L}(\sigma_\varepsilon, r, k, B_0 | I_y) = \prod_y (\frac{1}{\sigma_\varepsilon I_y \sqrt{2\pi}} e^{-\frac{(lnI_y - \ln(qB_y))^2}{2\sigma_\varepsilon^2}}) \quad (5.6)$$

$$B_{MSY} = k/2; F_{MSY} = r/2 \quad (5.7)$$

where I_y is the observed biomass in year y, ε_y denotes observation error in year y that is assumed to follow a normal distribution, and σ_ε is the standard deviation of the normal distribution.

Approach 4 (**A4**): This approach is the same with A3 except using the Pella-Tomlinson model instead of the Schaefer model to fit the biomass and catch data. The Pella-Tomlinson form of the population dynamics model, the observation model, the objective function and the biological reference points are written as follows:

$$B_{y+1} = B_y + \frac{r}{s} B_y(1 - (\frac{B_y}{k})^s) - C_y \quad (5.8)$$

$$I_y = B_y e^{\varepsilon_y} \quad (5.9)$$

$$\mathrm{L}(\sigma_\varepsilon, r, k, B_0, s | I_y) = \prod_y (\frac{1}{\sigma_\varepsilon I_y \sqrt{2\pi}} e^{-\frac{(lnI_y - \ln(qB_y))^2}{2\sigma_\varepsilon^2}}) \quad (5.10)$$

$$B_{MSY} = k \times \sqrt[s]{\frac{1}{s+1}}; F_{MSY} = r/(s+1) \quad (5.11)$$

For A3 and A4, the parameters are estimated by maximizing the objective function. This process is implemented in Template Model Builder (Kristensen et al., 2016).

5.2.1.2 Operating models for testing stock status identification approaches

We simulate a 45-year-old fishery. We select the last 16 years (year 30~year 45) to evaluate the accuracy of the four approaches on stock status identification. Two scenarios of data collection are used: Data collection 1 (**D1**): Data used in the approaches have been collected since year 21(ten years before the onset of management); Data collection 2 (**D2**): Data used in the approaches have been collected since the beginning of the fishery. The biomass data are assumed to be subject to four levels of observation errors (the standard deviation of observation error σ_{ε} = 0.05; 0.1; 0.25; and 0.5, respectively). We assume the catch data are accurate as the observation error associated with the catch is often orders of magnitude smaller than the observation error in observed biomass. Values for the parameters are set based on the results of a stock assessment for jumbo flying squid in the Southeast Pacific Ocean (SPRFMO, 2017). The operating models are parameterized such that k = 11.62 million tons and r = 0.64 year-1. The initial biomass is set equal to the carrying capacity k. To test the robustness of the results, another set of parameters based on the Pacific saury fishery is used to construct the operating models (NPFC, 2018). The results of this sensitivity analysis are included in the appendix.

We define three population dynamics scenarios based on two forms of surplus production models (Schaefer and Fox model): Population dynamics 1 (**P1**): The biomass is calculated using Schaefer model; Population dynamics 2 (**P2**): The biomass is calculated using Fox model; Population dynamics 3 (**P3**): Use Schaefer model to calculate the biomass for the first 30 years and then use Fox model to calculate the biomass for the last 15 years. **P3** is developed to mimic a simplified regime shift phenomenon (Fig. 5.2 and Fig. S5.1~S5.5 in appendix).

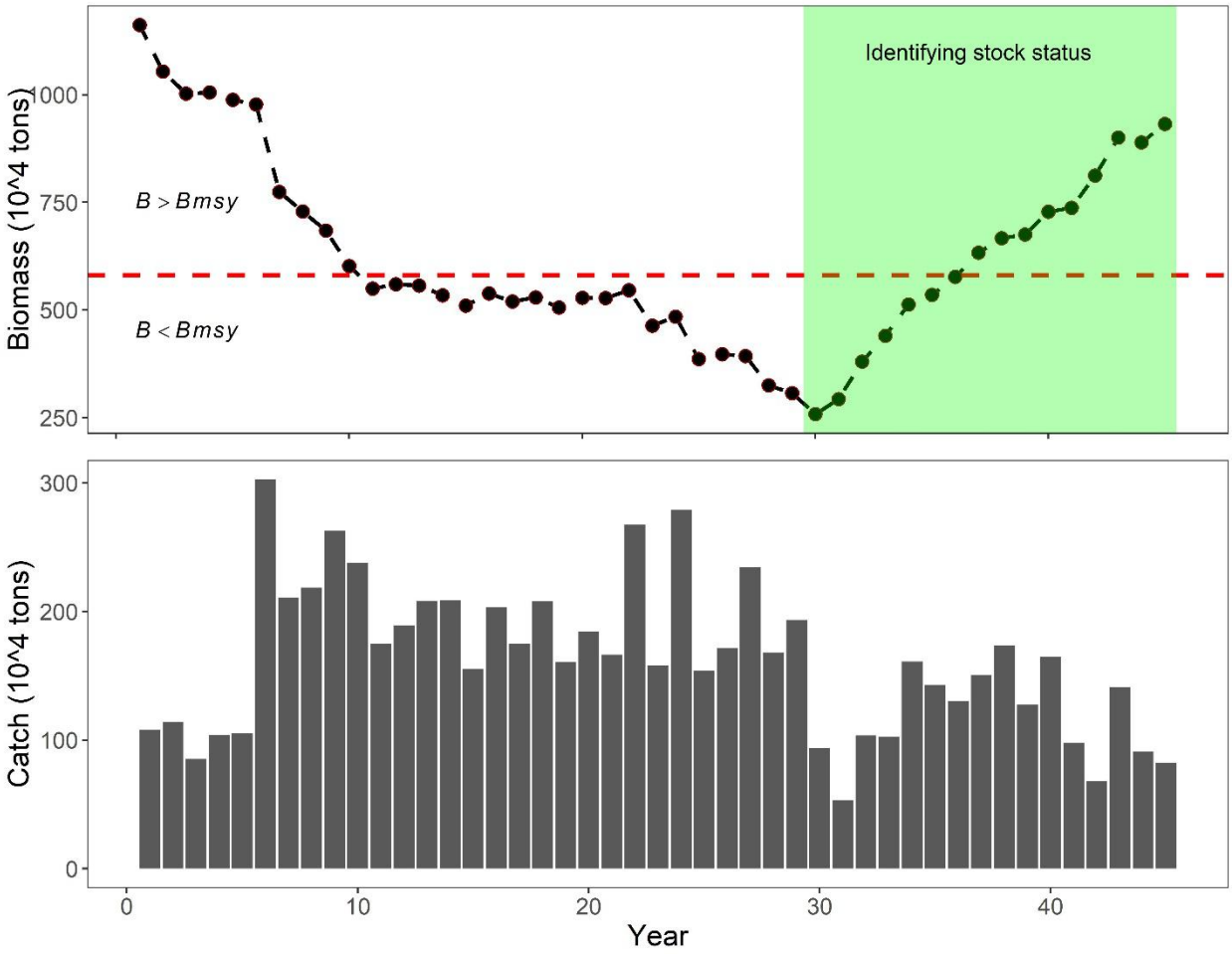

Figure 5.2. The historical catch and biomass in simulation 1 for population dynamics scenario 1 (P1: Schaefer model) and fishing history scenario 1 (F1: Good contrast). The years in the shaded part are used in testing the performance of the four approaches on identifying the stock status.

Two fishing histories are simulated for each population dynamics scenario: Fishing history 1 (**F1**): The stock is fished down to less than B_{MSY} and then recover to a status above B_{MSY} (good contrast); Fishing history 2 (**F2**): The stock continues to decline from the level of unexploited biomass without recovery (one-way trip).

The combinations of the operating models and the stock status identification approaches help us to answer specific questions. For example, **P2-A3** scenario demonstrates how a model structure mismatch

affects the surplus production model's stock status identification which depends on the accuracy of the estimated B_{MSY}. A factorial design of three population dynamics, two fishing histories, two data collection designs, four levels of observation error and four stock status identification approaches provides 1152 scenarios. For each scenario, the procedures of data generation and stock status assessments are repeated 200 times with stochasticity from observation error.

5.2.1.3 Performance measures

The performance of a stock status identification approach is quantified by comparing the result from each approach with the true stock status determined from the operating models. The performance indicator is the correct identification rate:

$$\text{correct identification rate} = \frac{\text{the number of years the stock status is correctly identified}}{\text{the total number of years the stock status is identified}} \times 100\% \quad (5.12)$$

We also compare the $B_{highest\_S}$ from **A2**, and estimated B_{MSY} from **A3** and **A4** with the true B_{MSY}. The relative errors of $B_{highest\_S}$ and estimated B_{MSY} are calculated as:

$$\text{relative error} = \frac{\hat{\theta} - \theta}{\theta} \quad (5.13)$$

where $\hat{\theta}$ represents the $B_{highest\_S}$ or estimated B_{MSY} and the θ represents the true B_{MSY}.

We analyze the sensitivity of $slope_{S/B}$ to the number of years used to calculate the indicator. We use data points from different numbers of previous years (7~13) to calculate $slope_{S/B}$ and compare the values with $slope_{S/B}$ calculated with data from the previous ten years (default setting). The relative difference of $slope_{S/B}$ is calculated:

$$\text{relative difference} = \frac{slope_{S/B}^{N} - slope_{S/B}^{10}}{|slope_{S/B}^{10}|} \quad (5.14)$$

where $|slope_{S/B}^{10}|$ is the absolute default calculated value of $slope_{S/B}$ and $slope_{S/B}^{N}$ is the value of $slope_{S/B}$ calculated by data from previous N years.

5.2.2 Simulation 2: Evaluating the management procedures

5.2.2.1 Harvest control rules of Gcontrol

The total allowable catch (TAC) under method *Gcontrol* is calculated step-wise as follows:

$$TAC_{preliminary} = S_y \times (1 - 2\, slope_{S/B}) \tag{5.15}$$

$$TAC_{final_y} = \begin{cases} 2 \times C_{y-1};\ TAC_{preliminary} \geq (2 \times C_{y-1}) \\ 0.5 \times C_{y-1};\ TAC_{preliminary} \leq (0.5 \times C_{y-1}) \\ TAC_{preliminary};\ (0.5 \times C_{y-1}) < TAC_{preliminary} < (2 \times C_{y-1}) \end{cases} \tag{5.16}$$

A positive $slope_{S/B}$ indicates that the stock is below B_{MSY} and $TAC_{preliminary}$ will be less than the calculated surplus production. The reverse is also true. The second step is necessary so that the final TAC is between half and twice the catch of the previous year. This rule prevents drastic changes in TAC in adjacent years, which could have large social and economic impacts for a given fishery.

5.2.2.2 Harvest control rules of five new management procedures

The harvest control rule of *Gcontrol* was modified by introducing $B_{highest\_S}$ or estimated B_{MSY} to construct three new MPs. Calculation of the TAC for the new MP using $B_{highest\_S}$ is as follows:

$$TAC_{preliminary} = S_y \times (1 - 2\, slope_{S/B}) \tag{5.17}$$

$$TAC_{final_y} = \begin{cases} 2 \times C_{y-1}; TAC_{preliminary} \geq (2 \times C_{y-1})\ and\ B_y \geq B_{highest_S} \\ C_{y-1};\ TAC_{preliminary} \geq (2 \times C_{y-1})\ and\ B_y < B_{highest\_S} \\ 0.5 \times C_{y-1};\ TAC_{preliminary} \leq (0.5 \times C_{y-1})\ and\ B_y \leq B_{highest\_S} \\ C_{y-1};\ TAC_{preliminary} \leq (0.5 \times C_{y-1})\ and\ B_y > B_{highest\_S} \\ TAC_{preliminary};\ (0.5 \times C_{y-1}) < TAC_{preliminary} < (2 \times C_{y-1}) \end{cases} \tag{5.18}$$

If the two indicators ($B_{highest\_S}$ and $slope_{S/B}$) show no contradiction in identifying the stock status, the TAC from the new MP is the same as that from *Gcontrol*. If the two indicators suggest opposite stock status and *Gcontrol* leads to the TAC either halving or doubling, the TAC will be kept unchanged in the new MP. A potential improvement of the new MP is that an inappropriate change of TAC will be stopped if the stock status is identified correctly by $B_{highest\_S}$. The other two MPs are all the same except that $B_{highest\_S}$ is replaced by estimated B_{MSY} from models.

As the biological reference point F_{MSY} can be estimated from the Schaefer or Pella-Tomlinson surplus production models, it is feasible to determine TAC from the product of F_{MSY} and observed biomass. The corresponding harvest control rule is as follows:

$$TAC_{preliminary} = B_y \times F_{MSY} \qquad (5.19)$$

$$TAC_{final_y} = \begin{cases} 2 \times C_{y-1}; TAC_{preliminary} \geq (2 \times C_{y-1}) \\ 0.5 \times C_{y-1}; TAC_{preliminary} \leq (0.5 \times C_{y-1}) \\ TAC_{preliminary}; (0.5 \times C_{y-1}) < TAC_{preliminary} < (2 \times C_{y-1}) \end{cases} \qquad (5.20)$$

We hereafter refer to the modified *Gcontrol* using $B_{highest\_S}$, B_{MSY} estimated from the Schaefer model, and B_{MSY} estimated from the Pella-Tomlinson model as *Gcontrol2*, *Gcontrol3* and *Gcontrol4.* The MPs based on the F_{MSY} estimated from the Schaefer and Pella-Tomlinson model are referred to *FSchaefer* and *FPT*, respectively.

5.2.2.3 Operating models for evaluating the six management procedures

The management procedures are compared in the MSE framework "DLMtool". Ten built-in fisheries in DLMtool are used to compare the performance of the two methods. The operating models in DLMtool are age-structured population dynamics models (Carruthers et al., 2016). Fish populations with varying

biological characteristics (e.g., longevity; Table 5.1) are simulated based on the outputs of data-rich stock assessments for North and South Atlantic Albacore (*Thunnus alalunga*; ICCAT, 2013), North Pacific blue shark (*Prionace glauca*; PIFSC, 2009), Atlantic Bluefin tuna (*Thunnus thynnus*; ICCAT, 2012), Pacific herring (*Clupea pallasii*; CSAS, 2018), Pacific canary rockfish (*Sebastes pinniger*; NWFSC, 2011a), Atlantic mackerel (*Scomber scombrus*; CSAS, 2017), red porgy (*Pagrus pagrus*; SEFSC, 2012), South Atlantic red snapper (*Lutjanus campechanus*; SEDAR, 2010), Petrale sole (*Eopsetta jordani*; NWFSC, 2011b), and South Georgia Patagonian tooth fish (*Dissostichus eleginoides*; GSGSSI, 2018). The initial biomass is set as 5%~35% of the unfished biomass to reflect the fully-exploited or overexploited status quo of most marine stocks. The observation error associated with the observed biomass is assumed to be lognormal and the standard deviation ranges from 0.25 to 0

Table 5.1. Overview of the operating models' design for different species

Attribute	Species									
	Albacore	Blue shark	Bluefin tuna	Herring	Rockfish	Mackerel	Porgy	Snapper	Sole	Tooth fish
Maximum age (Yr)	15	32	32	18	120	30	25	70	38	37
Natural mortality (Yr^{-1})*	0.35~0.45	0.15~0.25	0.20~0.28	0.28~0.38	0.04~0.08	0.15~0.3	0.20~0.25	0.07~0.11	0.13~0.22	0.13~0.20
Recruitment compensation (steepness)*	0.65~0.85	0.40~0.90	0.60~0.90	0.40~0.60	0.35~0.72	0.25~0.7	0.31~0.51	0.85~0.95	0.60~0.90	0.55~0.80
Asymptotic length (cm)*	121~135	195~205	315~325	25~29	64~68	38~42	50~54	88~92	48~54	98~104
Length at 50% maturity (cm)*	81~91	127~144	103~135	15~18	32~38	23~28	17~29	28~40	31~37	75~85
Growth rate*	0.16~0.22	0.18~0.24	0.08~0.1	0.43~0.53	0.12~0.13	0.18~0.28	0.18~0.22	0.17~0.21	0.15~0.19	0.11~0.12
Length-weight relationship (a)	1.34E-05	3.18E-06	1.96E-05	4.50E-06	1.55E-05	6.00E-06	1.05E-05	1.00E-06	2.08E-06	1.00E-06
Length-weight relationship (b)	3.16	3.13	3.01	3.13	3.03	3.15	3.08	3.07	3.47	3.07
Initial stock depletion*	0.5%~35%	0.5%~35%	0.5%~35%	0.5%~35%	0.5%~35%	0.5%~35%	0.5%~35%	0.5%~35%	0.5%~35%	0.5%~35%
Lognormal recruitment errors	0.15~0.3	0.15~0.3	0.15~0.3	0.15~0.3	0.15~0.3	0.15~0.3	0.15~0.3	0.15~0.3	0.15~0.3	0.15~0.3
Autocorrelation in recruitment	0.1~0.9	0.1~0.9	0.1~0.9	0.1~0.9	0.1~0.9	0.1~0.9	0.1~0.9	0.1~0.9	0.1~0.9	0.1~0.9

*Parameter ranges indicate that, for each simulation, the corresponding value was drawn from a uniform distribution within that particular range

For each simulation, a 50-year management period is projected forward by adopting the TAC recommendations from MPs, with catch and biomass data have been available for the ten years before the onset of management. We assume no implementation error and the TAC recommendations update every year. 100 simulations are carried out for each scenario to ensure the results are convergent.

5.2.2.4 Performance metrics

The performance of management procedures is summarized by seven metrics (Table 5.2): the ratio of average yield to the reference yield for the entire management period (Yield); the probability of long-term yield (last 10 years of projection period) is above half of the maximum sustainable yield (LTY); the probability of average annual variability in yield less than 50% (AAVY); the probability of fishing mortality less than F_{MSY} (PNO); the probability of biomass above 10% of B_{MSY} (P10); the probability of biomass above 50% of B_{MSY} (P50); and the probability of biomass above 100% of B_{MSY} (P100). The reference yield was obtained when the fishing mortality equaled F_{MSY}. These performance criteria are commonly used as objectives for fisheries management.

Table 5.2. The performance metrics of stock management based on the two data-limited methods.

Symbol	Performance metric	Remarks
Yield	Ratio of average yield to the reference yield for the entire management period	Catch level in the stock rebuilding period and the stable stock period
LTY	Probability of long-term yield (last 10 years of projection period) is above half of the maximum sustainable yield	Catch level in the stable stock period
AAVY	Probability of average annual variability in yield less than 50%	It is not desirable for catch-limits to strongly fluctuate over adjacent years.
PNO	Probability of fishing mortality less than F_{msy}	The probability of overfishing in the management period
P10	Probability of biomass above 10% of B_{msy}	The probability of stock not being severely depleted
P50	Probability of biomass above 50% of B_{msy}	The probability of stock not being severely overfished
P100	Probability of biomass above 100% of B_{msy}	The probability of stock not being overfished

5.3 Results

5.3.1 Compare $B_{highest\_S}$ and estimated B_{MSY} with true B_{MSY}

$B_{highest\_S}$ from the non-model approach (**A2**) is an accurate proxy for B_{MSY} in all three population dynamics scenarios. The two different data collection scenarios have no visible impact on the accuracy of $B_{highest\_S}$ (Fig. 5.3). That is because $B_{highest\_S}$ derived from the data at the years the biomass is around B_{MSY} is already a good approximation of B_{MSY} and will unlikely change by data collected at the years where the biomass is far from B_{MSY}. B_{MSY}s estimated from the Schaefer model are relatively accurate and precise when the operating model is developed by the same model (**P1-A3**). The Schaefer model slightly overestimates B_{MSY} when the operating model is developed by the Fox model (**P2-A3**). Compared with the Schaefer model, B_{MSY}s estimated by the Pella-Tomlinson model have larger ranges. In the scenarios where the assumed population dynamics shifted from Schaefer to Fox (**P3**), the non-model approach seems to outperform the model approaches (Fig. 5.3). The performance of the model approaches is affected by the data volume as more data lead to more accurate and precise estimations of B_{MSY}.

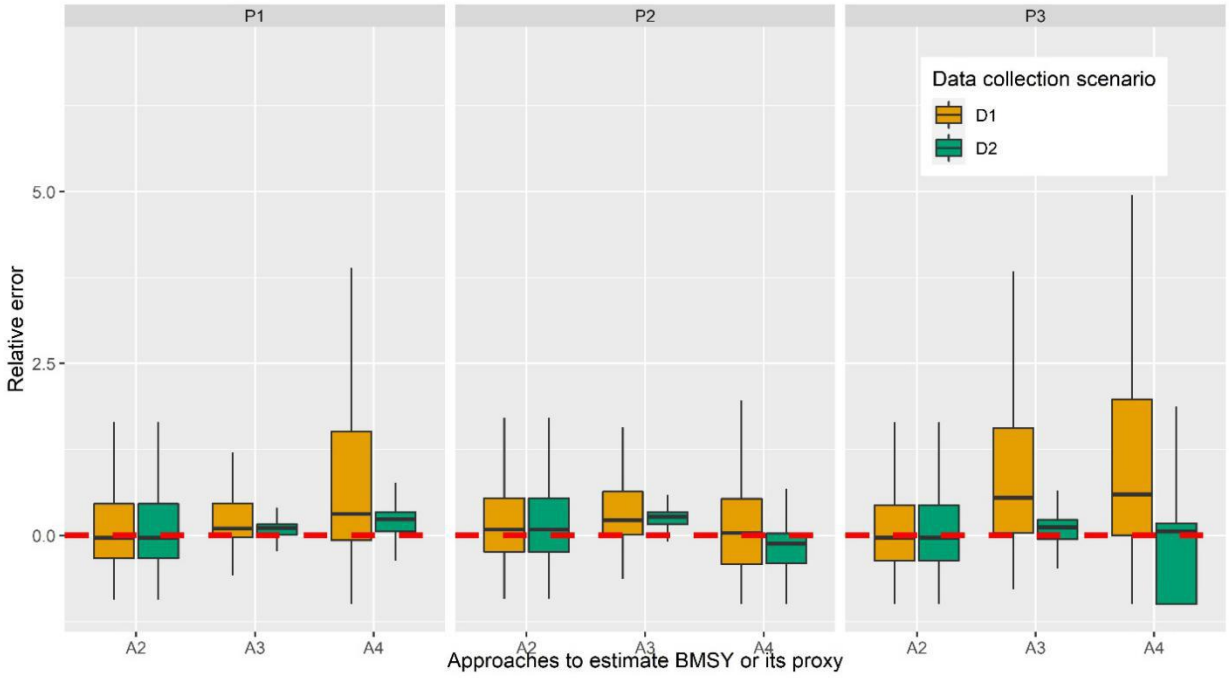

Figure 5.3. The relative error of Bhighest_S and estimated BMSY.

5.3.2 The correct stock status identification rate

Using $slope_{S/B}$ (**A1**) to identify the stock status is generally less reliable compared with the other three approaches (Fig.5.4). The exception is that **A4** (using B_{MSY} estimated form PT model) has a lower correct identification rate than **A1** in the regime shift scenarios (**P3-D2**). The data volume has no impact on **A1** as it only uses the recent ten-year data. When more data are being used (**D2** compared with **D1**), the correct identification rates of model approaches (**A3** and **A4**) are higher in **P1** and **P2,** but lower in **P3**. This may be because the historical and recent data provide inconsistent information to the models when the operating model shifted from one function form to another. For model approaches, **A3** outperforms **A4** in all scenarios. In the regime shift scenario, the non-model approach **A2** performs better than its counterparts (Fig. 5.4). The results concerning the correct stock status identification rate from the operating models based on the Pacific saury fishery are consistent with those described above (Fig. S5.6).

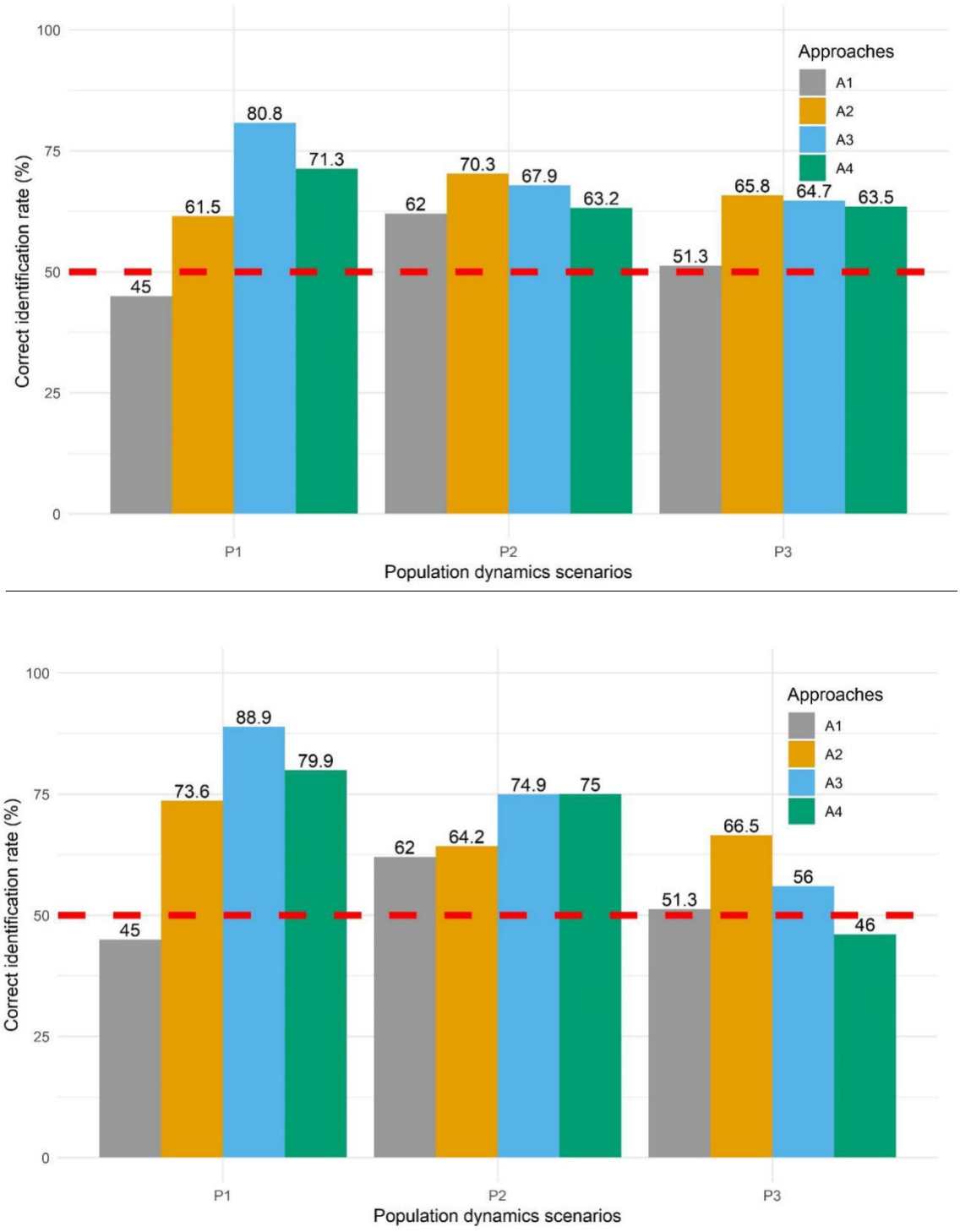

Figure 5.4. The correct stock status identification rate of four approaches in different scenarios. The upper panel summarizes the result from D1 data collection scenario. The bottom panel represents summarizes the result from D2 data collection scenario.

5.3.3 Sensitivity of $slope_{S/B}$ to the number of data points

The values of the indicator $slope_{S/B}$ are sensitive to the number of data points used to calculate the indicator. The value of $slope_{S/B}$ increases with the number of data points used in the regression analysis (Fig.5.5). The values of $slope_{S/B}$ are also affected by the level of observation error. Variation of values of $slope_{S/B}$ is greater when the standard deviation of observation error is larger (Fig. 5.5).

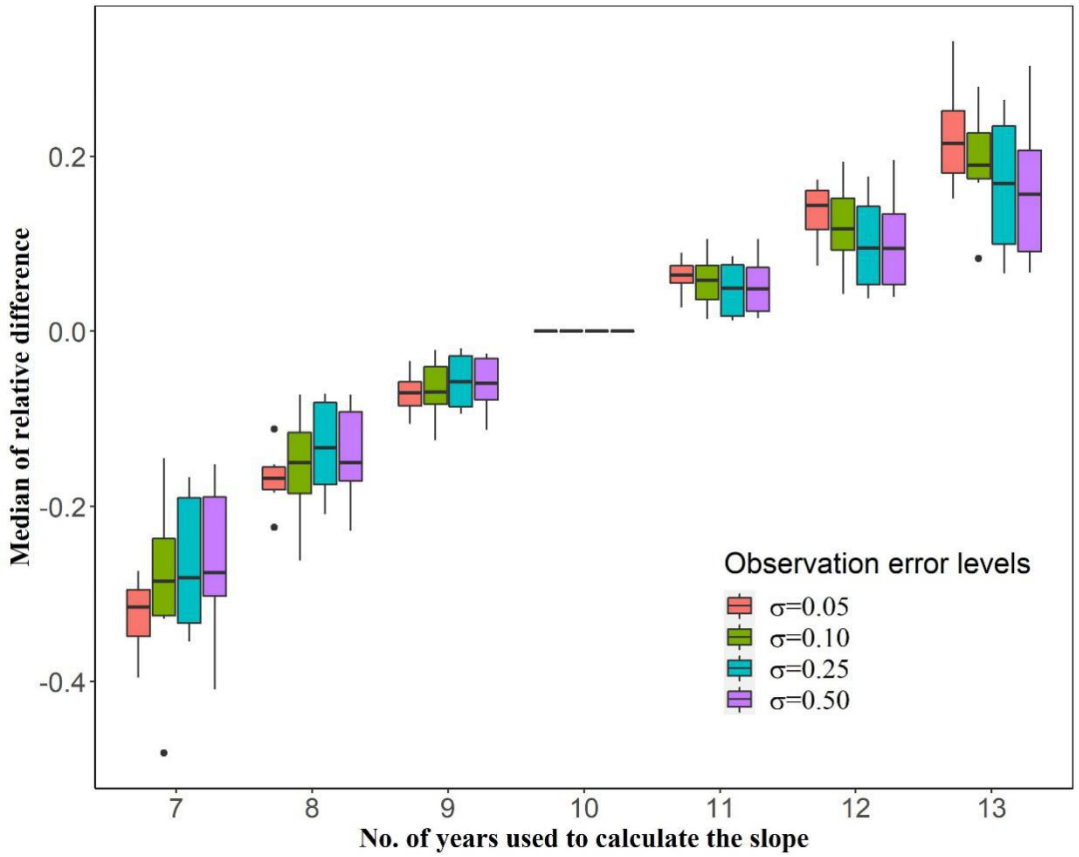

Figure 5.5. The relative difference of slopeS/B calculated by data from different number of years against default setting (ten years).

5.3.4 Performance of the four management procedures

For all simulated fisheries, TACs from *Gcontrol2*, *Gcontrol3,* and *Gcontrol4* are less variable over management years than those from *Gcontrol* (Fig. 5.6). The yields from *Gcontrol2*, *Gcontrol3,* and *Gcontrol4* are higher for all species compared with *Gcontrol*; the only exception being rockfish. The long-term yields from *Gcontrol* and its modified version are similar among different fisheries. The probabilities of long-term yields exceeding 50% of the maximum sustainable yield are 20% (Fig. 5.6). *Gcontrol* performs slightly better than its modified versions with regard to stock conservation, which means fewer chances of overfishing and a greater chance of the stock being above the three reference levels, for most fisheries except for rockfish and porgy (Fig. 5.6). *FSchaefer* and *FPT* generally provide higher yield and more long-term yield than *Gcontrol*. However, *FSchaefer* and *FPT* perform poorly in preventing overfishing and rebuilding the population. *FSchaefer* outperforms *FPT* for almost all the metrics among the different species tested (Fig. 5.7).

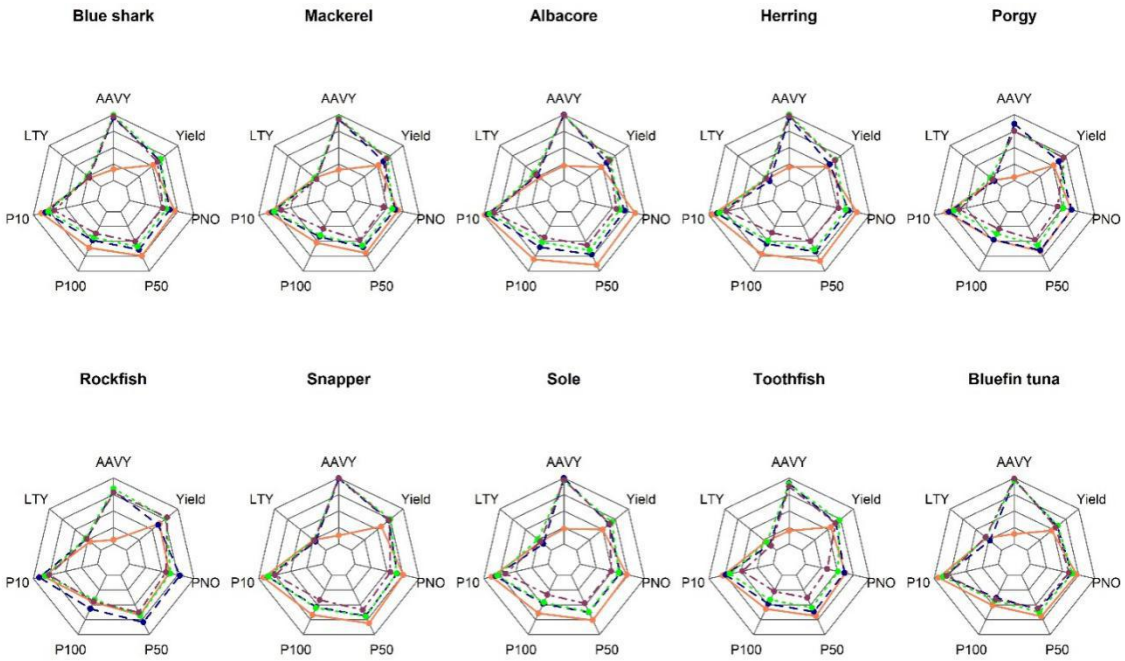

Figure 5.6. The radar chart that reflects the performance metrics of the management procedures. The orange solid line represents the performance of Gcontrol; the blue, green and purple dashed lines represent the performance of Gcontrol2, Gcontrol3, and Gcontrol4, respectively.

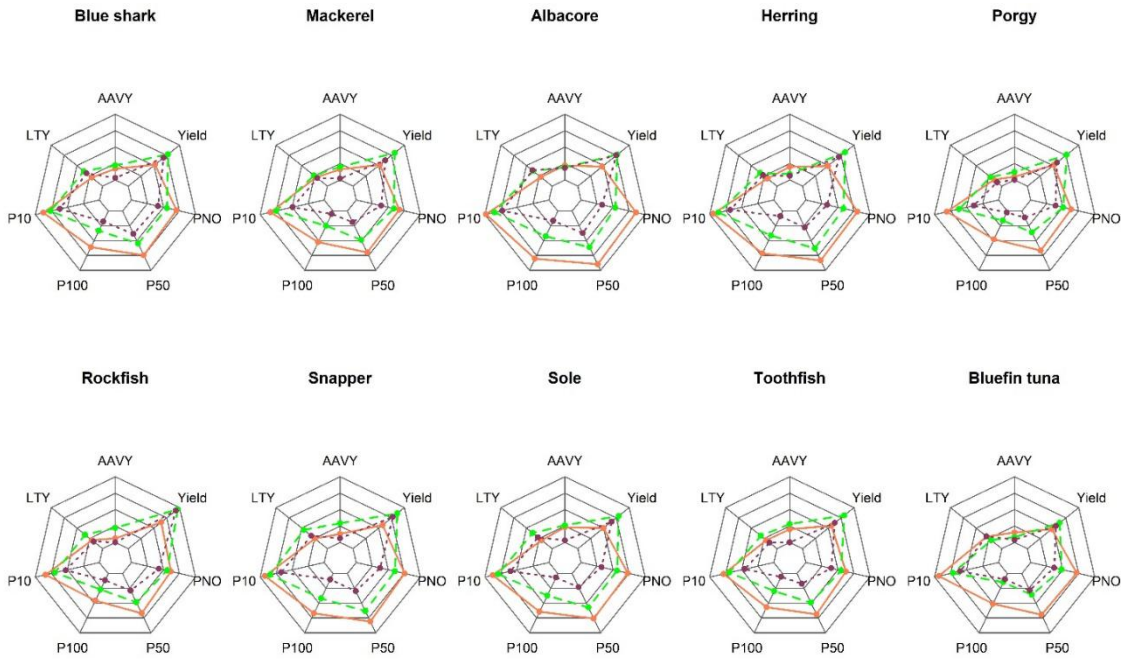

Figure 5.7. The radar chart that reflects the performance metrics of the management procedures. The orange solid line represents the performance of Gcontrol; the green and purple dashed lines represent the performance of FSchaefer and FPT, respectively

5.4 Discussion

The value of $slope_{S/B}$ is sensitive to the number of data points used in the linear regression analysis and the precision of $slope_{S/B}$ is affected by the level of observation error. These features make $slope_{S/B}$ less reliable in identifying stock status. In some scenarios of the first simulation, $slope_{S/B}$ is less likely to result in a correct stock status conclusion than a random guess (which has a 50% chance of being correct). The MP *Gcontrol* solely relying on $slope_{S/B}$ fails to take full advantage of all historical data. The MP in its default setting uses catch and biomass data from the last ten years and all the data collected before are not used to inform the harvest control rule. The consequence of this shortcoming is that TAC is determined without reference to the complete picture provided by the full use of all available information. $B_{highest\_S}$, which is derived by comparing the corresponding surplus production for all observed biomass, is proposed as an alternative indicator to identify the stock status. The simulation study demonstrates that $B_{highest\_S}$ is a more reliable indicator for identifying the stock status than $slope_{S/B}$. The modified MP *Gcontrol2* using $B_{highest\_S}$ in conjunction with $slope_{S/B}$ provides more stable and higher yields than *Gcontrol*. However, it should be noted that $B_{highest\_S}$ is a good approximation of B_{MSY} only if the data are collected in the years when the biomass is reduced to a level close to B_{MSY}.

Two forms of surplus production models are compared with the non-model approaches in this study. The result of the first simulation study reaffirms that the reliability of model output is subject to data quantity and quality, as well as fishing history. It also shows that even a modest model mismatch or temporal variation in productivity will affect the accuracy of surplus production model outputs. Estimating parameters and biological reference points by maximizing the likelihood function is a relatively sophisticated process even for structurally simplified models. Therefore, model approaches generally require accurate assumptions about population dynamics and observation error structures, and informative input data, which are often not available for data-limited fisheries.

The shape parameter in the Pella-Tomlinson model is notoriously difficult to estimate accurately. Although the function form of the Pella-Tomlinson model is more flexible (and therefore free from model mismatches in **P1** and **P2** scenarios in the first simulation) than the Schaefer model, the former generally performs worse than the latter in all the scenarios in both simulations. It indicates that appropriately simplifying model structure or restricting particular parameters within a reasonable range is sometimes necessary especially when the information provided by the input data is limited.

Non-model DLMs usually "assess" the stock and inform harvest control rules based on simple indicators (e.g., $slope_{S/B}$; $B_{highest\_S}$; mean length of catch). These DLMs are usually based on more fundamental assumptions so that they are recognized to be immune to misspecifications of fixed model functions and may be able to adapt to temporal shifts in productivity. However, using $slope_{S/B}$ to identify stock status is worse than model approaches in model mismatch and regime shift scenarios. Using $B_{highest\_S}$ to identify stock status is superior to model approaches in the regime shift scenario but not in the model mismatch scenario. The reliability of both model and non-model methods are affected by observation errors. Non-model approaches do not make explicit assumptions about the observation error distributions, which is an integral component of modeling approaches. The uncertainty of the parameters and biological reference points can be quantified and used to formulate the harvest control rule in the model approach. In non-model approaches, observation error is usually unable to be estimated and not considered in the harvest control rule. Thus, robustness to observation error is instrumental to the success of those methods, particularly because moderate to large observation errors continue to plague fisheries data.

All the information used in the harvest control rules for the said MPs is only from historical catch and biomass data. The information in conjunction with other inputs related to biological characteristics of the species could potentially create multiple other MPs. The depletion rate is a particularly valuable piece of information in data-limited fisheries given that the DLMs and corresponding MPs that utilize it (e.g.,

Depletion corrected average catch; Stock reduction analysis) generally lead to satisfactory management results (Guan et al., 2019). For many fisheries, the carrying capacity (k), which is acquired using model approaches, is unknown, but using $B_{highest\_S}$ as an approximation of B_{MSY} provides a possibility to estimate the depletion rate. Thorson et al. (2012) estimated the ratio of B_{MSY}/k for 147 marine species from different taxonomic orders. The stock depletion (B/k) can be estimated when the observed current biomass, $B_{highest\_S}$, and B_{MSY}/k are known with a certain level of precision for a given species (Thorson et al., 2012; Xu et al., 2019). Whether $B_{highest\_S}$ could improve the performance of the DLMs and MPs using stock depletion as a input needs further investigation.

CHAPTER 6

SLOW RECOVERY IN THE WAKE OF GLOBAL CRISES: INSIGHTS FROM AN ICONIC FISHERY

6.1 Introduction

Few commercial fisheries in the world have been as productive or lucrative as the American lobster (*Homarus americanus*) fishery in the Gulf of Maine. At present, it is the most valuable commercial fishery in the United States (+$600 million) and supports thousands of jobs in coastal communities (NOAA, 2020). As the fishery has expanded, so too has global trade of the crustacean (Fig. 6.1). The storied success of this fishery is particularly noteworthy given the downward trajectory of so many fisheries in the Gulf of Maine and worldwide during the last century (Jackson, 2001; Bolster, 2002). Multiple interrelated factors have contributed to its long term productivity, including physiological characteristics of the organism and its ability to withstand being caught repeatedly; hyper-optimal environmental conditions that have significantly expanded its territory; chronic overexploitation of its predators; and conservation measures employed by fishermen that have helped to preserve a robust spawning population (Le Bris et al., 2018). However, despite the remarkable durability of the lobster fishery, it has not been immune to socioeconomic shocks. Indeed, shocks are a widespread occurrence in fisheries that can be triggered by local drivers of change as well as distal impacts that affect markets where the catch is consumed (Marín et al., 2010; Gephart et al., 2017).

Our research focuses on recovery duration following crises that occurred over the last two and a half decades from 1995 to early 2020. Understanding recovery dynamics in food production systems such as those associated with the iconic lobster fishery following shocks is

critically important to developing effective strategies to ameliorate the economic, social, and even psychological impacts they place on those who depend on them for their livelihoods.

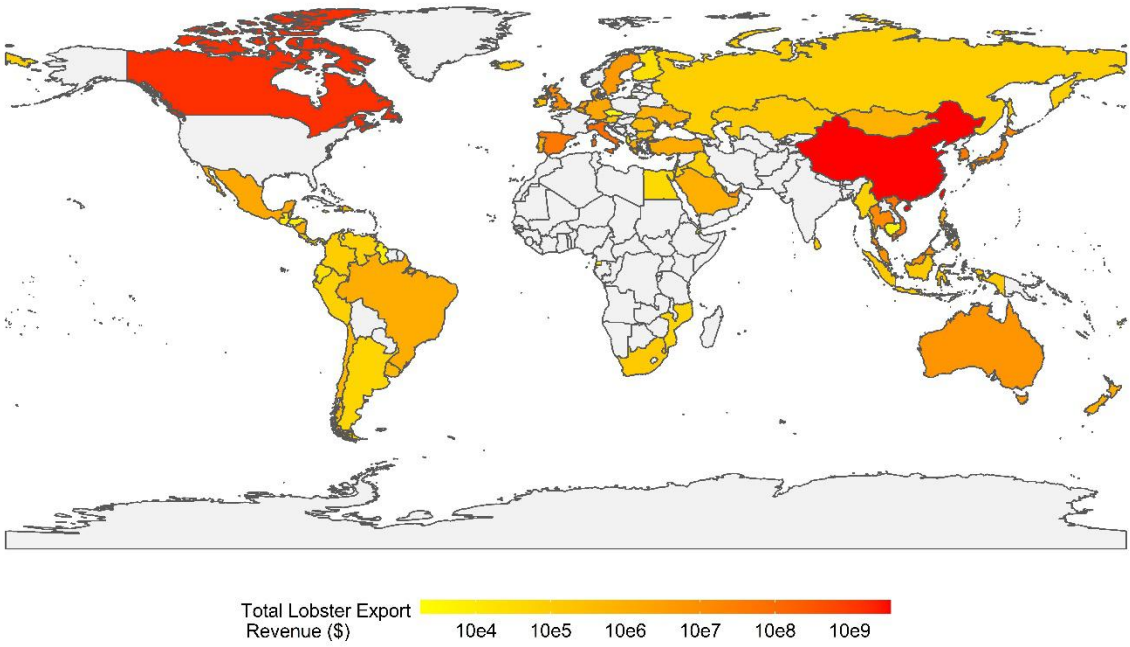

Figure 6.1. Average export (USD) of US lobster between 2017 and 2019 (Source: United Nations Comtrade).

Recovery is a key feature of resilient fisheries, which can be defined as those that are able to sustain disturbances without fundamentally changing. Systems that experience a shock generally follow a u-shaped trajectory that is punctuated by three key phases: (i) a rapid economic or ecological decline that triggers acute socioeconomic hardship and/or environmental catastrophe; (ii) a nadir at which the crisis reaches an extreme low point and begins to level-off; and (iii) a period of restoration and gradual recovery (Jesse et al., 2019). Using monthly total catch and ex-vessel revenue data for the American lobster fishery in the United States from 1995 to early 2020,

we conducted an inflation-adjusted simple moving average (SMA) analysis to evaluate recovery duration following shocks. To determine the specific timing of each shock, we paired the SMA with a review of 6,042 newspaper articles that referenced lobster from a daily newspaper in Maine. The publication was selected because its geographic focus overlaps with the coastal communities that have the highest landings of lobster in the country. These analyses allowed us to calculate the timeframe from the initial shock to the nadir of the crisis and the subsequent recovery duration from the nadir to the point at which the price recovered to the pre-crisis ex-vessel value.

6.2 Materials and methods

6.2.1 Data sources

The monthly ex-vessel price and total catch of lobster from January 1994 to March 2020 were provided by National Marine Fisheries Service (NMFS) of National Oceanic and Atmospheric Administration (NOAA). The data are collected in eight coastal states including Maine, New Hampshire, Massachusetts, Rhode Island, New York, New Jersey, Maryland, and Virginia.The monthly consumer price index (CPI) inflation rate data from January 1994 to March 2020 were provided by U.S. Bureau of Labor Statistics. The stock spawning biomass (SSB) data were from the 2015 benchmark stock assessment of lobster conducted and reviewed by Atlantic States Marine Fisheries Commission. Newspaper abstracts from the Bangor Daily were downloaded from ProQuest (Maine) from 1990 to 2020.

6.2.2 Correlation of monthly lobster price in different states across the United States

The correlation of the monthly ex-vessel price of lobster in different states were analyzed by Pearson correlation coefficient.

6.2.3 Price adjustment by CPI inflation rate

The CPI inflation rate data were used to adjust the monthly ex-vessel price to the same level of December 2019 (note the prices from January to March 2020 were not adjusted as the CPI was not released at the time of doing the analysis).

6.2.4 Simple moving average

Simple moving average (SMA) analysis was conducted to help us to catch the trend of the price. SMA price was calculated as follows:

$$\mathrm{SMA}_i = \frac{p_{i-n} + p_{i-n+1} + \ldots + p_{i-1}}{n}$$

where SMA_i is the moving average ex-vessel price of lobster in the *n* months prior to month-year *i* and p_i is the inflation-adjusted monthly ex-vessel price of lobster in month-year *i*. The length of the moving window, *n,* was set to 12 months to reduce the effects of monthly price fluctuations.

6.2.5 Newspaper article review

Newspaper titles and abstracts were downloaded and coded thematically based on the focus on the article to contextualize how the lobster fishery was responding to social, economic, and environmental events.

6.3 Results

The results show a strong correlation of the price between states (Fig. 6.2). Therefore, we aggregated the data in different states and calculated the monthly price by using total revenue divided by total catch.

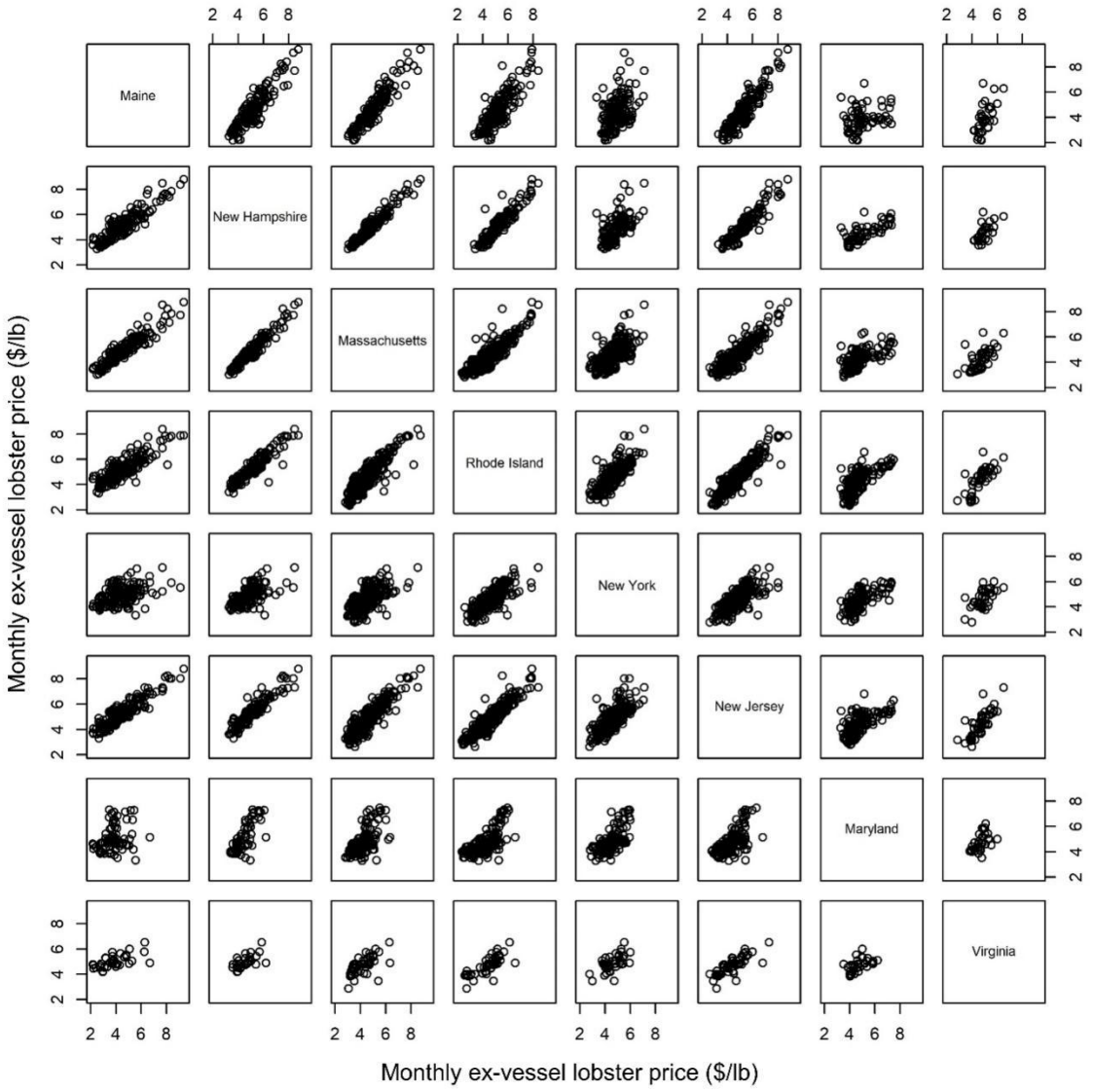

Figure 6.2. The monthly ex-vessel lobster price paired by different states

Our analysis shows that three shocks have caused the ex-vessel price of lobster to precipitously drop during our 25-year study period; each corresponds with a well-documented shock that has been previously characterized as a "crisis" by those involved in the fishery (Fig.

6.2). Each of these crises can be attributed to a specific socioeconomic or social-environmental event that ultimately altered trade dynamics. The first crisis occurred in 2001 and corresponds to the turbulence caused by the World Trade Center attacks in New York City in September 2001. Leading up to this event, the average ex-vessel price for lobster from January 1995 to August 2001 was $6.09 per pound; following the event, the price fell 14.8% over a 11 month-period. The relationships between lobster trade and the World Trade Center attack may seem tenuous, but in the wake of the event, air travel decreased significantly, causing airlines to downsize their operations, which meant that there was less cargo space to export live lobsters and less demand, in general, for high-end seafood. Following the crisis, it took an additional 16 months for ex-vessel price to return to pre-shock level (price reached $6.16 per pound in June 2003).

A second more prolonged price drop occurred as a result of the Great Recession that began in 2007. Prior to the start of the recession, the average monthly per pound price for lobster from July 2003 to November 2007 was $6.37 per pound. This is higher than the average price from January 1995 to August 2001. However, from December 2007 onward, the average price of lobster decreased over a 31-month period, reaching its lowest price of $4.24 per pound in June 2010. Prices then started to show signs of recovering, increasing for several months, before experiencing a third price drop, which reached a historical low of $4.19 per pound. This latter decline happened in association with an ocean warming anomaly in the Gulf of Maine that caused lobsters to molt a month earlier than normal (Mills et al., 2012). The event resulted in a spike in landings early in the season, which disrupted the long-standing trade dynamic between the United States and Canada by flooding the marketplace and overwhelming the Canadian-based lobster processing plants (Stoll et al., 2018). As a result, prices were so low that fishermen worked together to temporarily halt fishing in an attempt to reduce supply and re-establish the

market in Canada. In contrast to the crisis following the World Trade Center attack, which resulted in a 11-month decline, followed by a relatively short recovery period of 16 months, the crisis caused by the Great Recession and subsequent US-Canada lobster trade conflict was much more severe, resulting in a 33.4% decrease in price over 31 months and a recovery period that is ongoing after 144 months.

Importantly, the three price drops and their associated socioeconomic impacts were not caused by a decline in lobster catch or stock biomass (Fig. 6.3). Instead these crises were driven by socioeconomic and social-environmental shocks. In 2001, the lobster industry's ability to export product was severely limited as a result of reduced air travel and cargo space availability; in 2007 and 2008, the Great Recession dramatically decreased demand for luxury products worldwide; and in 2012, the processing sector in Canada was overwhelmed by the influx of lobsters early in the fishing season. Early signs from COVID-19 indicate that a fourth crisis may be imminent. Without appropriate policies to mitigate the rate of decline, the price is on track to reach a historical low within half a year.

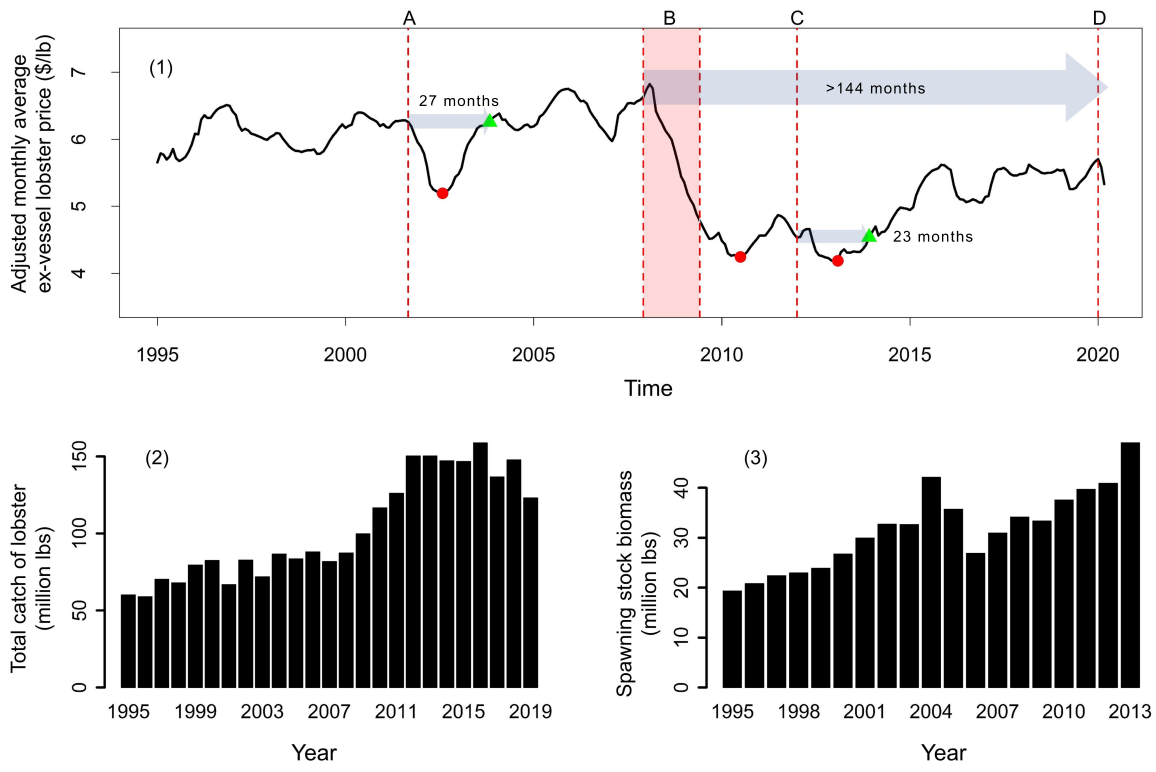

Figure 6.3. (Top) (1) Inflation-adjusted moving average monthly ex-vessel price of American lobster in the United States. Vertical red dashed lines denote shocks associated with: (A) World Trade Center attack; (B) Great Recession [note this event spanned several years as indicated by the shaded area between dashed lines]; (C) US-Canada lobster trade conflict; and (D) COVID-19 pandemic. Red circles represent price nadir in the aftermath of each shock. Green triangles show point at which recovery to pre-shock price occurs. The number of months from shock to nadir and recovery are indicated by blue arrows. (Bottom): Total catch (2) and spawning stock biomass (3) for American lobster over approximately the same time period show trends that are de-coupled from ex-vessel price.

6.4 Discussion

In the wake of shocks to fisheries and other food production systems, short-term mitigation is often emphasized. For example, the U.S. federal government alone has distributed $1.1 billion to fishing communities and industry stakeholders for disaster-related mitigation following fisheries related crises since 1990. These stop-gap measures are critically important. However, our findings show that shocks in fisheries can have long-term consequences that persist for extended periods of time. In the case of the lobster fishery, the impact of the Great Recession has persisted for 12 years and full recovery has not yet been achieved, in part because recovery stalled due to a local shock to the system. Although significant public and private investments are made to help fishing sectors in the wake of crises, relatively limited attention has been given to recovery duration. Understanding that recovery can be a slow process suggests that there may be utility in rethinking the model for providing disaster support to fishing sectors experiencing crises, for example, considering a "time release" approach that distributes resources more gradually through the extent of recovery rather than large and immediate injections of resources. Alternative approaches like this may be particularly important for global shocks such as the Great Recession, and likely the COVID-19 pandemic, which may have a prolonged effect on fisheries.

CHAPTER 7

CONCLUDING REMARKS

The dissertation has discussed four different sources of uncertainties commonly seen in fishery stock assessment and management. Using simulations and case studies, we have compared existing methods, proposed new methods in some cases, and recommended statistical methods and management strategies that can better quantify the uncertainties or that are potentially more robust to the uncertainties.

In chapter 2, we have demonstrated that the outliers caused by atypical observation error in the biomass index data can be identified by evaluating residuals in a robust-distribution-based estimator for surplus production models. By removing the detected outliers in biomass index data, though in some cases there are still undetected outliers in the data or some good data points are removed, the performance in parameter estimation is generally improved. The biomass index data have been widely used as an input in different stock assessment models. We suggest that this method can potentially be used to provide a higher-quality input for more sophisticated stock assessment models (e.g., ASAP, SAM, SS3).

This simulation study in chapter 3 shows that the state-space production model generally outperforms the observation-error estimator when process, observation and model errors are all assumed in the operating model. However, differences in performance between these two estimators decrease with increased model errors. The observation-error estimator could even outperform the state-space model when the model errors became large. Therefore, ensuring low model errors is critical for state-space models to perform well. It is found that the ratio of process error standard deviation to observation error standard deviation could affect their estimates. This finding was also reported by Auger-méthé et al (2016) for a state-space

Gompertz model. The question of how to accurately estimate process and observation error standard deviations in a state-space production model remains. The impact of different error levels on model performance is evaluated using a GLM. This approach allows managers to understand the relative values of reducing different errors. Reducing the observation error of a biomass index often requires increasing sample effort, which may be economically and/or logically difficult. Many studies for optimizing survey designs aim to find a balance between the costs of the survey and the quality of the observed data. The evaluation of the link between the quality of the observed data and the reliability of the model outputs can serve as additional information to those tasks with designing surveys.

In chapter 4, two simulations have been conducted to compare a suite of surplus-production-based data-limited methods (DLMs) and management procedures (MPs). The first simulation is to evaluate the performance of the surplus production model (Schaefer and Pella-Tomlinson) and indicator approach ($slope_{S/B}$ and $B_{highest\_S}$) on identifying stock status. The precision of $slope_{S/B}$, which is a coefficient of the linear regression between the calculated surplus production and the observed biomass in recent years, is sensitive to the number of data points used in the regression and is greatly affected by the observation error. Using $slope_{S/B}$ to identify the stock status is generally less reliable compared with the other three approaches. In the scenario where the population productivity shifts from one level to another, $B_{highest\_S}$, which is the biomass at which surplus production was at its highest, performs better than the model approaches on identifying stock status. The second simulation is conducted to compare the five new-proposed MPs with *Gcontrol*, which provides catch limits recommendations solely relying on $slope_{S/B}$. Using $B_{highest\_S}$ or estimated B_{MSY} in conjunction with $slope_{S/B}$ in the harvest control rule provides more stable and higher yields than *Gcontrol*. Catch limits determined by the

product of estimated F_{MSY} and current biomass generally lead to higher yield but perform poorly in preventing overfishing and rebuilding the population.

In chapter 5, a simulation study has been conducted to demonstrate that the routine survey data processing approach of aggregating all observations into a single annual biomass index causes fitting problems for state-space models. Such practice loses considerable information on parameters and undermines state-space models' ability to distinguish between process error and observation error. Using multiple time series of biomass index as model inputs substantially improves the performance of state-space models and especially improves the accuracy of the error estimates. Without additional sampling efforts, appropriately adjusting the protocol of processing survey data can gain considerable benefits when state-space models are used for fishery stock assessment.

In Chapter 6, we have applied an inflation-adjusted simple moving average analysis of the monthly ex-vessel price of American lobster in tandem with a content analysis of more than 6,000 newspaper articles about lobster to systematically analyze the recovery process following socioeconomic shocks of different magnitude over a 25-year time frame from 1995 to early 2020. Results show that recovery duration ranges from 23 months to more than 12 years and the process can be stalled by compounding local and regional disturbances. Understanding that recovery can be a slow process suggests that there may be utility in rethinking the model for providing disaster support to fishing sectors experiencing crises, for example, considering a "time-release" approach that distributes resources more gradually through the extent of recovery rather than large and immediate injections of resources. Alternative approaches like this may be important for the industry to confront future socioeconomic uncertainties.

BIBLIOGRAPHY

Anderson, S.C., Branch, T.A., Cooper, A.B., and Dulvy, N.K. 2017. Black-swan events in animal populations. Proc. Natl. Acad. Sci. 114: 3252-3257.

Andrew, N. 1999. Stock Assessment of Paua in PAU5 and 7. Progress Report for Ministry of Fisheries Research Project PAU9701. NIWA, Wellington, New Zealand, 35 pp.

Auger-Méthé, M., Field, C., Albertsen, C. M., Derocher, A. E., Lewis, M. A., Jonsen, I. D., and Mills F. J. 2016. State-space models' dirty little secrets: even simple linear Gaussian models can have estimation problems. Sci. Rep. 6: 26677.

Barnett V., and Lewis T. 1994. Outliers in Statistical Data 3rd edition. John Wiley and Sons, New York.

Berg, C.W., and Nielsen, A. 2016. Accounting for correlated observations in an age-based state-space stock assessment model. ICES J. Mar. Sci. J. du Cons. 73: 1788-1797.

Bolster, J. 2002. The Mortal Sea: Fishing the Atlantic in the Age of Sail. Harvard University Press, New York.

Brian, D., Ponciano, J.M., and Taper, M.L. 2010. Replicated sampling increases efficiency in monitoring biological populations. Ecology 91: 610-620.

Cadigan, N.G. 2016. A state-space stock assessment model for northern cod, including under-reported catches and variable natural mortality rates. Can. J. Fish. Aquat. Sci. 73: 296-308.

Cao, J., Thorson, J.T., Punt, A.E., and Szuwalski, C. 2020. A novel spatiotemporal stock assessment framework to better address fine-scale species distributions: Development and simulation testing. Fish Fish. 21: 350-367.

Carruthers, T.R., and Hordyk, A.R. 2018. The Data-Limited Methods Toolkit (DLMtool): An R package for informing management of data-limited populations. Methods Ecol. Evol. 9: 2388-2395.

Carruthers, T.R., Kell, L.T., Butterworth, D.D.S., Maunder, M.N., Geromont, H.F., Walters, C., McAllister, M.K., Hillary, R., Levontin, P., Kitakado, T., and Davies, C.R. 2016. Performance review of simple management procedures. ICES J. Mar. Sci. 73: 464-482.

Carruthers, T.R., Punt, A.E., Walters, C.J., MacCall, A., McAllister, M.K., Dick, E.J., and Cope, J. 2014. Evaluating methods for setting catch limits in data-limited fisheries. Fish. Res. 153: 48-68.

Chen, Y. 2003. Quality of fisheries data and uncertainty in stock assessment. Sci. Mar. 67: 75-87.

Chen, Y., and Andrew, N. 1998. Parameter estimation in modelling the dynamics of fish stock biomass: are currently used observation-error estimators reliable? Can. J. Fish. Aquat. Sci. 55: 749-760.

Chen, Y., and Fournier, D. 1999. Impacts of atypical data on Bayesian inference and robust Bayesian approach in fisheries. Can. J. Fish. Aquat. Sci. 56: 1525-1533.

Chen, Y., Breen, P.A., and Andrew, N.L. 2000. Impacts of outliers and misspecification of priors on Bayesian fisheries-stock assessment. Can. J. Fish. Aquat. Sci. 57: 2293-2305.

Chen, Y., Jiao, Y., and Chen, L. 2003. Developing robust frequentist and Bayesian fish stock assessment methods. Fish Fish. 4: 105-120.

CSAS. 2017. Assessment of the Atlantic mackerel stock for the Northwest Atlantic (subareas 3 and 4) in 2016. Available at: https://waves-vagues.dfo-mpo.gc.ca/Library/40619576.pdf. (accessed 31 March 2020).

CSAS. 2018. Stock assessment for pacific herring in British Columbia in 2017 and forecast for 2018. Available at: https://waves-vagues.dfo-mpo.gc.ca/Library/40687752.pdf. (accessed 31 March 2020).

DAFF. 2007. Commonwealth Fisheries Harvest Strategy: Policy and Guidelines. Australian Government, Department of Agriculture, Fisheries and Forestry, Available at: https://www.issuelab.org/resources/17772/17772.pdf (accessed 31 March 2020).

de Valpine, P. 2002. Review of methods for fitting time-series models with process and observation error and likelihood calculations for nonlinear, non-Gaussian state-space models. Bull. Mar. Sci. 70: 455-471.

de Valpine, P. 2004. Monte Carlo state-space likelihoods by weighted posterior kernel density estimation. J. Am. Stat. Assoc. 99: 523-536.

de Valpine, P., and Hastings, A. 2002. Fitting population models incorporating process noise and observation error. Ecol. Monogr. 72: 57-76.

de Valpine, P., and Hilborn, R. 2005. State-space likelihoods for nonlinear fisheries time-series. Can. J. Fish. Aquat. Sci. 62: 1937-1952.

Dennis, B., Ponciano, J.M., Lele, S.R., Taper, M.L., and Staples, D.F. 2006. Estimating density dependence, process noise, and observation error. Ecol. Monogr. 76: 323-341.

Denwood, M.J. 2016. runjags: An R package providing interface utilities, model templates, parallel computing methods and additional distributions for MCMC models in JAGS. J. Stat. Softw. 71: 1-24.

Deroba, J.J., Butterworth, D.S., Methot, R.D., De Oliveira, J.A.A., Fernandez, C., Nielsen, A., Cadrin, S.X., Dickey-Collas, M., Legault, C.M., Ianelli, J., Valero, J.L., Needle, C.L., O'Malley, J.M., Chang, Y., Thompson, G.G., Canales, C., Swain, D.P., Miller, D.C.M., Hintzen, N.T., Bertignac, M., Ibaibarriaga, L., Silva, A., Murta, A., Kell, L.T., de Moor, C.L., Parma, A.M., Dichmont, C.M., Restrepo, V.R., Ye, Y., Jardim, E., Spencer, P.D., Hanselman, D.H., Blaylock, J., Mood, M., and Hulson, P.F. 2015. Simulation testing the robustness of stock assessment models to error: some results from the ICES strategic initiative on stock assessment methods. ICES J. Mar. Sci. 72: 19-30.

Dowling, N.A., Smith, A.D.M., Smith, D.C., Parma, A.M., Dichmont, C.M., Sainsbury, K., Wilson, J.R., Dougherty, D.T., and Cope, J.M. 2019. Generic solutions for data-limited fishery assessments are not so simple. Fish Fish. 20: 174-188.

Fournier, D.A. 1996. AUTODIFF: A C++ Array Language Extension with Automatic Differentiation for Use in Non-linear Modelling and Statistics. Otter Research Ltd, Nanaimo BC, Canada, 98 pp.

Fournier, D.A., Sibert, J.R., Majkowski, J., and Hampton, J. 1990. MULTIFAN a likelihood-based method for estimating growth parameters and age composition from multiple length frequency data sets illustrated using data for Southern Bluefin Tuna (*Thunnus maccoyii*). Can. J. Fish. Aquat. Sci. 47: 301-317.

Fournier, D.A., Skaug, H.J., Ancheta, J., Ianelli, J., Magnusson, A., Maunder, M.N., Nielsen, A., and Sibert, J. 2012. AD Model Builder: Using automatic differentiation for statistical inference of highly parameterized complex nonlinear models. Optim. Methods Softw. 27: 233-249.

Francis, R.I.C.C., and Shotton, R. 1997. “Risk” in fisheries management: a review. Can. J. Fish. Aquat. Sci. 54: 1699-1715.

Froese, R., Demirel, N., Coro, G., Kleisner, K.M., and Winker, H. 2017. Estimating fisheries reference points from catch and resilience. Fish Fish. 18: 506-526.

Froese, R., Zeller, D., Kleisner, K., and Pauly, D. 2012. What catch data can tell us about the status of global fisheries. Mar. Biol. 159: 1283-1292.

Fulton, E.A., Link, J.S., Kaplan, I.C., Savina-Rolland, M., Johnson, P., Ainsworth, C., Horne, P., Gorton, R., Gamble, R.J., Smith, A.D.M., and Smith, D.C. 2011. Lessons in modelling and management of marine ecosystems: The Atlantis experience. Fish Fish. 12: 171-183.

Gephart, J.A., Deutsch, L., Pace, M.L., Troell, M., and Seekell, D.A. 2017. Shocks to fish production: Identification, trends, and consequences. Glob. Environ. Change 42: 24-32.

Geromont, H.F., and Butterworth, D.S. 2014. Generic management procedures for data-poor fisheries: Forecasting with few data. ICES J. Mar. Sci. 72: 251-261.

GSGSSI. 2018. South Georgia Patagonian Toothfish longline public certification report. Available at:https://cert.msc.org/FileLoader/FileLinkDownload.asmx/GetFile?encryptedKey=THAdw8qXIMV6cRGtXachp+vqgd99s8Gzg2xczcpAWdpxj7J4vC9O6/B5RVyGq4MG. (accessed 31 March 2020).

Guan, L., Chen, Y., Boenish, R., Jin, X., and Shan, X. 2019. Improving data-limited stock assessment with sporadic stock index information in stock reduction analysis. Can. J. Fish. Aquat. Sci. 77: 139-142.

Haddon, M. 2011. Modelling and Quantitative Methods in Fisheries. Taylor & Francis Group, Boca Raton.

Hampel, F.R., Ronchetti, E.M., Rousseeuw, P.J., and Stahel, W.A. 1986. Robust Statistics: The Approach Based on Influence Functions. John Wiley and Sons, New York.

Hilborn, R., and Walters, C.J. 1992. Quantitative Fisheries Stock Assessment Choice, Dynamic and Unvertainty. Chapman and Hall, London.

Hinrichsen, R.A. 2011. The importance of influence diagnostics: examples from Snake River chinook salmon spawner-recruit models. Can. J. Fish. Aquat. Sci. 58: 551-559.

Hordyk, A. R., Huynh, Q. C., and Carruthers, T. R. 2019. Misspecification in stock assessments: common uncertainties and asymmetric risks. Fish Fish. 20: 888-902.

Hordyk, A.R., Ono, K., Prince, J.D., and Walters, C.J. 2016. A simple length-structured model based on life history ratios and incorporating size-dependent selectivity: application to spawning potential ratios for data-poor stocks. Can. J. Fish. Aquat. Sci. 73: 1787-1799.

ICCAT. 2012. Report of the 2012 Atlantic bluefin tuna stock assessment. Available at: https://www.iccat.int/Documents/Meetings/Docs/2012_BFT_ASSESS.pdf. (accessed 31 March 2020).

ICCAT. 2013. Report of the 2013 ICCAT north and south albacore stock assessment. Available at: https://www.iccat.int/Documents/Meetings/Docs/2013_ALB_ASSESS_REP_ENG.pdf. (accessed 31 March 2020).

Jackson, J.B.C., Kirby, M.X., Berger, W.H., Bjorndal, K.A., Botsford, L.W., Bourque, B.J., Bradbury, R.H., Cooke, R., Erlandson, J., Estes, J.A., Hughes, T.P., Kidwell, S., Lange, C.B., Lenihan, H.S., Pandolfi, J.M., Peterson, C.H., Steneck, R.S., Tegner, M.J., Warner, R.R. 2001. Historical Overfishing and the Recent Collapse of Coastal Ecosystems. Science. 293: 629-638.

Jesse, B., Heinrichs, H.U., and Kuckshinrichs, W. 2019. Adapting the theory of resilience to energy systems: a review and outlook. Energ. Sustain. Soc. 9: 1-19.

Kell, L.T., Mosqueira, I., Grosjean, P., Fromentin, J.M., Garcia, D., Hillary, R., Jardim, E., Mardle, S., Pastoors, M.A., Poos, J.J., Scott, F., and Scott, R.D. 2007. FLR: an open-source framework for the evaluation and development of management strategies. ICES J. Mar. Sci. 64: 640-646.

Kimura, D.K., Balsiger, J.W., and Ito, D.H. 1996. Kalman filtering the delay-difference equation: practical approaches and simulations. Fish. Bull. 94: 678-691.

Knape, J., Jonzén, N., and Sköld, M. 2011. On observation distributions for state space models of population survey data. J. Anim. Ecol. 80: 1269-1277.

Kristensen, K., Nielsen, A., Berg, C.W., Skaug, H., and Bell, B. 2016. TMB: Automatic differentiation and Laplace approximation. J. Stat. Softw. 70: 1-21.

Le Bris, A., Mills, K.E., Wahle, R.A., Chen, Y., Alexander, M.A., Allyn, A.J., Schuetz, J.G., Scott, J.D., and Pershing, A.J. 2018. Climate vulnerability and resilience in the most valuable North American fishery. Proc. Natl. Acad. Sci. USA. 115: 1831-1836.

Ludwig, D., and Walters, C. J. 1981. Measurement errors and uncertainty in parameter estimates for stock and recruitment. Can. J. Fish. Aquat. Sci. 38: 711-720.

Magnusson, A., Punt, A. E., and Hilborn, R. 2013. Measuring uncertainty in fisheries stock assessment: the delta method, bootstrap, and MCMC. Fish Fish. 14: 325-342.

Marín, A., Gelcich, S., Araya, G., Olea, G., Espíndola, M., and Castilla, J.C. 2010. The 2010 tsunami in Chile Devastation and survival of coastal small-scale fishing communities. Mar. Policy. 34: 1381-1384.

Methot, R.D., and Wetzel, C.R. 2013. Stock synthesis: A biological and statistical framework for fish stock assessment and fishery management. Fish. Res. 142: 86-99.

Meyer, R., and Millar, R.B., 1999. BUGS in Bayesian stock assessments. Can. J. Fish. Aquat. Sci. 56: 1078-1087.

MFNZ. 2008. Harvest Strategy Standard for New Zealand Fisheries. Ministry of Fisheries, Wellington, New Zealand, Available at: https://www.mpi.govt.nz/dmsdocument/728-harvest-strategy-standard-for-new-zealand-fisheries (accessed 31 March 2020).

Millar, R.B., and Meyer, R. 2000. Non-linear state space modelling of fisheries biomass dynamics by using Metropolis-Hastings within-Gibbs sampling. J. R. Stat. Soc. Ser. C. 49: 327-342.

Miller, S.K., Anganuzzi, A., Butterworth, D.S., Davies, C.R., Donovan, G.P., Nickson, A., Rademeyer, R.A., and Restrepo, V. 2019. Improving communication: the key to more effective MSE processes. Can. J. Fish. Aquat. Sci. 76: 643-656.

Mills, K.E., Pershing, A.J., Brown, C.J., Chen, Y., Chiang, F., Holland, D.S., Lehuta, S., Nye, J.A., Sun, J.C., Thomas, A.C., and Wahle, R.A. 2013. Fisheries management in a changing climate: Lessons from the 2012 ocean heat wave in the Northwest Atlantic. Oceanog. 26: 191-195.

Motulsky, H.J., and Brown, R.E. 2006. Detecting outliers when fitting data with nonlinear regression: a new method based on robust nonlinear regression and the false discovery rate. BMC Bioinform. 20: 1-20.

MSA. 2007. Magnuson-Stevens Fishery Conservation and Management Act, Public Law 94–265. As amended by the Magnuson-Stevens Fishery Conservation and Management Reauthorization Act, Available at: https://www.nefmc.org/files/msa_amended_2007.pdf (accessed 31 March 2020).

Newman, D., Berkson, J., and Suatoni, L. 2015. Current methods for setting catch limits for data-limited fish stocks in the United States. Fish. Res. 164: 86-93.

Nielsen, A., and Berg, C.W. 2014. Estimation of time-varying selectivity in stock assessments using state-space models. Fish. Res. 158: 96-101.

Nigmatullin, C.M., Nesis, K.N., and Arkhipkin, A.I. 2001. A review of the biology of the jumbo squid *Dosidicus gigas* (Cephalopoda: *Ommastrephidae*). Fish. Res. 54: 9-19.

NOAA. 2020. Fisheries of the United States. Available at: https://www.fisheries.noaa.gov/national/sustainable-fisheries/fisheries-united-states (accessed 31 March 2020).

NPFC. 2018. Updates of Pacific saury (*Cololabis saira*) stock assessment in the North Pacific Ocean. Available at: https://www.npfc.int/updates-pacific-saury-cololabis-saira-stock-assessment-north-pacific-ocean-china. (accessed 31 June 2020)

NWFSC. 2011a. Rebuilding analysis for canary rockfish based on the 2011 updated stock assessment. Available at: https://www.pcouncil.org/documents/2011/10/rebuilding-analysis-for-canary-rockfish-based-on-the-2011-updated-stock-assessment-october-2011.pdf/. (accessed 31 March 2020).

NWFSC. 2011b. 2011 petrale sole rebuilding analysis. Available at: https://www.pcouncil.org/documents/2011/11/2011-petrale-sole-rebuilding-analysis-november-23-2011.pdf/ (accessed 31 March 2020).

Ono, K., Punt, A. E., and Rivot, E. 2012. Model performance analysis for Bayesian biomass dynamics models using bias, precision and reliability metrics. Fish. Res. 125: 173-183.

Pedersen, M.W., and Berg, C.W. 2017. A stochastic surplus production model in continuous time. Fish Fish. 18: 226-243.

PIFSC. 2009. North pacific blue shark assessment. Available at: https://origin-apps-pifsc.fisheries.noaa.gov/library/pubs/tech/NOAA_Tech_Memo_PIFSC_17.pdf. (accessed 31 March 2020).

Polacheck, T., Hilborn, R., and Punt, A.E. 1993. Fitting surplus production models: comparing methods and measuring uncertainty. Can. J. Fish. Aquat. Sci. 50: 2597-2607.

Punt, A. E. 2003. Extending production models to include process error in the population dynamics. Can. J. Fish. Aquat. Sci. 60: 1217-1228.

Punt, A.E., and Szuwalski, C. 2012. How well can F_{MSY} and B_{MSY} be estimated using empirical measures of surplus production? Fish. Res. 136: 113-124.

Punt, A.E., Butterworth, D.S., de Moor, C.L., de Oliveira, J.A.A., and Haddon, M. 2014. Management strategy evaluation: best practices. Fish Fish. 17: 303-334.

Punt, A.E., Butterworth, D.S., de Moor, C.L., De Oliveira, J.A.A., and Haddon, M. 2016. Management strategy evaluation: best practices. Fish Fish. 17: 303-334.

Quinn, T.J. II, and Deriso, R.B. 1999. Quantitative Fish Dynamics. Oxford University Press, New York.

Reed, W.J. 1986. Analyzing catch–effort data allowing for randomness in the catching process. Can. J. Fish. Aquat. Sci. 43: 174-186.

Rousseeuw, P.J. and Leroy, A.M. 1987. Robust Regression and Outlier Detection. Wiley, New York.

Rudd, M.B., and Thorson, J.T. 2018. Accounting for variable recruitment and fishing mortality in length-based stock assessments for data-limited fisheries. Can. J. Fish. Aquat. Sci. 75: 1019-1035.

Sagarese, S.R., Harford, W.J., Walter, J.F., Bryan, M.D., Isely, J.J., Smith, M.W., Goethel, D.R., Rios, A.B., Cass-Calay, S.L., Porch, C.E., Carruthers, T.R., and Cummings, N.J. 2019. Lessons learned from data-limited evaluations of data-rich reef fish species in the Gulf of Mexico: implications for providing fisheries management advice for data-poor stocks. Can. J. Fish. Aquat. Sci. 76: 1624-1639.

Schaefer, M.B. 1954. Some aspects of the dynamics of populations important to the management of commercial marine fisheries. IATTC Bull. 1: 25-56.

Schaefer, M.B. 1957. A study of the dynamics of the fishery for yellowfin tuna in the eastern tropical Pacific Ocean. IATTC Bull. 2: 245-285.

SEDAR, 2010. South Atlantic red snapper stock assessment. Available at: https://sedarweb.org/docs/sar/SEDAR%2024_SARRedSnap_Final.pdf. (accessed 31 March 2020).

SEFSC, 2012. Stock Assessment of Red Porgy off the Southeastern United States SEDAR Update Assessment. Available at: sedarweb.org/docs/suar/2012_SARPUpdate_Revised.pdf. (accessed 31 March 2020).

SPRFMO. 2017. A Stock assessment of the jumbo flying squid (*Dosidicus gigas*) in Southeast Pacific Ocean. Available from: https://www.sprfmo.int/assets/SC5-2017/SC5-SQ02-Stock-assessment-for-jumbo-flying-squid-in-SE-Pacific-2017.pdf (accessed 2 July 2020).

Stewart, I.J., Hicks, A.C., Taylor, I.G., Thorson, J.T., Wetzel, C., and Kupschus, S. 2013. A comparison of stock assessment uncertainty estimates using maximum likelihood and Bayesian methods implemented with the same model framework. Fish. Res. 142: 37-46.

Stoll, J.S., Crona, B.I., Fabinyi, M., and Farr, E.R. 2018. Seafood trade routes for lobster obscure teleconnected vulnerabilities. Front. Mar. Sci. 5: 239.

Sun, M., Zhang, C., Chen, Y., Xu, B., Xue, Y., and Ren, Y. 2018. Assessing the sensitivity of Data-Limited Methods (DLMs) to the estimation of life-history parameters from length-frequency data. Can. J. Fish. Aquat. Sci. 75: 1563-1572.

Taylor, I.G., and Methot, R.D. 2013. Hiding or dead? A computationally efficient model of selective fisheries mortality. Fish. Res. 142: 75-85.

Thorson, J.T., and Cope, J.M. 2017. Uniform, uninformed or misinformed? The lingering challenge of minimally informative priors in data-limited Bayesian stock assessments. Fish. Res. 194: 164-172.

Thorson, J.T., Cope, J.M., Branch, T.A., and Jensen, O.P. 2012. Spawning biomass reference points for exploited marine fishes, incorporating taxonomic and body size information. Can. J. Fish. Aquat. Sci. 69: 1556-1568.

Thorson, J.T., Hicks, A.C., and Methot, R.D. 2015. Random effect estimation of time-varying factors in Stock Synthesis. ICES J. Mar. Sci. 72: 178-185.

Thorson, J.T., Ono, K., and Munch, S.B. 2014. A Bayesian approach to identifying and compensating for model misspecification in population models. Ecology 95: 329-341.

Wiedenmann, J., Wilberg, M.J., and Miller, T.J. 2013. An Evaluation of Harvest Control Rules for Data-Poor Fisheries. North Am. J. Fish. Manag. 33: 845-860.

Winker, H., Carvalho, F., and Kapur, M. 2018. JABBA: Just Another Bayesian Biomass Assessment. Fish. Res. 204: 275-288.

Xu, L., Li, B., Chen, X., and Chen, Y. 2019. A comparative study of observation-error estimators and state-space production models in fisheries assessment and management. Fish. Res. 219: 105322.

Yu, W., Yi, Q., Chen, X., and Chen, Y. 2016. Modelling the effects of climate variability on habitat suitability of jumbo flying squid, *Dosidicus gigas*, in the Southeast Pacific Ocean off Peru. ICES J. Mar. Sci. 73: 239-249.

APPENDIX

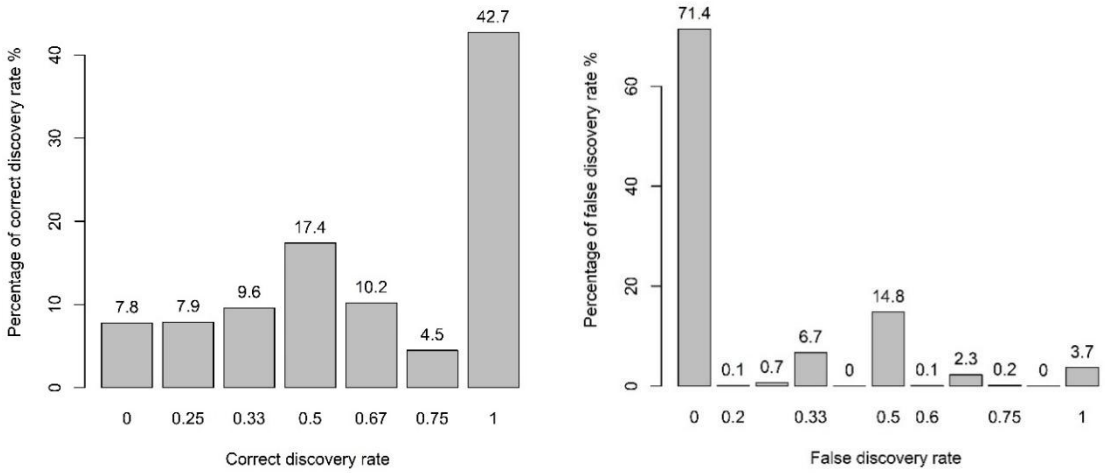

Figure S2.1. The percentage of different levels of correct discovery rates (CDRs) (left) and false discovery rates (FDRs) (right) of the proposed method when the input data are uninformative. The number above each bar represents the percentage of the corresponding CDR or FDR.

(a) (b)

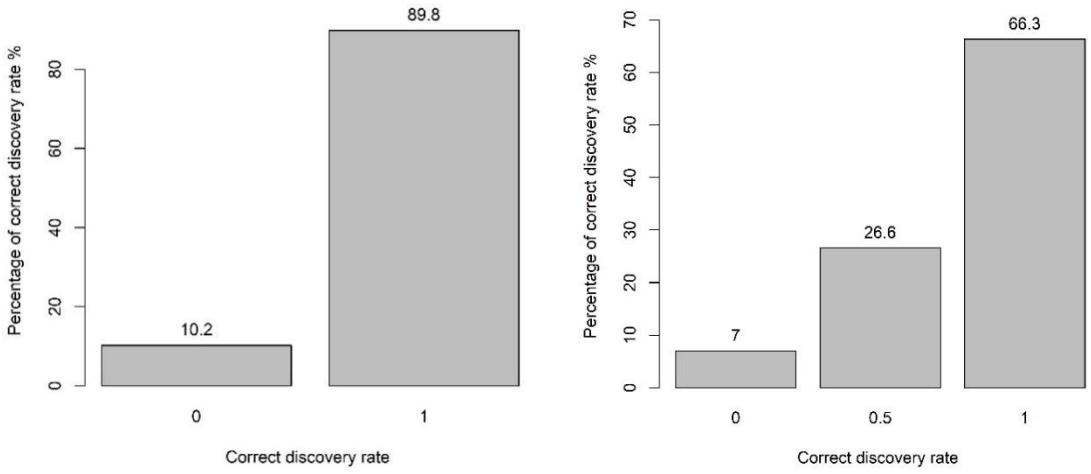

(c) (d)

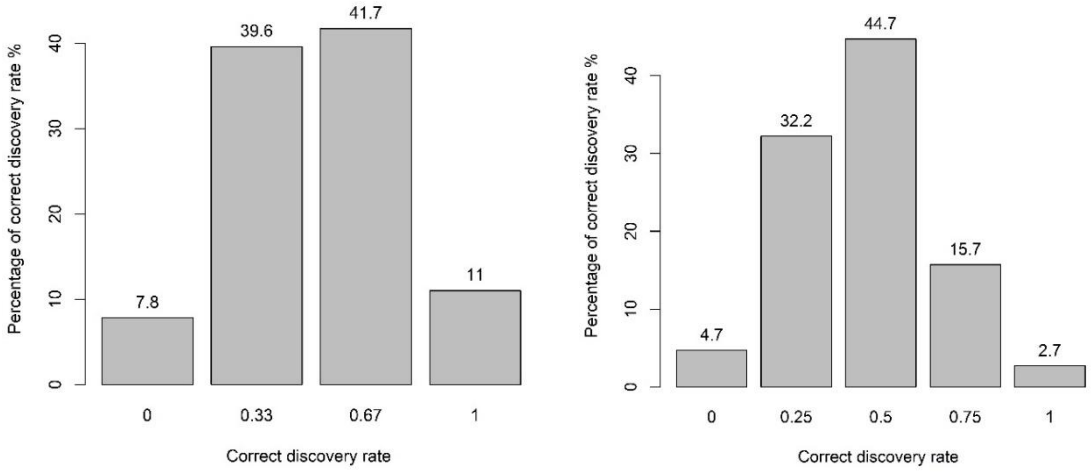

Figure S2.2. The percentages of different levels of correct discovery rates (CDRs) of the proposed method with informative input data when the number of true outliers is (a) one; (b) two; (c) three; and (d) four.

(a) (b)

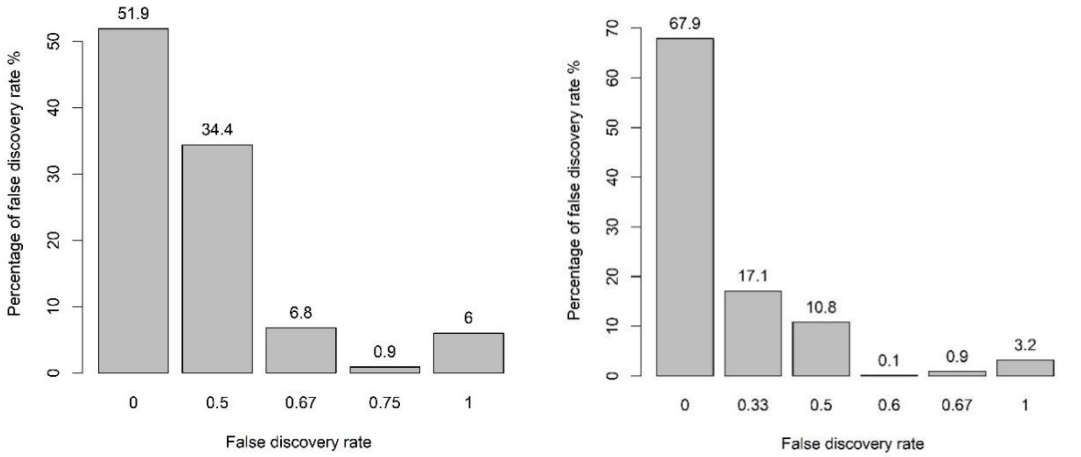

(c) (d)

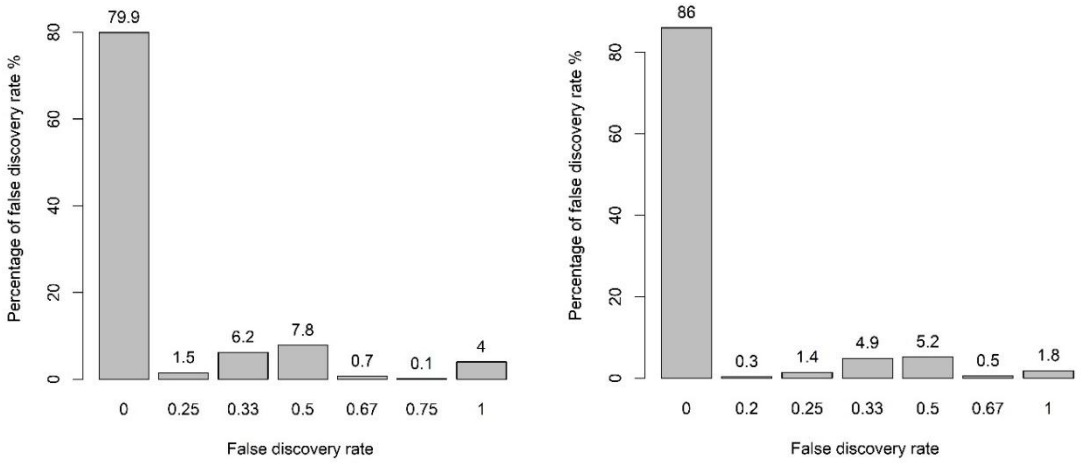

Figure S2.3. The percentages of different levels of false discovery rates (FDRs) of the proposed method with informative input data when the number of true outliers is (a) one; (b) two; (c) three; and (d) four.

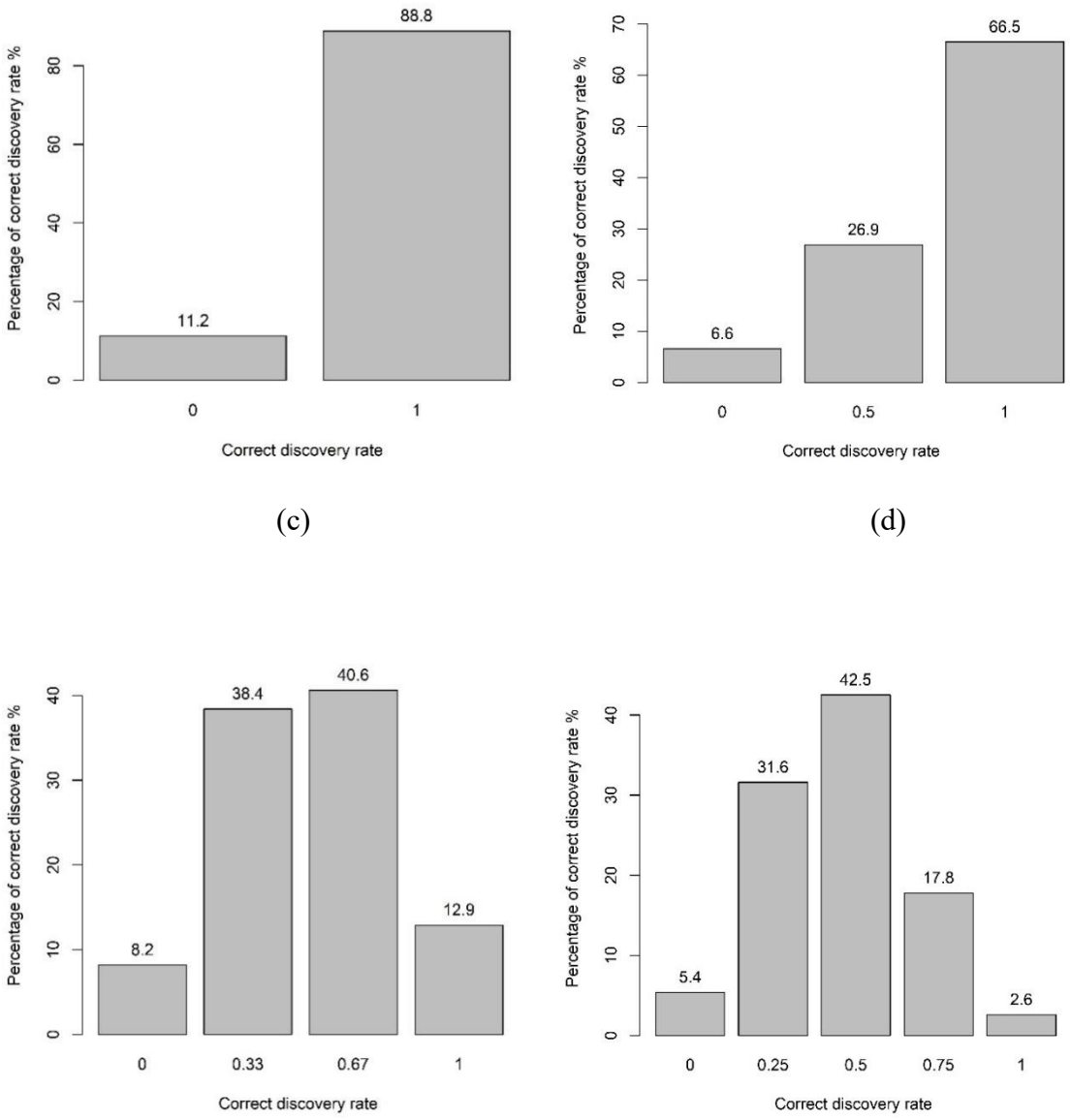

Figure S2.4. The percentages of different levels of correct discovery rates (CDRs) of the proposed method with uninformative input data when the number of true outliers is (a) one; (b) two; (c) three; and (d) four.

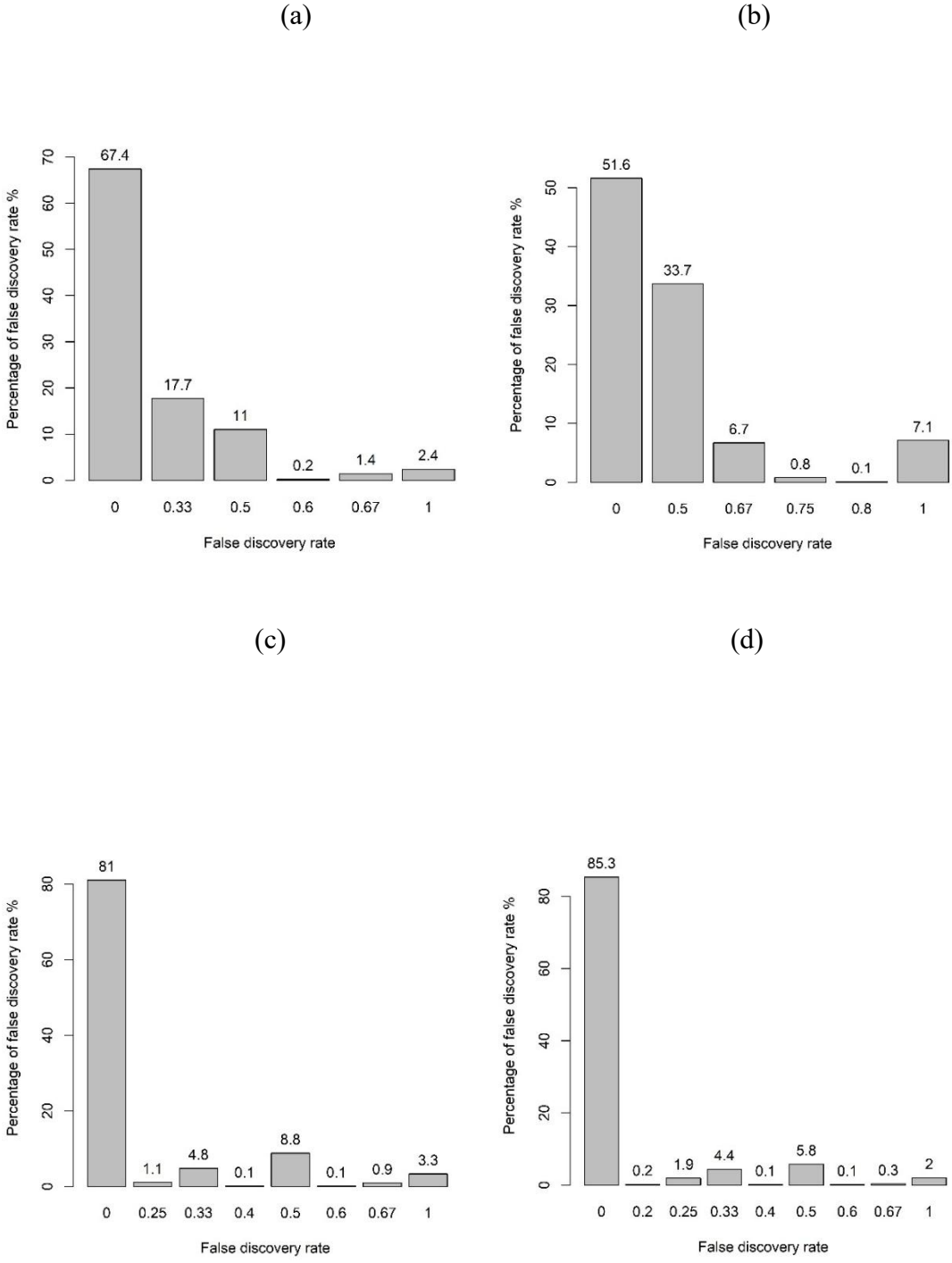

Figure S2.5. The percentages of different levels of false discovery rates (FDRs) of the proposed method with uninformative input data when the number of true outliers is (a) one; (b) two; (c) three; and (d) four.

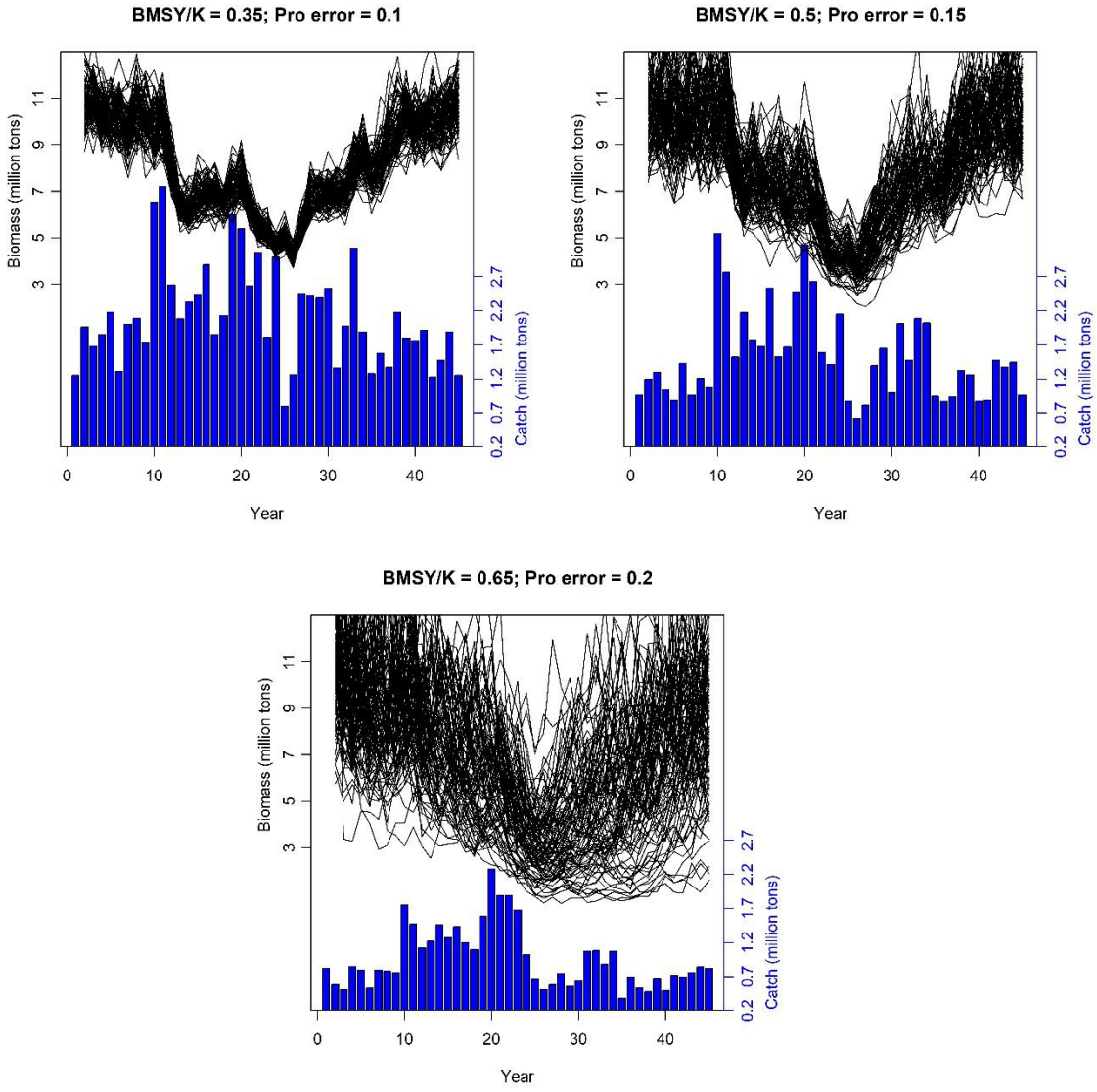

Figure S3.1. Average catch over simulation trials and 100 simulated biomass trajectories in three different scenarios; topleft (Bmsy/k = 0.35; process error standard deviation=0.1), topright (Bmsy/k = 0.5; process error standard deviation =0.15),bottomleft (Bmsy/k = 0.65; process error standard deviation =0.2)

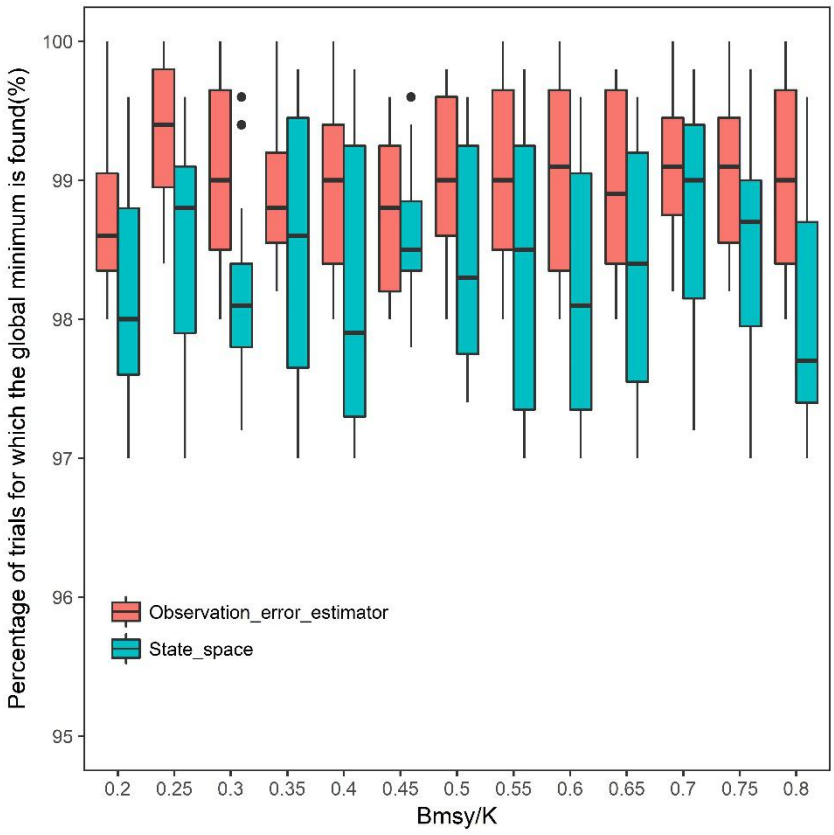

Figure S3.2. The percentages of trials for which the global minimum is found against levels of model error for the state-space model and the observation-error estimator

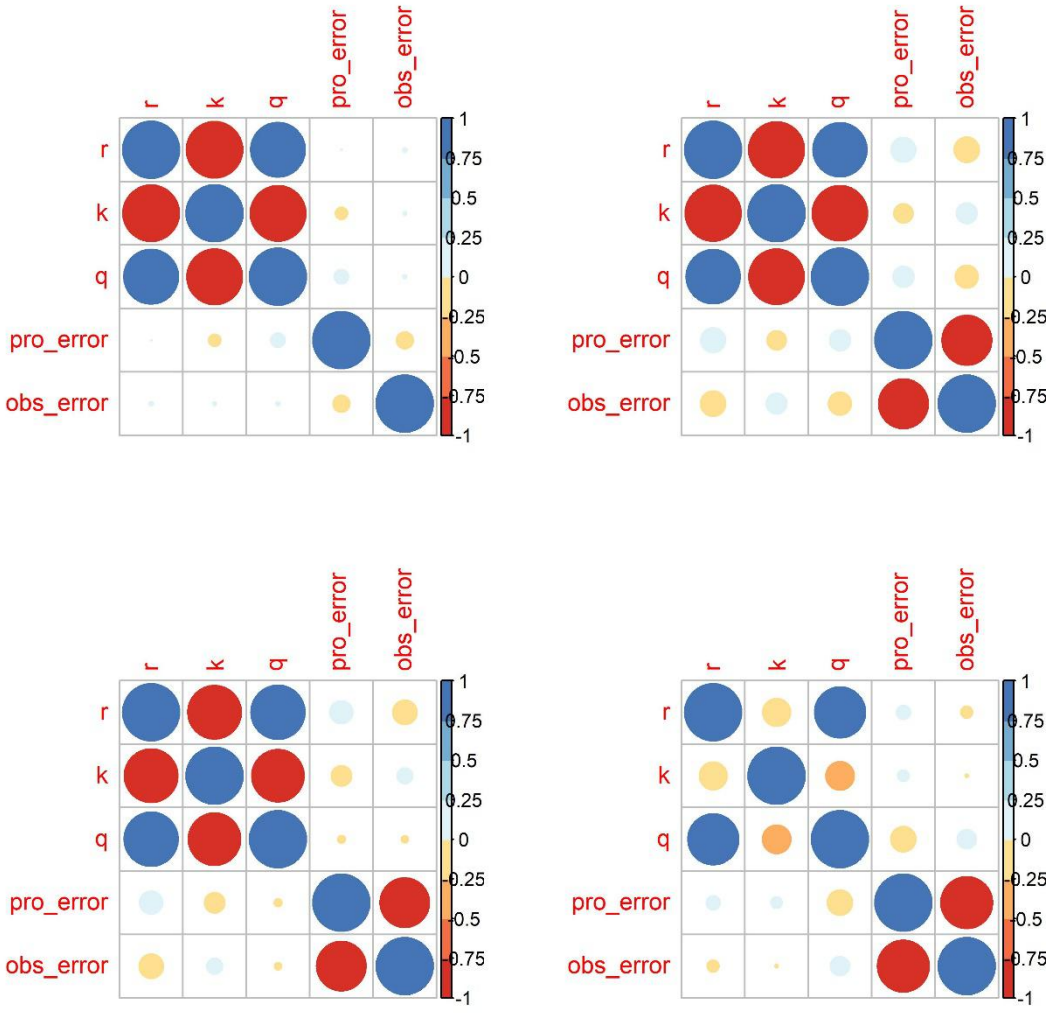

Figure S3.3. The Pearson correlation coefficients of estimated parameters from state-space models when the ration of Bmsy over k equals 0.2 and the standard deviations of true process and observation errors are 0.05 (top-left), 0.1 (top-right), 0.15 (bottom-left), and 0.2 (bottom-right).

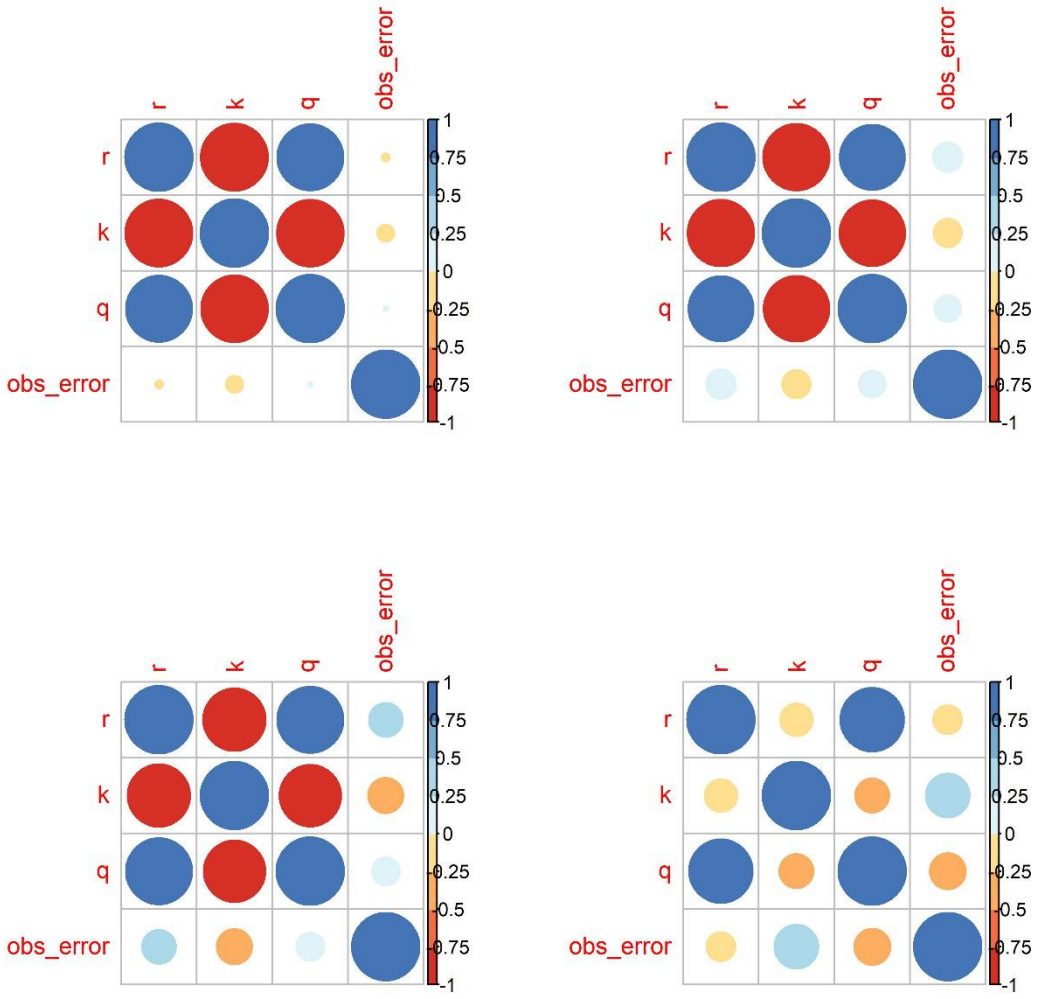

Figure S3.4. The Pearson correlation coefficients of estimated parameters from observation-error estimators when the ration of Bmsy over k equals 0.2 and the standard deviations of true process and observation errors are 0.05 (top-left), 0.1 (top-right), 0.15 (bottom-left), and 0.2 (bottom-right).

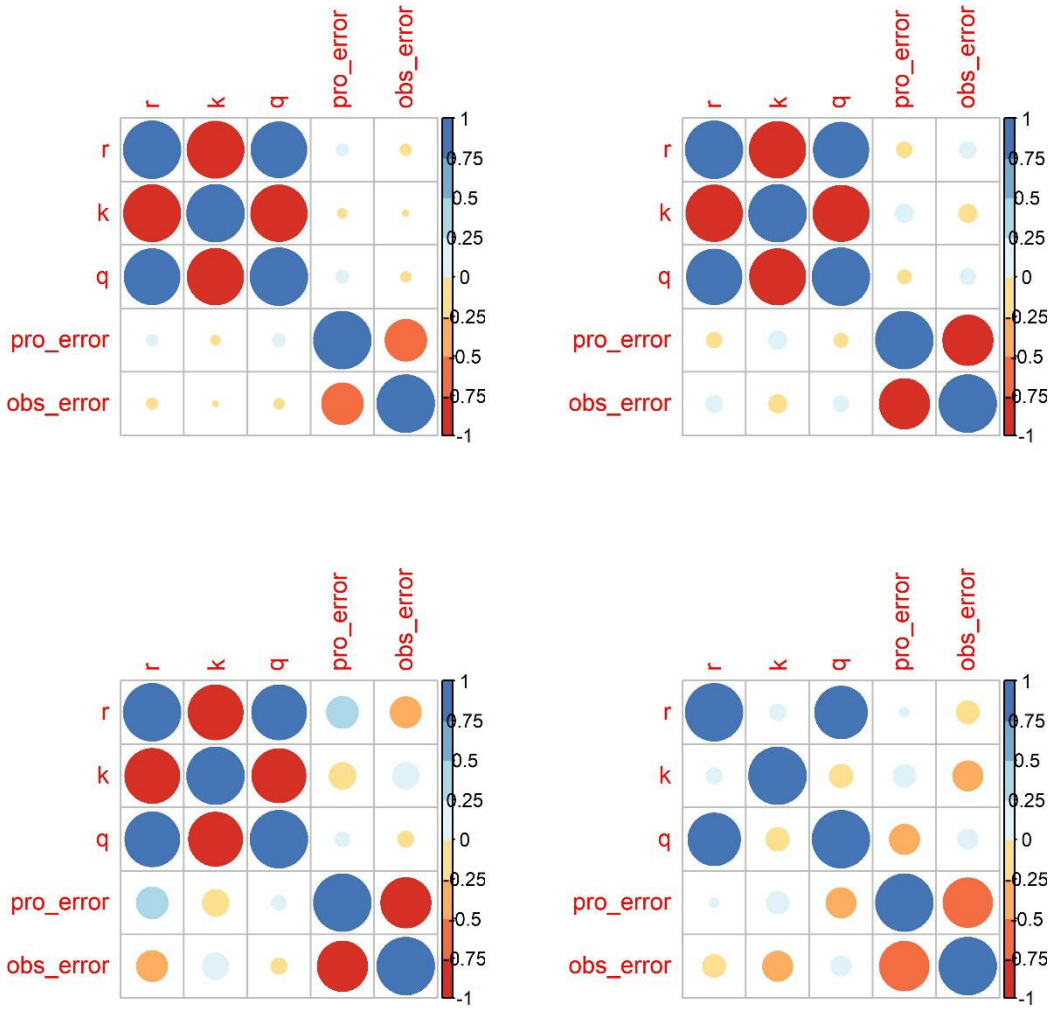

Figure S3.5. The Pearson correlation coefficients of estimated parameters from state-space models when the ration of Bmsy over k equals 0.3 and the standard deviations of true process and observation errors are 0.05 (top-left), 0.1 (top-right), 0.15 (bottom-left), and 0.2 (bottom-right).

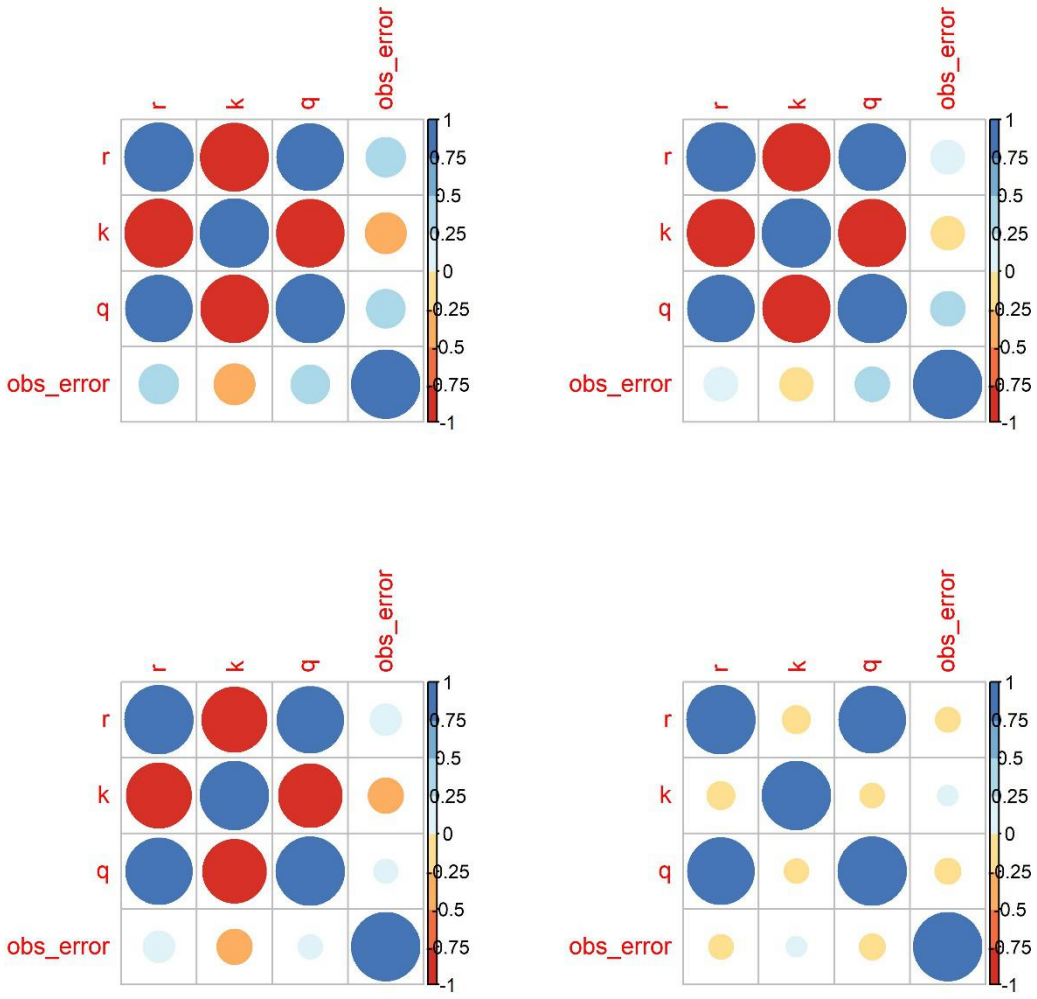

Figure S3.6. The Pearson correlation coefficients of estimated parameters from observation-error estimators when the ration of Bmsy over k equals 0.3 and the standard deviations of true process and observation errors are 0.05 (top-left), 0.1 (top-right), 0.15 (bottom-left), and 0.2 (bottom-right).

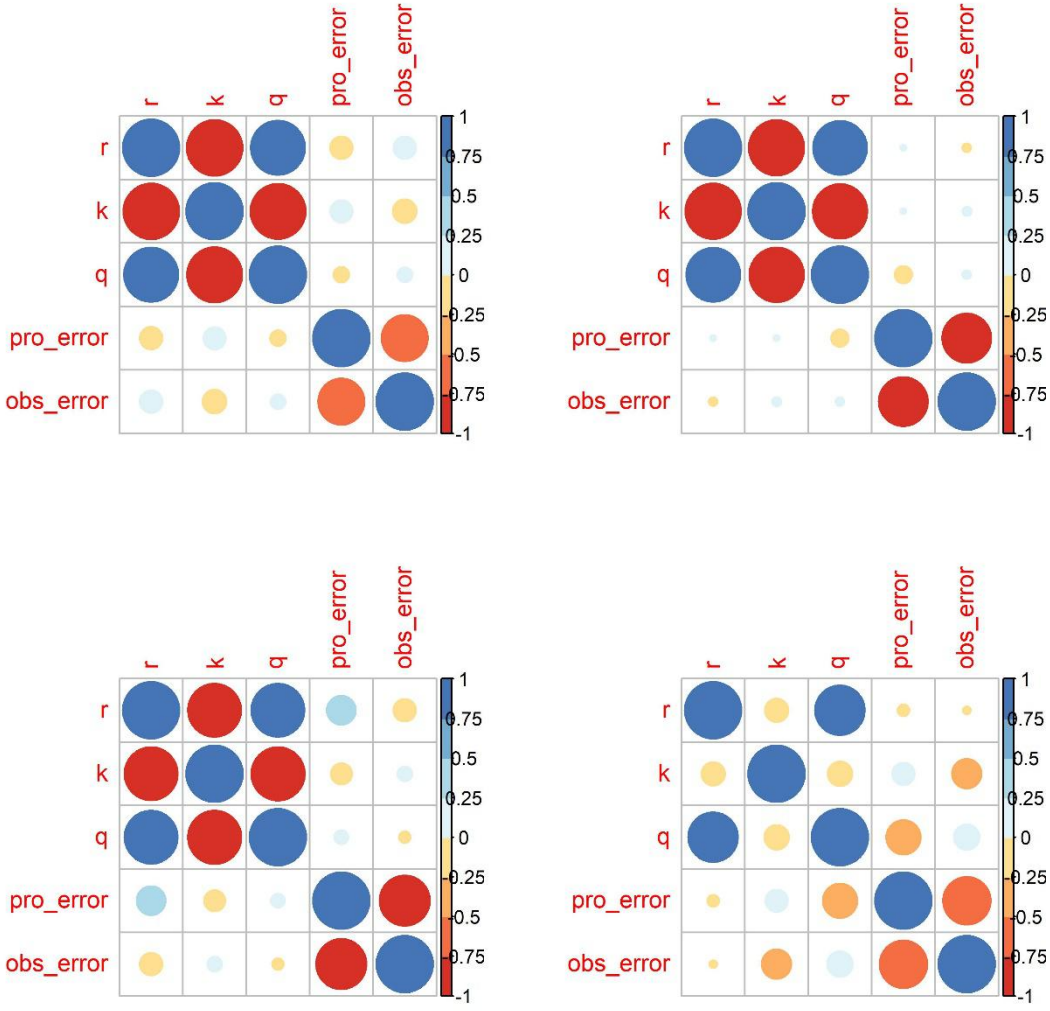

Figure S3.7. The Pearson correlation coefficients of estimated parameters from state-space models when the ration of Bmsy over k equals 0.4 and the standard deviations of true process and observation errors are 0.05 (top-left), 0.1 (top-right), 0.15 (bottom-left), and 0.2 (bottom-right).

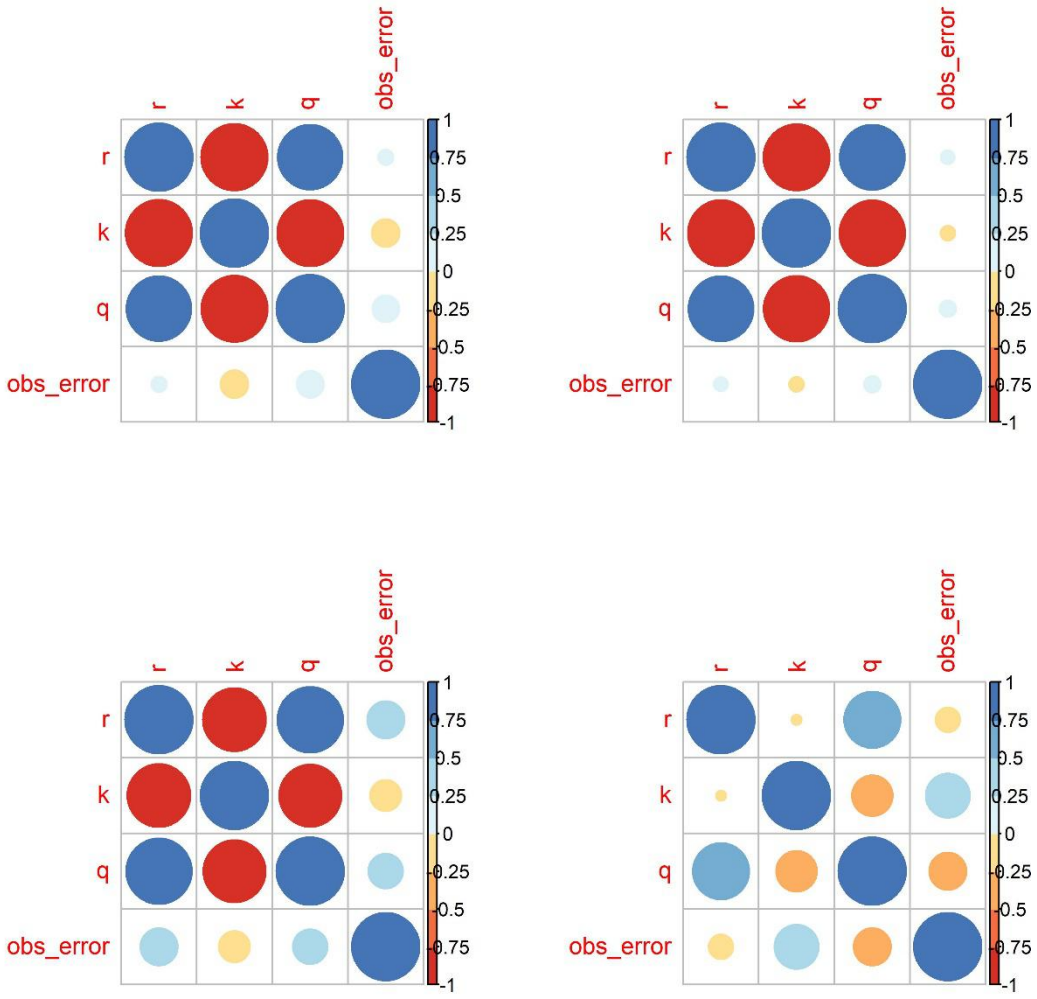

Figure S3.8. The Pearson correlation coefficients of estimated parameters from observation-error estimators when the ration of Bmsy over k equals 0.4 and the standard deviations of true process and observation errors are 0.05 (top-left), 0.1 (top-right), 0.15 (bottom-left), and 0.2 (bottom-right).

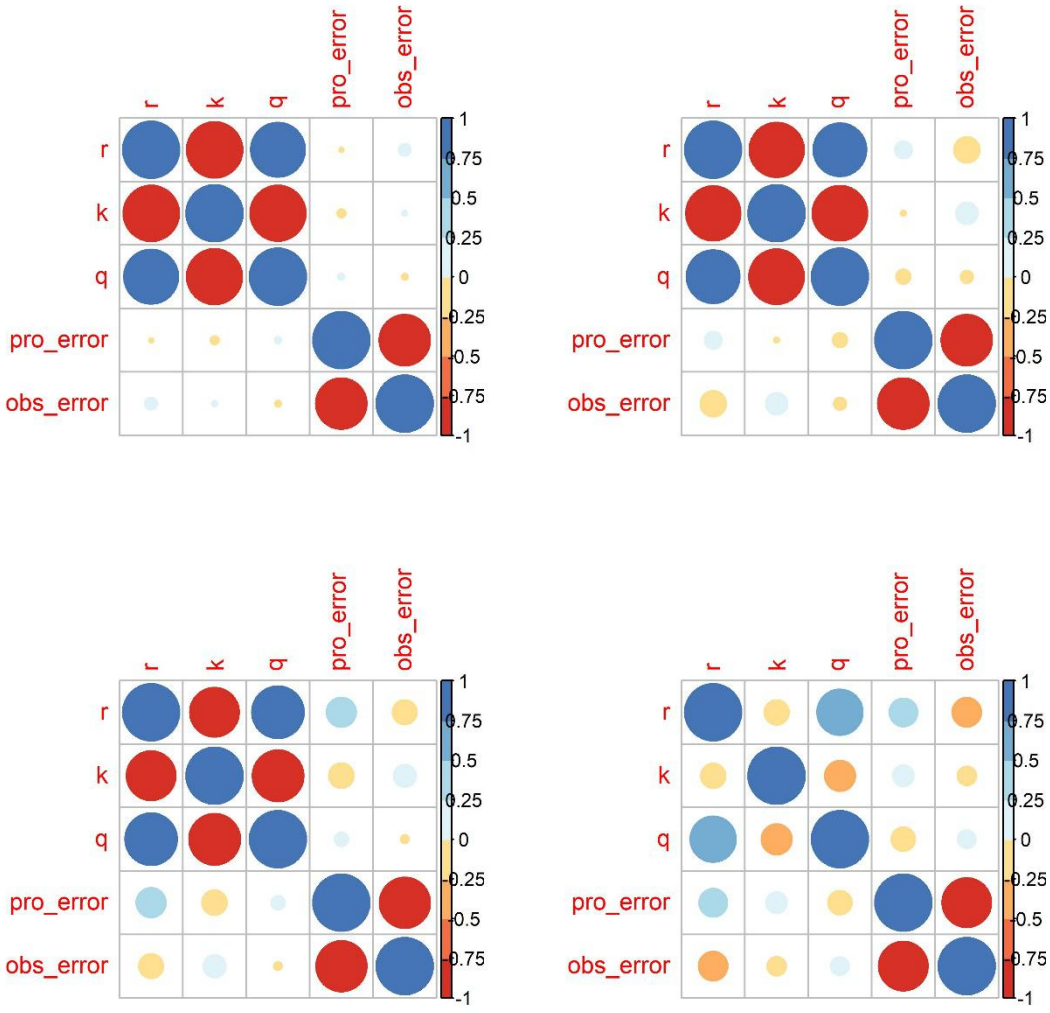

Figure S3.9. The Pearson correlation coefficients of estimated parameters from state-space models when the ration of Bmsy over k equals 0.6 and the standard deviations of true process and observation errors are 0.05 (top-left), 0.1 (top-right), 0.15 (bottom-left), and 0.2 (bottom-right).

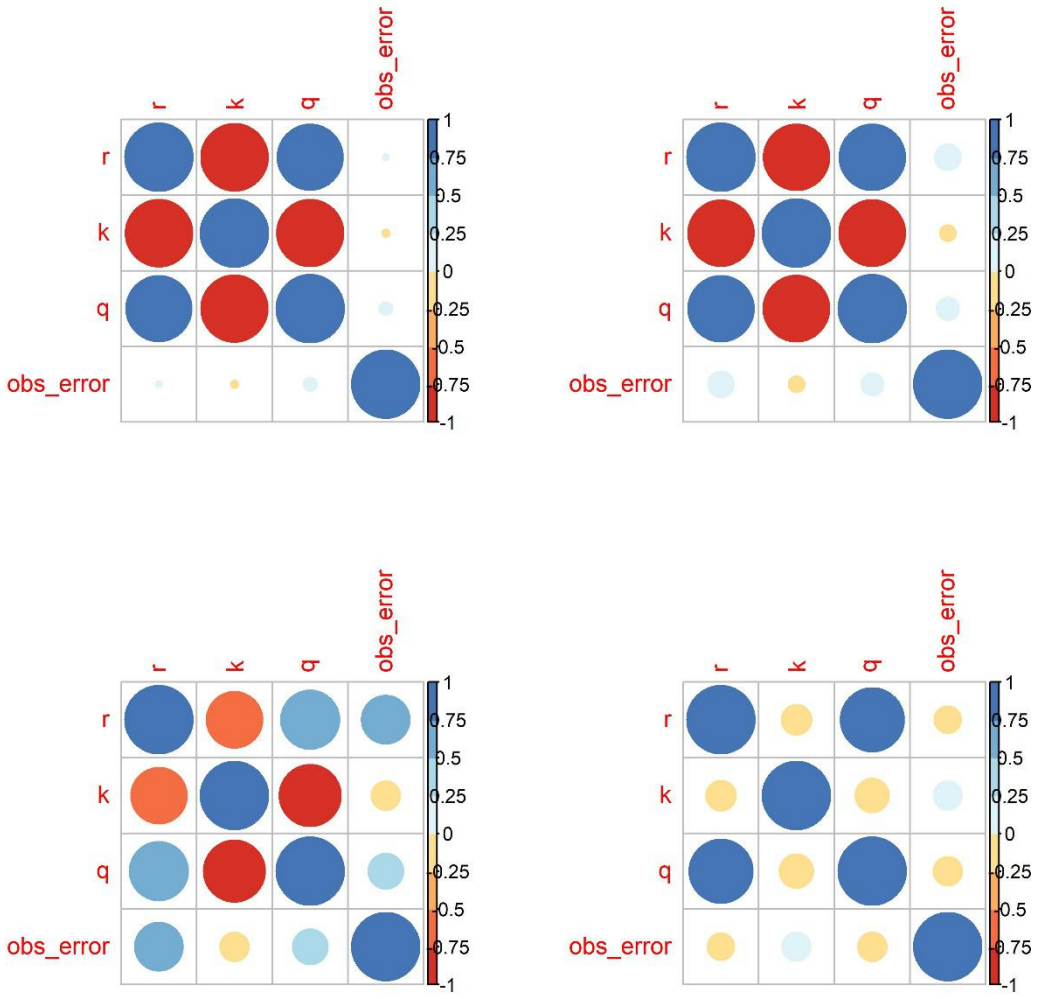

Figure S3.10. The Pearson correlation coefficients of estimated parameters from observation-error estimators when the ration of Bmsy over k equals 0.6 and the standard deviations of true process and observation errors are 0.05 (top-left), 0.1 (top-right), 0.15 (bottom-left), and 0.2 (bottom-right).

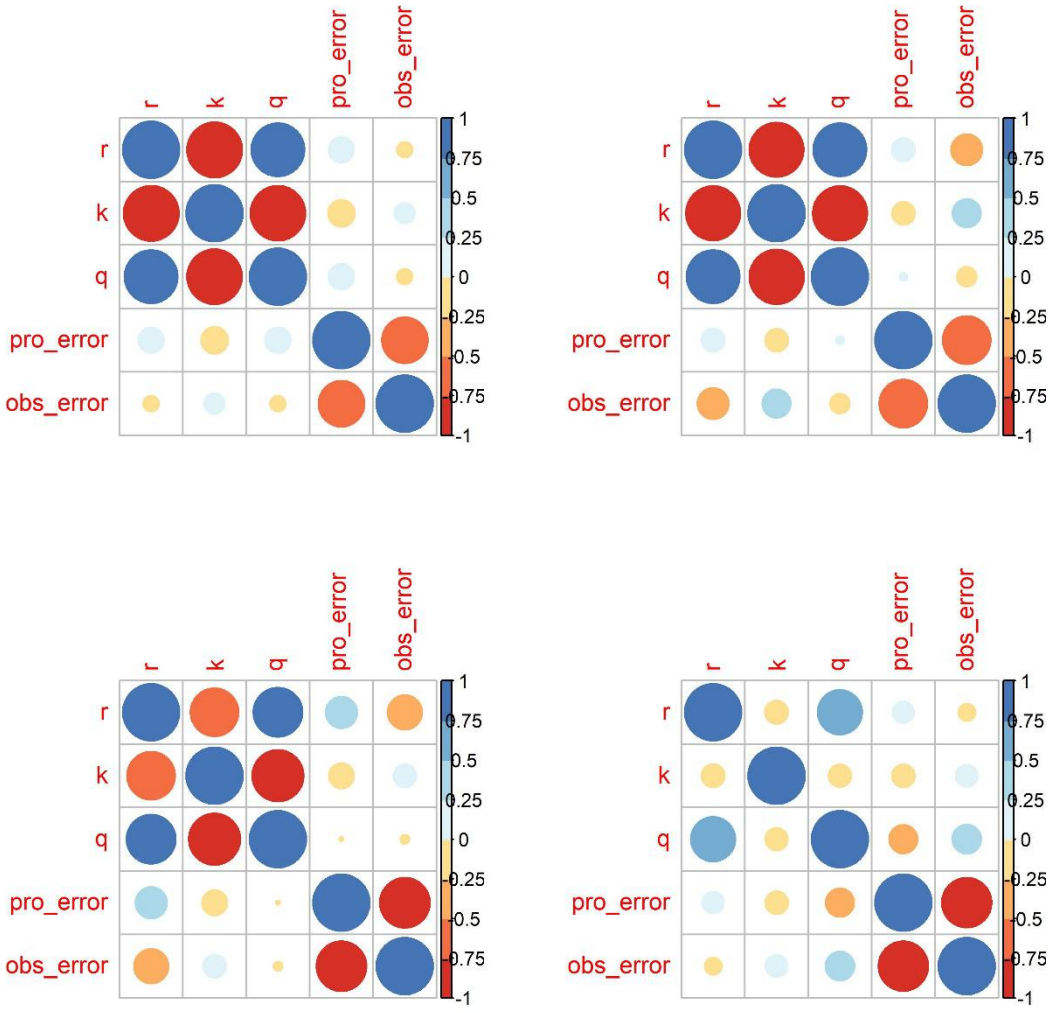

Figure S3.11. The Pearson correlation coefficients of estimated parameters from state-space models when the ration of Bmsy over k equals 0.7 and the standard deviations of true process and observation errors are 0.05 (top-left), 0.1 (top-right), 0.15 (bottom-left), and 0.2 (bottom-right).

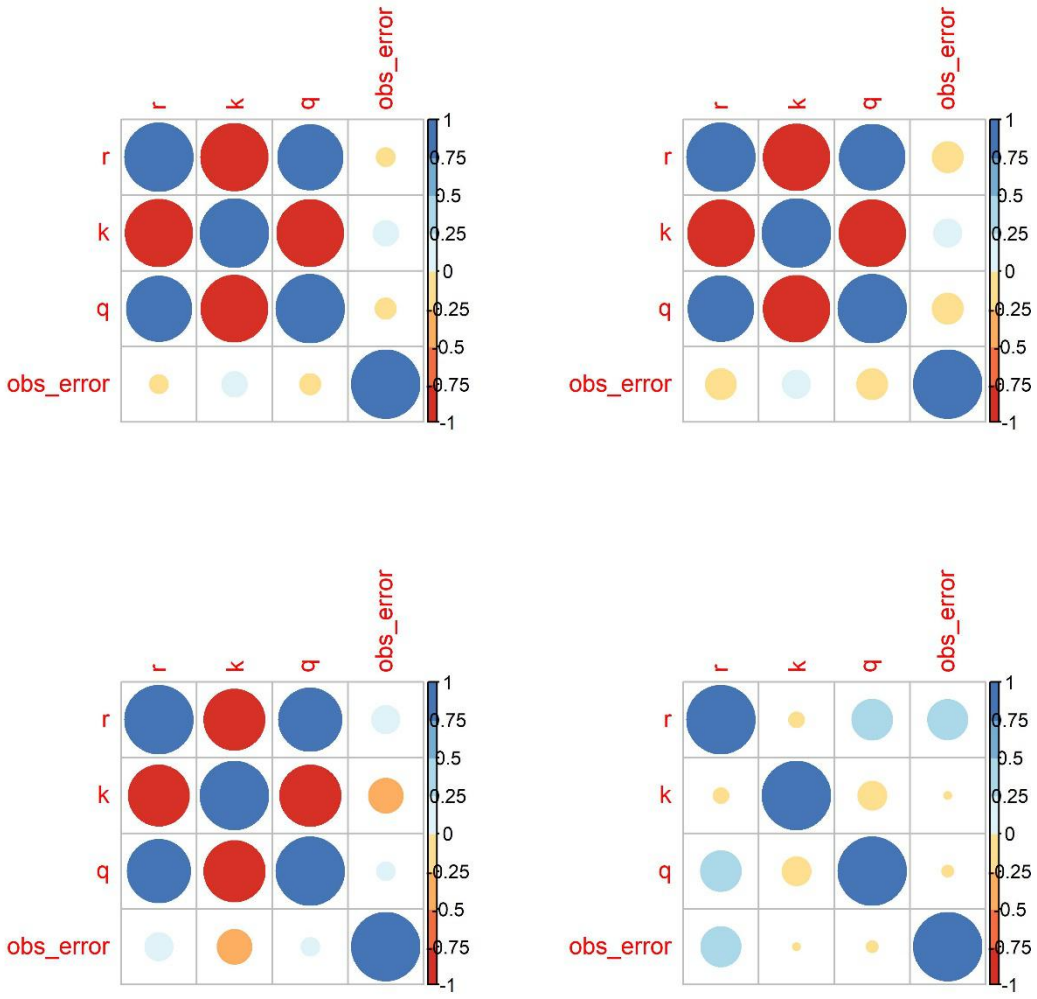

Figure S3.12. The Pearson correlation coefficients of estimated parameters from observation-error estimators when the ration of Bmsy over k equals 0.7 and the standard deviations of true process and observation errors are 0.05 (top-left), 0.1 (top-right), 0.15 (bottom-left), and 0.2 (bottom-right).

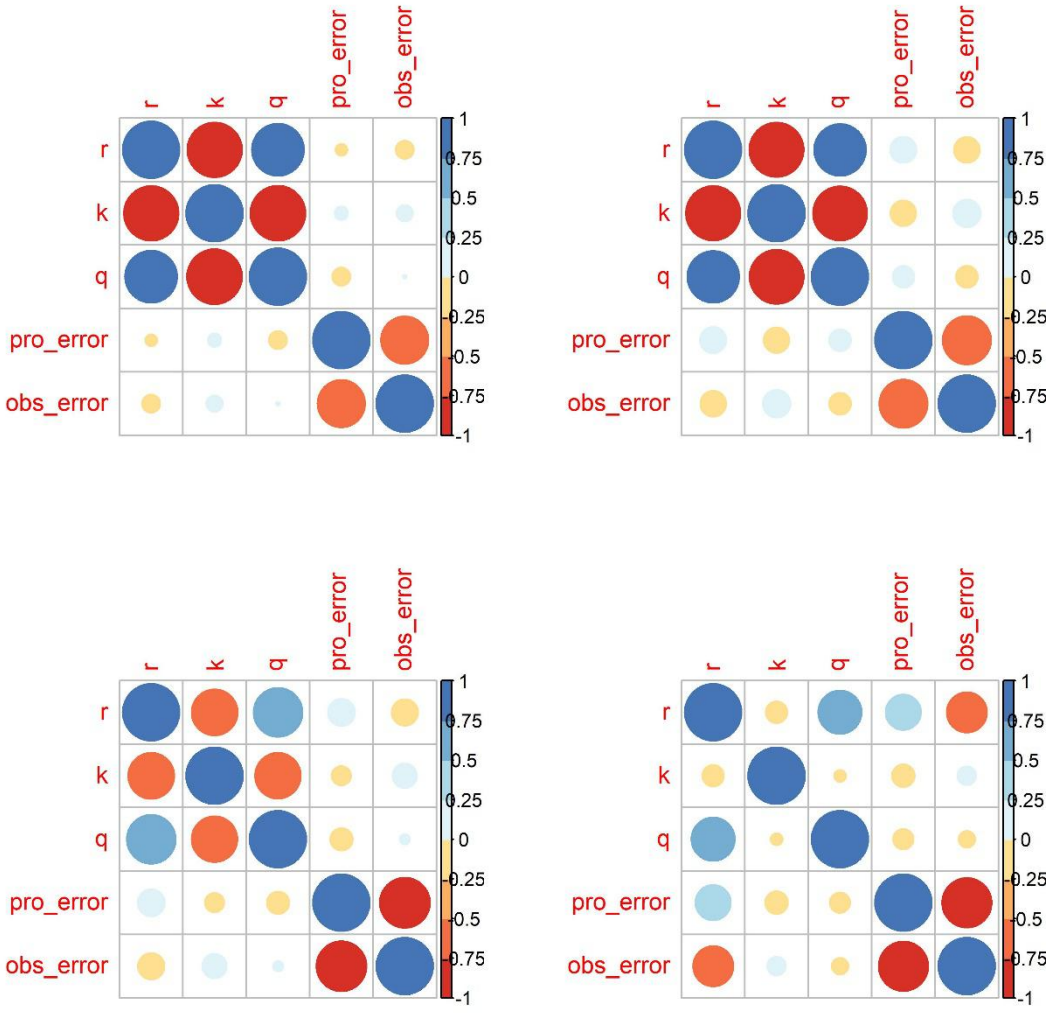

Figure S3.13. The Pearson correlation coefficients of estimated parameters from state-space models when the ration of Bmsy over k equals 0.8 and the standard deviations of true process and observation errors are 0.05 (top-left), 0.1 (top-right), 0.15 (bottom-left), and 0.2 (bottom-right).

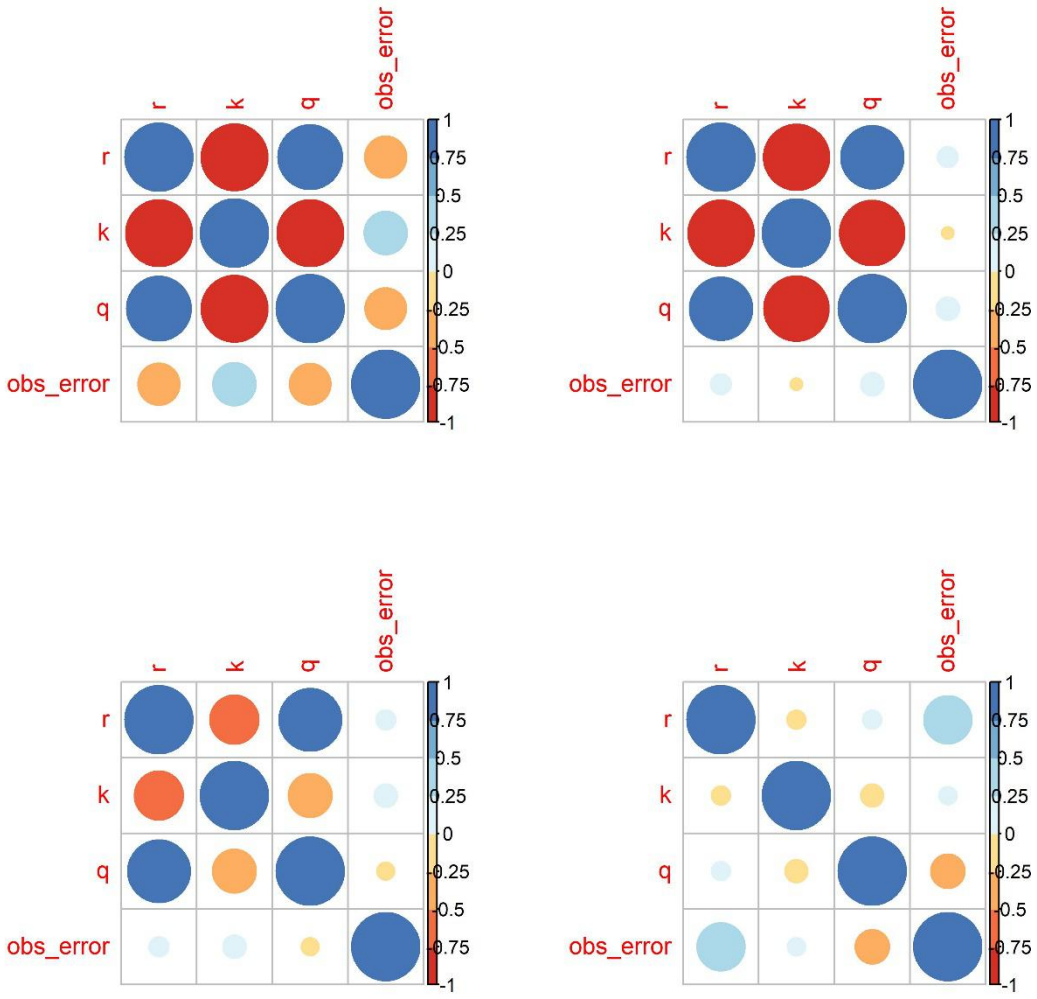

Figure S3.14. The Pearson correlation coefficients of estimated parameters from observation-error estimators when the ration of Bmsy over k equals 0.8 and the standard deviations of true process and observation errors are 0.05 (top-left), 0.1 (top-right), 0.15 (bottom-left), and 0.2 (bottom-right).

Table S3.1. The ranges from which the initial values of parameters were randomly selected for conventional and state-space models.

Parameter	Model	Initial value range
r	both	(0.34,0.94)
k	both	(5,20)
q	both	(0.002,0.008)
B_0	Observation-error	(0.8k,1.2k)
B_y	state-space	(0.1k,k)
$\sigma\varepsilon$	both	(0.01,0.5)
$\sigma\eta$	state-space	(0.01,0.5)

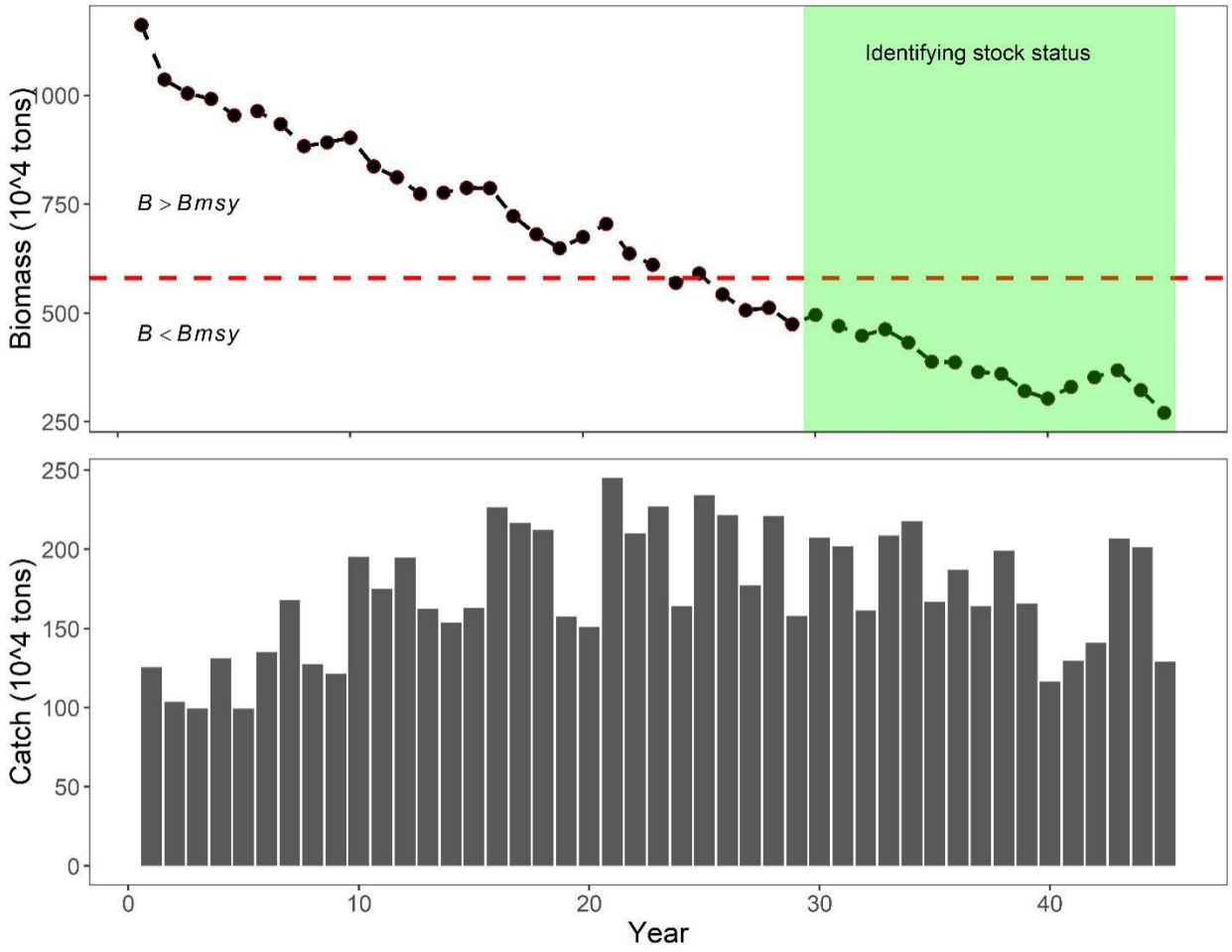

Figure S5.1. The historical catch and biomass in simulation 1 for population dynamics scenario 1 (P1: Schaefer model) and fishing history scenario 2 (F2: One way trip). The years in the shaded part are used in testing the performance of the four approaches on identifying the stock status.

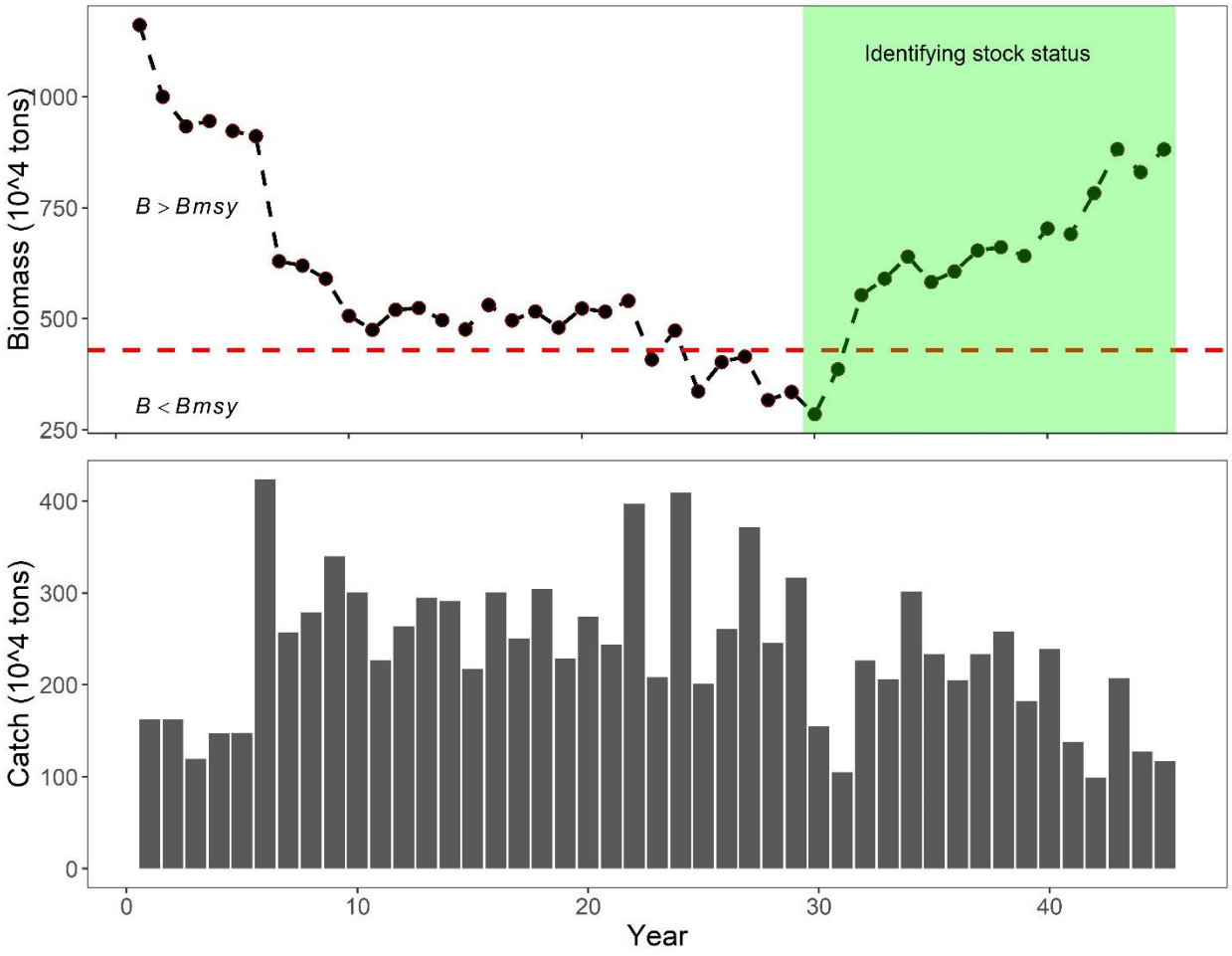

Figure S5.2. The historical catch and biomass in simulation 1 for population dynamics scenario 2 (P2: Fox model) and fishing history scenario 1 (F2: Good contrast). The years in the shaded part are used in testing the performance of the four approaches on identifying the stock status.

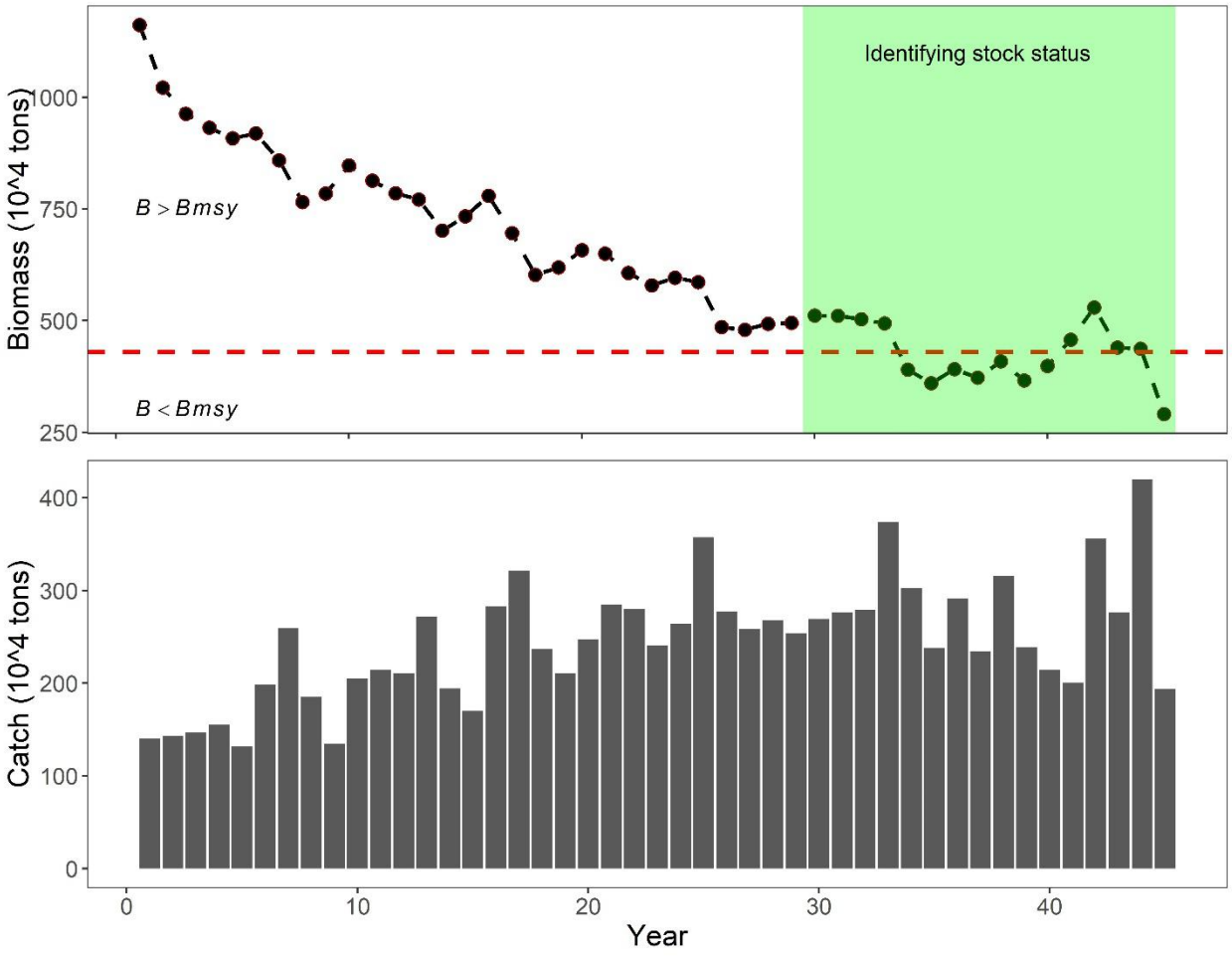

Figure S5.3. The historical catch and biomass in simulation 1 for population dynamics scenario 2 (P2: Fox model) and fishing history scenario 2 (F2: One way trip). The years in the shaded part are used in testing the performance of the four approaches on identifying the stock status.

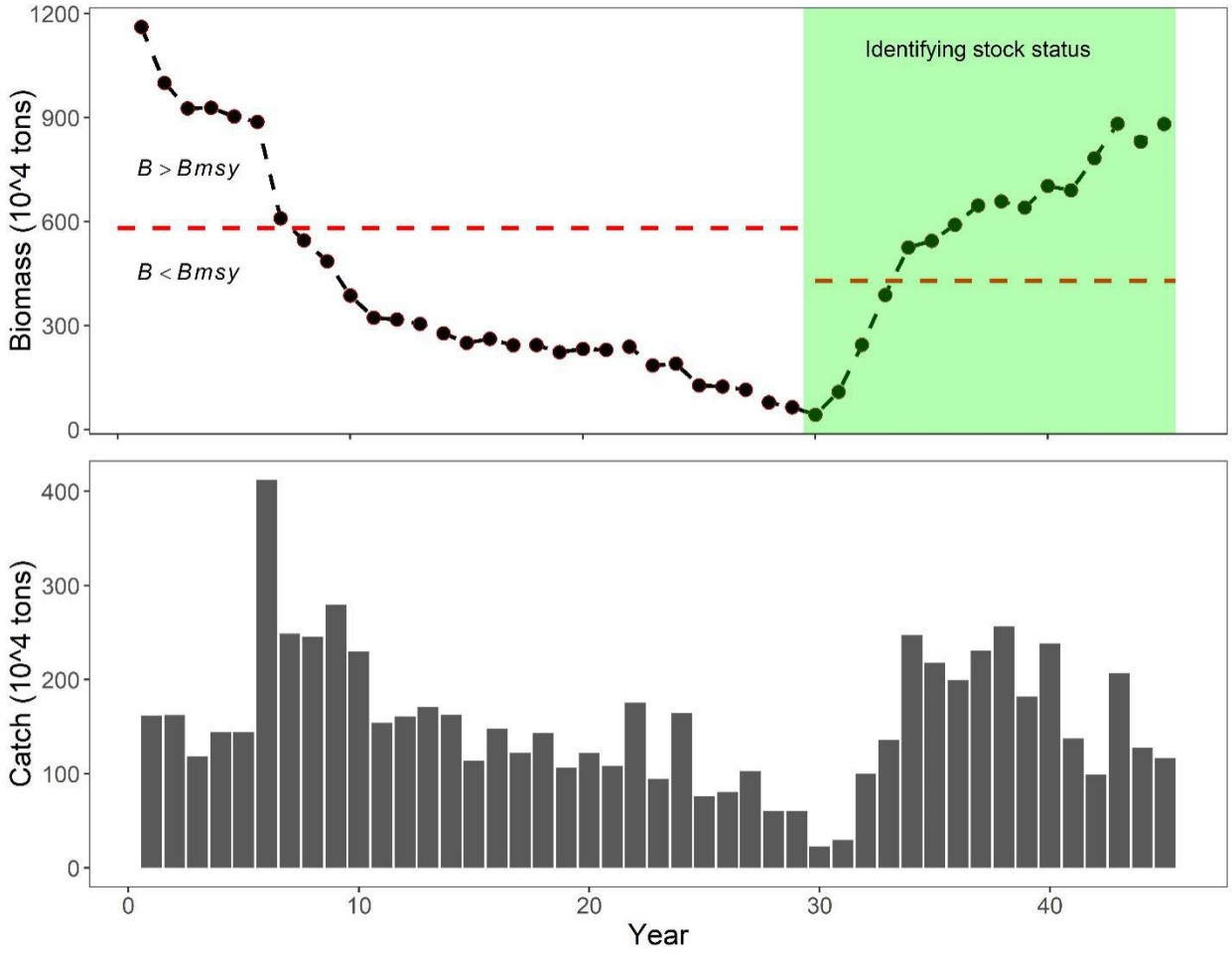

Figure S5.4. The historical catch and biomass in simulation 1 for population dynamics scenario 3 (P3: Regime shift) and fishing history scenario 1 (F1: Good contrast). The years in the shaded part are used in testing the performance of the four approaches on identifying the stock status.

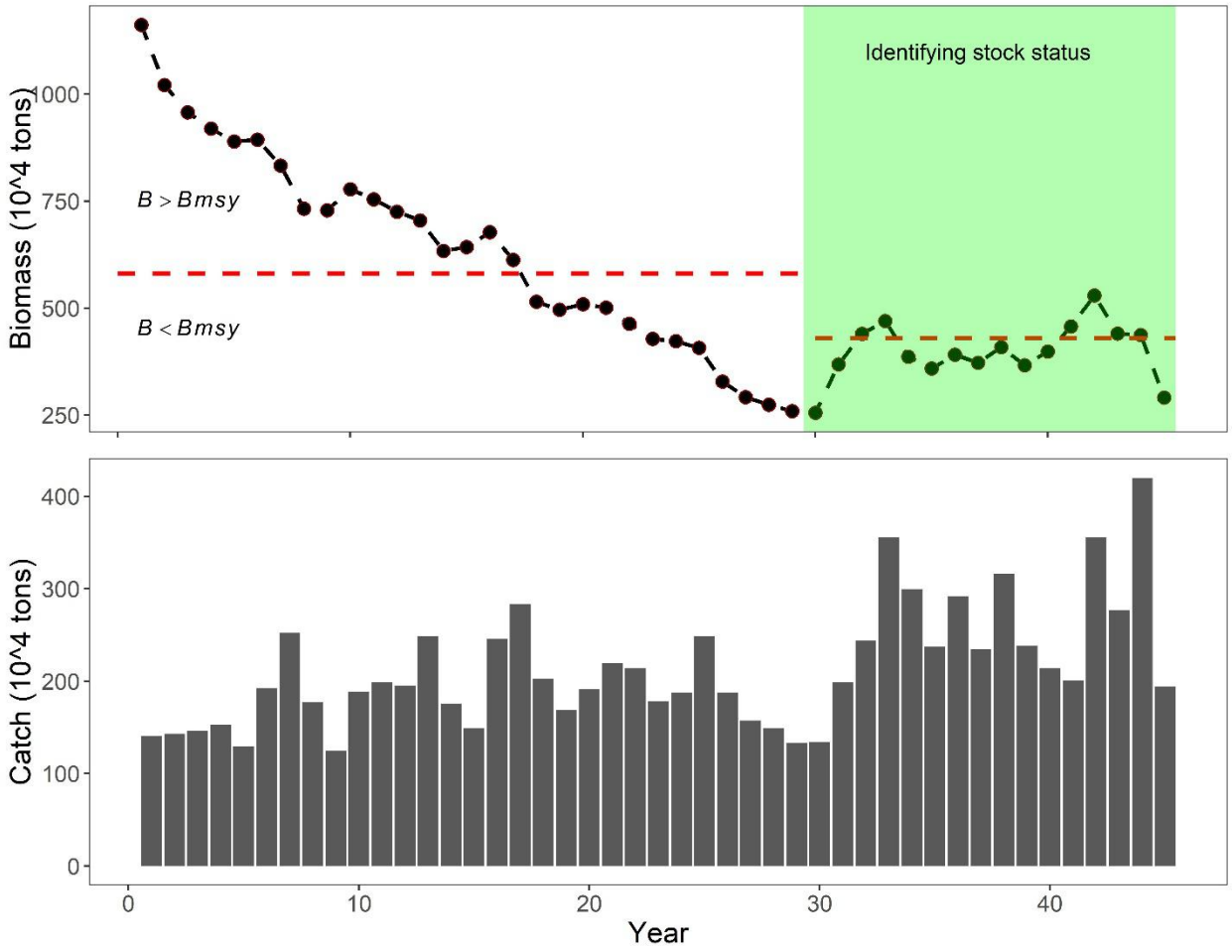

Figure S5.5. The historical catch and biomass in simulation 1 for population dynamics scenario 3 (P3: Regime shift) and fishing history scenario 2 (F2: One way trip). The years in the shaded part are used in testing the performance of the four approaches on identifying the stock status.

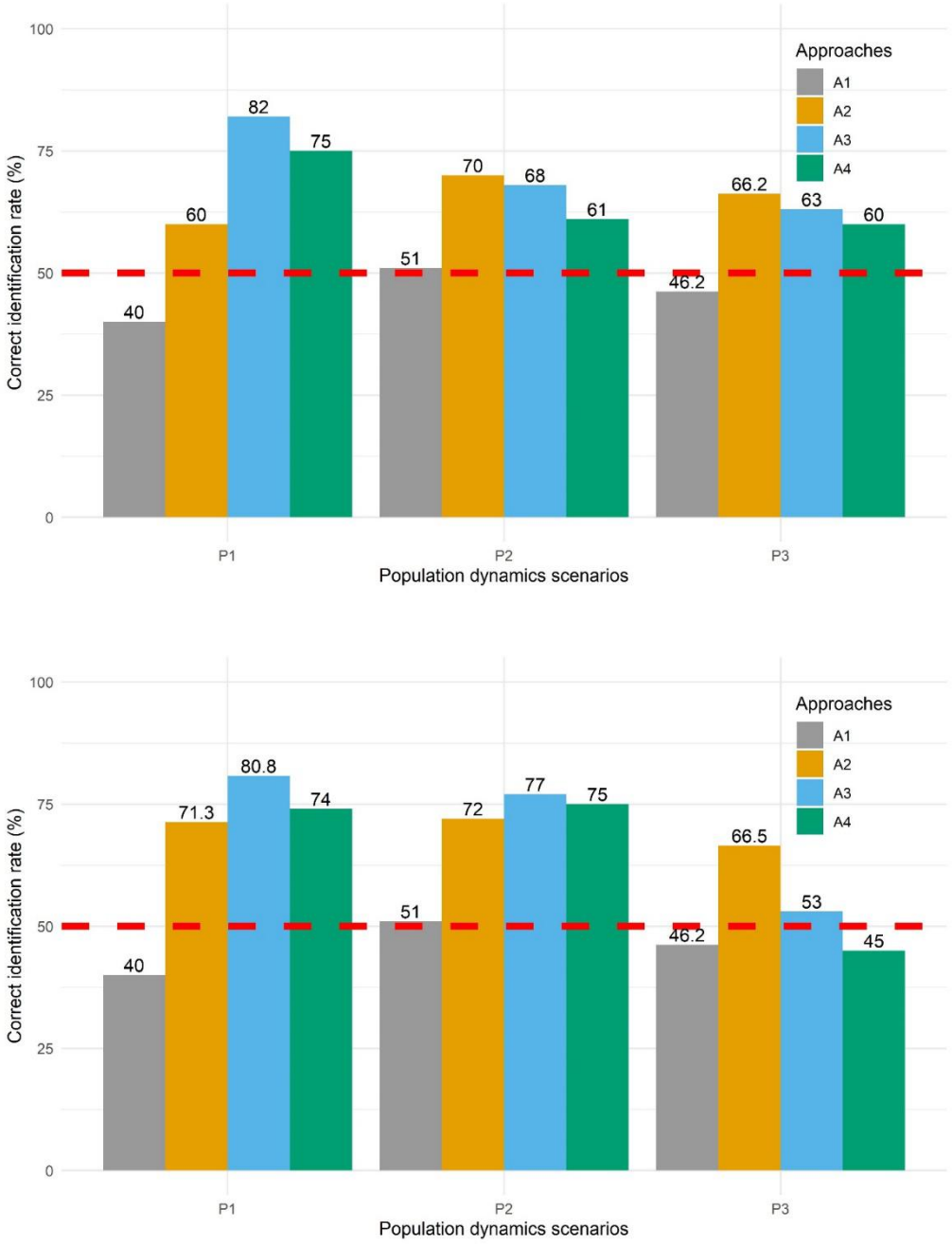

Figure S5.6. The correct stock status identification rate of four approaches in different scenarios when the operating model is parameterized based on the Pacific saury fishery. The upper panel summarizes the result from D1 data collection scenario. The bottom panel represents summarizes the result from D2 data collection scenario.

Newly proposed management procedures in DLMtools:

```
Schaefer = function (x, Data, reps = 100)
{
 dependencies = "Data@Year, Data@Cat, Data@Ind, Data@Abun"
 ind <- 1:length(Data@Year)
 C_dat <- log(Data@Cat[x, ind])
 C_dat[C_dat == -Inf] <- 0
 B_dat <- log(Data@Ind[x, ind]/Data@Ind[x, ind[length(ind)]] *
              Data@Abun[x])
 B_dat[B_dat == -Inf] <- 0
 C_hist <- exp(C_dat)
 B_hist <- exp(B_dat)
 PAR = c(log(0.3),log(B_hist[1]),log(B_hist[1]),log(0.2))

 RKQTSMOpt<-function(PAR)
 {
  r<-exp(PAR[1])
  K<-exp(PAR[2])
  B1<-exp(PAR[3])
  Sigma<-exp(PAR[4])
  N<-length(C_hist)+1
  B<-numeric(N)
  Effort<-numeric(N-1)
  B[1]=B1
  for (i in 2:N){
    B[i]=max(B[i-1]+r*B[i-1]*(1-B[i-1]/K)-C_hist[i-1],0.01)
  }
  -sum(stats::dlnorm(B_hist,meanlog = log(B),sdlog=Sigma,log=T))
 }
```

```
  OPModel<-optim(PAR,RKQTSMOpt)
  r = exp(OPModel$par)[1]
  TAC <- B_hist[length(B_hist)]*r/2
  Rec <- new("Rec")
  Rec@TAC <- TACfilter(TAC)
  Rec
}
class(Schaefer) = "MP"
```

```
Pella = function (x, Data, reps = 100)
      {
       dependencies = "Data@Year, Data@Cat, Data@Ind, Data@Abun"
       ind <- 1:length(Data@Year)
       C_dat <- log(Data@Cat[x, ind])
       C_dat[C_dat == -Inf] <- 0
       B_dat <- log(Data@Ind[x, ind]/Data@Ind[x, ind[length(ind)]] *
                    Data@Abun[x])
       B_dat[B_dat == -Inf] <- 0
       C_hist <- exp(C_dat)
       B_hist <- exp(B_dat)
       PAR = c(log(0.3),log(B_hist[1]),log(B_hist[1]),log(0.2),log(2))

       RKQTSMOpt<-function(PAR)
       {
        r<-exp(PAR[1])
        K<-exp(PAR[2])
        B1<-exp(PAR[3])
        Sigma<-exp(PAR[4])
        S = exp(PAR[5])
        N<-length(C_hist)+1
        B<-numeric(N)
        Effort<-numeric(N-1)
        B[1]=B1
        for (i in 2:N){
          B[i]=max(B[i-1]+r*B[i-1]*(1-(B[i-1]/K)^(S-1))/(S-1)-C_hist[i-1],0.01)
        }
        -sum(stats::dlnorm(B_hist,meanlog = log(B),sdlog=Sigma,log=T))
       }
       OPModel<-optim(PAR,RKQTSMOpt)
```

```
  r = exp(OPModel$par)[1]
  s = exp(OPModel$par)[5]
  TAC <- B_hist[length(B_hist)]*r/s
  Rec <- new("Rec")
  Rec@TAC <- TACfilter(TAC)
  Rec
}
class(Pella) = "MP"
```

```
Gcontrol2 =  function (x, Data, reps = 100, yrsmth = 10, gg = 2, glim = c(0.5, 2),bin=5)
{
  dependencies = "Data@Year, Data@Cat, Data@Ind, Data@Abun"
  ind <- (length(Data@Year) - (yrsmth - 1)):length(Data@Year)
  C_dat <- log(Data@Cat[x, ind])
  C_dat[C_dat == -Inf] <- 0
  B_dat <- log(Data@Ind[x, ind]/Data@Ind[x, ind[yrsmth]] * Data@Abun[x])
  B_dat[B_dat == -Inf] <- 0
  C_hist <- exp(predict(loess(C_dat ~ ind, degree = 1)))
  B_hist <- exp(predict(loess(B_dat ~ ind, degree = 1)))
  ind <- 2:yrsmth
  ind1 <- 1:(yrsmth - 1)
  SP_hist <- B_hist[ind] - B_hist[ind1] + C_hist[ind1]
  yind <- 1:length(SP_hist)
  SP_mu <- predict(lm(SP_hist ~ yind), newdat = list(yind =length(SP_hist) + 1))
  SP_se <- predict(lm(SP_hist ~ yind), newdat = list(yind = length(SP_hist) + 1), se =
T)$se.fit
  SP_new <- rnorm(reps, SP_mu, SP_se/2)
  Glm <- summary(lm(SP_hist ~ B_hist[ind1]))$coefficients[2, 1:2]
  G_new <- rnorm(reps, Glm[1], Glm[2]/2)
  TAC <- SP_new * (1 - gg * G_new)
  TAC[TAC < glim[1] * C_hist[yrsmth]] <- glim[1] * C_hist[yrsmth]
  TAC[TAC > glim[2] * C_hist[yrsmth]] <- glim[2] * C_hist[yrsmth]

  C_dat_n <- log(Data@Cat[x, ])
  C_dat_n[C_dat_n == -Inf] <- 0
  B_dat_n <- log(Data@Ind[x,]* Data@Abun[x])
  B_dat_n[B_dat_n == -Inf] <- 0
  C_hist_n <- exp(predict(loess(C_dat_n ~ c(1:length(Data@Year)), degree = 1)))
  B_hist_n <- exp(predict(loess(B_dat_n ~ c(1:length(Data@Year)), degree = 1)))
```

```
SP_hist_n <- B_hist_n[2:length(B_hist_n)] - B_hist_n[1:(length(B_hist_n)-1)] + C_hist_n[1:(length(B_hist_n)-1)]


highest = B_hist_n[which.max(SP_hist_n)]
second = B_hist_n[which.max(SP_hist_n[SP_hist_n!=max(SP_hist_n)])]


if(tail(B_hist_n,1) < highest )
{
  TAC[TAC>(C_hist[yrsmth])] =  C_hist[yrsmth]
}
if(tail(B_hist_n,1) > highest)
{
  TAC[TAC<( C_hist[yrsmth])] =  C_hist[yrsmth]
}
Rec <- new("Rec")
Rec@TAC <- TACfilter(TAC)
Rec
}
class(Gcontrol2) = "MP"
```

```
Gcontrol3 =  function (x, Data, reps = 100, yrsmth = 10, gg = 2, glim = c(0.5, 2),bin=5)
{
  dependencies = "Data@Year, Data@Cat, Data@Ind, Data@Abun"
  ind <- (length(Data@Year) - (yrsmth - 1)):length(Data@Year)
  C_dat <- log(Data@Cat[x, ind])
  C_dat[C_dat == -Inf] <- 0
  B_dat <- log(Data@Ind[x, ind]/Data@Ind[x, ind[yrsmth]] * Data@Abun[x])
  B_dat[B_dat == -Inf] <- 0
  C_hist <- exp(predict(loess(C_dat ~ ind, degree = 1)))
  B_hist <- exp(predict(loess(B_dat ~ ind, degree = 1)))
  ind <- 2:yrsmth
  ind1 <- 1:(yrsmth - 1)
  SP_hist <- B_hist[ind] - B_hist[ind1] + C_hist[ind1]
  yind <- 1:length(SP_hist)
  SP_mu <- predict(lm(SP_hist ~ yind), newdat = list(yind =length(SP_hist) + 1))
  SP_se <- predict(lm(SP_hist ~ yind), newdat = list(yind = length(SP_hist) + 1), se =
T)$se.fit
  SP_new <- rnorm(reps, SP_mu, SP_se/2)
  Glm <- summary(lm(SP_hist ~ B_hist[ind1]))$coefficients[2, 1:2]
  G_new <- rnorm(reps, Glm[1], Glm[2]/2)
  TAC <- SP_new * (1 - gg * G_new)
  TAC[TAC < glim[1] * C_hist[yrsmth]] <- glim[1] * C_hist[yrsmth]
  TAC[TAC > glim[2] * C_hist[yrsmth]] <- glim[2] * C_hist[yrsmth]


  C_dat_n <- log(Data@Cat[x, ])
  C_dat_n[C_dat_n == -Inf] <- 0
  B_dat_n <- log(Data@Ind[x,]* Data@Abun[x])
  B_dat_n[B_dat_n == -Inf] <- 0
  C_hist_n <- exp(predict(loess(C_dat_n ~ c(1:length(Data@Year)), degree = 1)))
  B_hist_n <- exp(predict(loess(B_dat_n ~ c(1:length(Data@Year)), degree = 1)))
```

```
PAR = c(log(0.3),log(B_hist_n[1]),log(B_hist_n[1]),log(0.2))

RKQTSMOpt<-function(PAR)
{
 r<-exp(PAR[1])
 K<-exp(PAR[2])
 B1<-exp(PAR[3])
 Sigma<-exp(PAR[4])
 N<-length(C_hist_n)+1
 B<-numeric(N)
 Effort<-numeric(N-1)
 B[1]=B1
 for (i in 2:N){
  B[i]=max(B[i-1]+r*B[i-1]*(1-B[i-1]/K)- C_hist_n[i-1],0.01)
 }
 -sum(stats::dlnorm(B_hist_n,meanlog = log(B),sdlog=Sigma,log=T))
}
OPModel<-optim(PAR,RKQTSMOpt)
r = exp(OPModel$par)[1]
k = exp(OPModel$par)[2]
bmsy = k/2

highest = bmsy


if(tail(B_hist_n,1) < highest )
{
 TAC[TAC>(C_hist[yrsmth])] =  C_hist[yrsmth]
}
```

```
  if(tail(B_hist_n,1) > highest)
  {
    TAC[TAC<( C_hist[yrsmth])] =  C_hist[yrsmth]
  }
  Rec <- new("Rec")
  Rec@TAC <- TACfilter(TAC)
  Rec
}
class(Gcontrol3) = "MP"
```

```
Gcontrol4 =  function (x, Data, reps = 100, yrsmth = 10, gg = 2, glim = c(0.5, 2),bin=5)
{
  dependencies = "Data@Year, Data@Cat, Data@Ind, Data@Abun"
  ind <- (length(Data@Year) - (yrsmth - 1)):length(Data@Year)
  C_dat <- log(Data@Cat[x, ind])
  C_dat[C_dat == -Inf] <- 0
  B_dat <- log(Data@Ind[x, ind]/Data@Ind[x, ind[yrsmth]] * Data@Abun[x])
  B_dat[B_dat == -Inf] <- 0
  C_hist <- exp(predict(loess(C_dat ~ ind, degree = 1)))
  B_hist <- exp(predict(loess(B_dat ~ ind, degree = 1)))
  ind <- 2:yrsmth
  ind1 <- 1:(yrsmth - 1)
  SP_hist <- B_hist[ind] - B_hist[ind1] + C_hist[ind1]
  yind <- 1:length(SP_hist)
  SP_mu <- predict(lm(SP_hist ~ yind), newdat = list(yind =length(SP_hist) + 1))
  SP_se <- predict(lm(SP_hist ~ yind), newdat = list(yind = length(SP_hist) + 1), se =
T)$se.fit
  SP_new <- rnorm(reps, SP_mu, SP_se/2)
  Glm <- summary(lm(SP_hist ~ B_hist[ind1]))$coefficients[2, 1:2]
  G_new <- rnorm(reps, Glm[1], Glm[2]/2)
  TAC <- SP_new * (1 - gg * G_new)
  TAC[TAC < glim[1] * C_hist[yrsmth]] <- glim[1] * C_hist[yrsmth]
  TAC[TAC > glim[2] * C_hist[yrsmth]] <- glim[2] * C_hist[yrsmth]


  C_dat_n <- log(Data@Cat[x, ])
  C_dat_n[C_dat_n == -Inf] <- 0
  B_dat_n <- log(Data@Ind[x,]* Data@Abun[x])
  B_dat_n[B_dat_n == -Inf] <- 0
  C_hist_n <- exp(predict(loess(C_dat_n ~ c(1:length(Data@Year)), degree = 1)))
```

```
B_hist_n <- exp(predict(loess(B_dat_n ~ c(1:length(Data@Year)), degree = 1)))

PAR = c(log(0.3),log(B_hist_n[1]),log(B_hist_n[1]),log(0.2),log(2))

RKQTSMOpt<-function(PAR)
{
 r<-exp(PAR[1])
 K<-exp(PAR[2])
 B1<-exp(PAR[3])
 Sigma<-exp(PAR[4])
 S = exp(PAR[5])
 N<-length(C_hist_n)+1
 B<-numeric(N)
 Effort<-numeric(N-1)
 B[1]=B1
 for (i in 2:N){
  B[i]=max(B[i-1]+r*B[i-1]*(1-(B[i-1]/K)^(S-1))/(S-1)-C_hist_n[i-1],0.01)
 }
 -sum(stats::dlnorm(B_hist_n,meanlog = log(B),sdlog=Sigma,log=T))
}
OPModel<-optim(PAR,RKQTSMOpt)
r = exp(OPModel$par)[1]
k = exp(OPModel$par)[2]
m = exp(OPModel$par)[5]
bmsy = (1/m)^(1/(m-1))*k

highest = bmsy

if(tail(B_hist_n,1) < highest )
{
```

```
    TAC[TAC>(C_hist[yrsmth])] =  C_hist[yrsmth]
  }
  if(tail(B_hist_n,1) > highest)
  {
    TAC[TAC<( C_hist[yrsmth])] =  C_hist[yrsmth]
  }
  Rec <- new("Rec")
  Rec@TAC <- TACfilter(TAC)
  Rec
}
class(Gcontrol4) = "MP"
```

BIOGRAPHY OF THE AUTHOR

Luoliang Xu was born in Jixi, Anhui Province, China in 1990. He graduated from Tunxi No.1 high school. He attended Shanghai Ocean University and majored in Marine Fisheries Sciences and Technologies in 2009. Luoliang received his Bachelor's degree in 2013 and started a Master's program in Fisheries Resources at Shanghai Ocean University. He was sent to University of Maine as a visiting student in the summer of 2016. In January of 2017, he was officially enrolled in University of Maine and started his Ph.D. program.

The following chapters of the dissertation have been published in or submitted to peer-review journals.

Chapter 2 has been published as:

Xu, L., Mazur, M., Chen, X., and Chen, Y. 2020. Improving the robustness of fisheries stock assessment models to outliers in input data. Fish. Res. 230: 105641.

Chapter 3 has been published as:

Xu, L., Li, B., Chen, X., and Chen, Y. 2019. A comparative study of observation-error estimators and state-space production models in fisheries assessment and management. Fish. Res. 219: 105322.

Chapter 4 has been submitted for review as:

Xu, L., Chen, J., Chen, X., and Chen, Y. 2020. Multiple time series of input data improve the performance of state-space fishery stock assessment models. (submitted to Fish Fish.)

Chapter 5 has been submitted for publication as:

Xu, L., Hodgdon, C., Sun, M., Mazur, M., Chen, X., and Chen, Y. 2020. Comparing a suite of surplus-production-based stock status identification approaches and management procedures. (submitted to Can. J. Fish. Aquat. Sci.)

Luoliang is a candidate for the Doctor of Philosophy degree in Ecology and Environmental Sciences from University of Maine in December 2020.